Arts & Sciences Electronic Theses and Dissertations   Arts & Sciences

Summer 8-15-2016

Infantile Batten Disease: Effective Therapy and Novel Model

Charles Shyng
Washington University in St. Louis

WASHINGTON UNIVERSITY IN ST. LOUIS

Division of Biology and Biomedical Sciences
Molecular Cell Biology

Dissertation Examination Committee:
Mark S Sands, Chair
John Cirrito
David H. Gutmann
Jin-Moo Lee
Steven J. Mennerick
Daniel S. Ory

Infantile Batten Disease: Effective Therapy and Novel Model

by
Charles Shyng

A dissertation presented to the
Graduate School of Arts & Sciences
of Washington University in
partial fulfillment of the
requirements for the degree
of Doctor of Philosophy

August 2016
St. Louis, Missouri

Table of Contents

List of Figures

List of Abbreviations

AAV	Adeno-associated virus
AFSM	Autofluorescent storage material
ANOVA	Analysis of Variance
CNS	Central Nervous System
ERG	Electroretinography
ERT	Enzyme replacement therapy
GFAP	Glial Fibrillary Acidic Protein
GROD	Granular Osmophilic Deposits
IC	Intracranial
IC/IT	Intracranial/Intrathecal
INCL	Infantile Neuronal Ceroid Lipofuscinosis
IT	Intrathecal
LAMP1	Lysosome-associated membrane protein-1
LSD	Lysosomal storage disease
NCL	Neuronal Ceroid Lipofuscinoses
PBS	Phosphate-buffered Saline
PFA	Paraformaldehyde
PPT1	Palmitoyl-protein thioesterase-1
PPT1-/-	PPT1-deficient
S1BF	Somatosensory barrel field cortex
TBS	Tris-buffered saline
VPM/VPL	Ventral posterior thalamic nucleus
WT	Wild-type

Acknowledgements

I could not be at this point in my life without the sacrifice and generosity of my parents, my family, my thesis advisor, my friends, my beloved fiancé, and my thesis lab members. I am sincerely thankful for their encouragement and love.

I would like to thank my mom and dad. Without their constant and unwavering support, love, and encouragement, I would not be where I am today. Their sacrifice so that I could be who I am today and who I will become tomorrow is not one that can be repaid. I thank them for instilling in me perseverance and dedication. I thank them for teaching me to see the light and to find joy when nothing seems to go right. I thank them for teaching me that one never stops growing. From a young age, they encouraged me to open my mind and explore the world, to absorb as much knowledge as I could, and to use my talent and skills to help others. I take that with me every day.

I would like to thank my thesis advisor, Dr. Mark Sands. Mark took me into his lab as a goofy kid who knew little and has molded me into a well-rounded scientist. He gave me the opportunity to apply myself and to succeed in graduate school. Mark provided constant guidance through his open door policy. His willingness to answer my constant questions, listen to my crazy ideas, help with writing grants and papers, and allowing me to observe daily PI life helped me to grow scientifically. Mark taught me so much about science and about people. From him, I learned how to conduct sound basic and translational science. I learned why we perform these studies. His dedication to helping patients and families is inspirational. His effort to instill that in his graduate students is commendable. Through scientific and patient conferences, I was able to see first-hand the impact our work would have on patients and their families. I cannot thank him enough for these eye-opening opportunities. I thank Mark for believing in and supporting me, for

giving me the opportunity to find my own interests, and for being such an amazing role model for a goofy kid.

I would like to thank my thesis lab for their laughter and insights. I have learned a great deal about science and about life from my interactions with current and former lab mates. I would like to thank Marie for being the awesome 'lab mom' and dealing with all the messes and general craziness. I would like to thank her for helping me get on my feet when I first joined the lab. Marie has always being there when I had questions or if I just needed someone to talk to. I would like to thank Kevin for always bringing laughter to my bay. I thank him for working so diligently, and for teaching me how to run a mouse colony and how to cryosection. I thank Bruno for being such a great friend both in and out of the lab. I thank him for all the guidance he has provided with experiments and for being so willing to pass on knowledge.

I would like to thank my closest friends for their constant support and their ability to keep me grounded. I have had the opportunity to make friends inside and outside of graduate school. To my friends within the graduate school, I thank you for all the scientific conversations we've had throughout the years and for all the fun times we've had outside of lab such as our monthly food club. I could not imagine going through graduate school without such wonderful friends to share the experience with. To my friends outside of graduate school, I thank you for all the joys and laughter. I have watched our circle of friends grow with new additions, with two more tiny ones on the way. Thank you for keeping me grounded, for continuing to support me through all of my highs and lows, and for dealing with my peculiarities.

I want to thank my beloved fiancé Brea Jewell. I never imagined that I would meet the love of my life right down the hall. Thank you for always believing in me and for always grounding me. Thank you for always being a source of joy and laughter. You have shown me

that there is more to life than just lab and soccer. Thank you for all the countless things you do for me daily. Most of all, thank you for always being there for me. I look forward to our many years ahead.

Lastly, I want to thank all the mentors I have had and my thesis committee. I would not be here today without the scientific mentorship from these individuals. I want to thank my uncle, Dr. Yao-wen Huang, for giving me my first foray into the lab. Thank you for teaching me about the scientific method and allowing me to conduct my first scientific experiment. Thank you for supporting me throughout this entire PhD process. I want to thank the Young Scholars Program at the University of Georgia for giving me the opportunity to continue my scientific curiosities while in high school. I thank Drs. Steven Stice and Amy Batal for providing an encouraging environment for a young scientist to grow. I want to thank Dr. James Huettner for the opportunity to work in his lab while in college. Thank you for allowing me to pursue my interests and teaching me along the way. The experience I gained in your lab has been instrumental while in graduate school. I want to thank Dr. Jonathan Cooper and Hemanth Nelvagal for their collaboration, hard work, and help with our mutual work. Finally, I want to thank my thesis committee members for their insight and support over these last four years.

Abstract of the Dissertation

Infantile Batten Disease: Effective Therapy and Novel Model

by

Charles Shyng

Doctor of Philosophy in Biology and Biomedical Sciences

Molecular Cell Biology

Washington University in St. Louis, 2016

Mark S. Sands, Chairperson

Infantile neuronal ceroid lipofuscinosis (INCL, Infantile Batten) is typically an early

onset, neurodegenerative lysosomal storage disorder. INCL is caused by mutations to the gene

CLN1 which codes for the lysosomal enzyme palmitoyl-protein thioesterase-1 (PPT1). PPT1 is a

soluble lysosomal enzyme that functions to cleave fatty acyl chains from proteins destined for

degradation. Deficiency in PPT1 leads to the accumulation of autofluorescent storage material, a

hallmark of the NCLs. The storage material has been implicated in progressive histopathological

changes in the brain such as neuronal loss, astrocytosis, microgliosis, and immune cell

infiltration. These histopathological changes result in a progression of clinical signs including

vision loss, decline in motor function, cognitive deficits, seizures, and premature death.

Currently, there are no cures or treatments for INCL. However, a murine model of INCL has

been used in pre-clinical therapy studies. The PPT1-/- mouse has been shown to be a reliable

model for the human INCL disease. Detailed temporal and spatial histopathological

examinations of murine INCL in the brain have led to intracranial gene therapy studies. These

pre-clinical studies have resulted in significant improvements in biochemical, histopathological,

and functional deficits seen in the untreated PPT1-/- mouse. However, there have only been

modest improvements in lifespan. Given the identification and development of improved gene therapy vectors, this was a surprising finding. Therefore, the first section of the dissertation, we pursued a more thorough characterization of the central nervous system to identify potential regions of disease not targeted by intracranial gene therapy. We identified the spinal cord as a significant site of disease that was not previously characterized or corrected. This allowed us to target both the brain and spinal cord with AAV-based gene therapy. We demonstrated that targeting the entirety of the central nervous system was necessary to treat INCL more effectively.

From these and historical studies, we identified a multitude of cell types that are involved with INCL pathogenesis. In the central nervous system, INCL has been shown to progress sequentially from astrocytosis, to neuronal loss, to microgliosis and immune cell infiltration. PPT1 is ubiquitously expressed; therefore, its deficiency in INCL could lead to pathology in every cell type. Currently, we are unable to model cellular and metabolic changes in specific cell types in INCL due to 'cross-correction'. While 'cross-correction' is beneficial for the development of therapeutics, it interferes with our ability to understand the role of PPT1 in specific cell types. Therefore, in the second section of the dissertation, we sought to determine the cell-autonomous nature of PPT1. Because PPT1 is a soluble lysosomal hydrolase that can undergo 'cross-correction', we developed a chimeric enzyme whereby PPT1 is tethered to the lysosomal membrane. We demonstrated that tethered PPT1 retains its enzymatic function and does not 'cross-correct' *in vitro* and *in vivo*. We further demonstrated that near-ubiquitous expression of tethered PPT1 could prevent INCL. This lays the groundwork for future studies designed to determine the role of specific cell types in the pathogenesis of INCL.

Chapter 1: Introduction

Lysosomal Storage Diseases

Lysosomal storage diseases (LSDs) are a group of rare, inherited metabolic disorders that include over 45 different diseases (Boustany, 2013; Cox & Cachon-Gonzalez, 2012; Hers, 1965; Neufeld, 1991; Schultz et al, 2011). LSDs occur with an incidence of approximately one in 8000 live births, making them one of the most common childhood genetic diseases (Fuller et al, 2006; Schultz et al, 2011). Each LSD is due to mutations to a single gene and occurs mostly with an autosomal recessive inheritance pattern (Neufeld, 1991). These mutations lead to deficiency or reduction in function of proteins involved in the lysosomal pathway. Functional loss or reduction of a lysosomal protein ultimately results in the accumulation of storage material either in the lysosome or extra-lysosomal. These deficiencies have been shown to cause an increase in lysosome proliferation and secondary effects on cellular metabolism (Vitner et al, 2010). The storage materials have been implicated in the pathogenesis of the clinical disease; however, precise studies to determine their role in pathology have not been performed.

Lysosomal enzymes are ubiquitously expressed and their deficiency affects multiple cell types and organ systems. Their deficiency leads to a complex clinical presentation. Many LSDs present with clinical signs of organomegally, skeletal deformities, cardiac abnormalities, and/or immunologic deficiencies (Madhavarao et al, 2009). Interestingly, approximately two-thirds of all LSDs present with a neurological phenotype (Jardim et al, 2010). Those disorders that present with neurological dysfunction exhibit behavioral problems, regression in cognition, loss of visual acuity and hearing, verbal deterioration, and/or loss of motor function. Patients are typically diagnosed after disease onset which can range from early infancy to adulthood (Platt & Lachmann, 2009). Interestingly, the mutated gene does not necessarily determine the age of onset (Maire, 2001). It has been shown that these mutations lead to a variable scale of lysosomal

enzyme activity, which ultimately influences the progression of the disease. This most likely is caused by the presence of yet unknown modifying genes. Ultimately, patients suffer an early death after an undefined period of cognitive or behavioral regression. Currently, there are no comprehensive treatments for lysosomal storage disorders. However, there has been progress towards the development of effective therapies involving gene and cell therapy as well as the development of small molecule drugs and recombinant enzyme (Parenti et al, 2015).

Neuronal Ceroid Lipofuscinoses

The Neuronal Ceroid Lipofuscinoses (Batten Disease, NCL) are a group of mostly pediatric neurodegenerative diseases (Goebel & Wisniewski, 2004). The incidence of Batten disease is ~1 in 12,500 live births making it the most common inherited pediatric neurologic disorder. This subgroup of lysosomal storage disorders are grouped together due to their common histologic hallmark of autofluorescent storage material (AFSM) accumulation (Mole & Williams, 1993). There is a variety of forms of Batten disease which have been historically classified based on age of onset (Dyken, 1989). However, in recent years, it has been determined that age of onset and the mutated gene are not necessarily correlated (Wisniewski et al, 2001). Presently, the various forms of Batten disease are classified based on the mutated gene. Currently there are over 14 different genes associated with NCL (Anderson et al, 2013). The progression of histopathogenesis in the brain has been well documented among the NCL variants (Bennett & Rakheja, 2013). The similarities in disease progression include neuronal loss, retinal deterioration, cortical thinning, brain atrophy, and neuroinflammation. The accumulation of AFSM is present in all variants, though the identification of AFSM substrates and whether AFSM is pathogenic has not been elucidated (Palmer et al, 2013). It has also been recently

3

shown in patients and murine models that NCL variants have metabolic and cardiac abnormalities (Galvin et al, 2008; Ostergaard et al, 2011; Woloszynek et al, 2007). Since the NCL field had largely focused on disease associated with the brain, these recent discoveries have led to studies focusing on systemic disease. Most studies have been directed to study the brain, while the spinal cord (central nervous system), the peripheral nervous system (PNS), and the autonomic nervous system (ANS) have been largely overlooked.

Infantile Neuronal Ceroid Lipofuscinosis

The infantile form of NCL is one of the earliest onset and most aggressive forms of Batten disease. Infantile NCL (INCL) was first described in 1973 by Haltia et al and subsequently referred to as Santavuori-Haltia disease (Haltia et al, 1973b; Santavuori et al, 1973). While most cases of INCL were located in the Scandinavian region, with the improvement in genomic techniques, INCL has been described worldwide with ages ranging from infancy to adulthood (Hofmann et al, 2001b; Kousi et al, 2012). Children with INCL are pre-symptomatic at birth but begin exhibiting psychomotor retardation between 6-12 months. Developmental regression begins first with loss of motor and visual functions followed by cognitive decline. As the disease progresses, patients become blind and ataxic, eventually losing complete muscle coordination and tone. Patients also develop myoclonic seizures. Near end of life, patients are wheelchair bound and are often on feeding tubes and ventilation (Jadav et al, 2014; Santavuori et al, 1974; Santavuori et al, 1973; Simonati et al, 2009). Currently, there are no effective treatments for INCL.

Mutations leading to INCL were identified in the *CLN1* gene in 1991 (Schonherr et al, 1991). Since then, over 61 novel mutations have been identified in the *CLN1* gene (Kousi et al,

2012). They consist of missense, nonsense, splicing affected, insertions, deletions, or a combination of mutations. These mutations lead to reduced enzymatic activity of PPT1. The enzymatic deficiency leading to INCL was not discovered until 1995 (Vesa et al, 1995). The authors showed that palmitoyl-protein thioesterase-1 (PPT1), a soluble lysosomal hydrolase, was deficient in INCL patients. A follow-up study showed that replacement of PPT1 via recombinant enzyme was able to correct the disease in *in vitro* lymphoblast cultures (Camp & Hofmann, 1993; Camp et al, 1994; Hellsten et al, 1996; Hofmann et al, 2001a; Verkruyse & Hofmann, 1996; Verkruyse et al, 1997). PPT1 functions to cleave fatty acyl groups from modified cysteine residues in proteins destined for degradation. It is ubiquitously expressed and has been shown to be developmentally and spatially regulated (Isosomppi et al, 1999). Recently, PPT1 has been shown to co-localize with synaptic vesicles and synaptosomes in neurons, however, the reason has yet to be discovered (Kim et al, 2008; Lehtovirta et al, 2001). Deficiency in PPT1 leads to the biochemical, histological, and behavioral changes associated with INCL.

The cellular pathology in PPT1 deficiency has the hallmark of NCLs, autofluorescent storage material. The ultrastructural appearance of storage material has been described as granular osmiophilic deposits (GRODs) (Goebel et al, 1995; Siegismund et al, 1982). These deposits are localized to the lysosome and their complete composition has yet to be determined. However, it has been shown in the brain to contain a complex mixture of protein and lipids with major products of saposin A and D and glial fibrillary acidic protein (GFAP) (Tyynela et al, 1993).

Analyses of the INCL brain show gross anatomical changes. There is severe brain atrophy such that the mass of the INCL brain is only 50% of an age-matched normal child (Haltia et al, 1973a). There is dramatic thinning of the cortical layers. The accumulation of

lipopigments has been found ubiquitously, however, the extent of their accumulation varies.

They are prevalent in the brain, reticuloendothelial system, intestine, bone marrow, and Kupffer

cells (Siegismund et al, 1982). Using magnetic resonance imaging, atrophy was seen in the

thalamus and basal ganglia by T2 hypointensity as well as in the cerebral cortex (Jadav et al,

2014; Jadav et al, 2012; Santavuori et al, 1992; Vanhanen et al, 1995a). This was correlated with

loss of cortical neurons as well as loss of axons and myelin sheaths (Vanhanen et al, 1995a;

Vanhanen et al, 1995b). There is also atrophy of the retinal pigment epithelial cells and

accumulation of GRODs ultimately leading to loss of an electroretinography (ERG) signal

(Vanhanen et al, 1997; Weleber et al, 2004)

The murine INCL model

A mouse model of INCL was created in 2001 that is deficient in PPT1 activity (PPT1-/-)

(Gupta et al, 2001). This model had a neomycin cassette inserted into exon 9 of the murine PPT1

gene via homologous recombination. This mutation introduced a premature stop codon as well as

abolished two of the amino acids involved in the catalytic triad. Characterization of the mouse

model has been extensive with much of the studies focused on the brain (Dearborn et al, 2015;

Galvin et al, 2008; Gupta et al, 2001; Kielar et al, 2007; Macauley et al, 2009). The PPT1-/-

mouse has a median lifespan of 8.5 months and accumulations AFSM ubiquitously (Gupta et al,

2001). Similar to the human disease, there is widespread neurodegeneration and

neuroinflammation (Kielar et al, 2007; Macauley et al, 2009). Temporal studies have shown that

astrocytosis, detectable at 3 months, precedes neurodegeneration, detectable at 5 months.

Microgliosis and infiltrating immune cells are detectable at 7 months. Overall, there is brain

atrophy and cortical thinning, with brain weights of PPT1-/- mice at a terminal time point

approximately 60% that of normal age-matched animals (Bible et al, 2004). There are significant decreases in retinal function measured by ERG and motor dysfunction measured by rotarod beginning at 4 months and 5 months, respectively (Griffey et al, 2005; Griffey et al, 2006). While mice have been shown to have decreased ERGs, they maintain some visual acuity in the early stages of disease (Dearborn et al, 2015; Griffey et al, 2005). Motor function continues to decrease over time and PPT1-/- mice are unable to stay on the rotarod past 7 months. Spontaneous seizure activity begins at 7 months in 50% of tested animals and occurs in 100% of PPT1-/- animals at 7.5 months (Bible et al, 2004).

While INCL studies have primarily focused on the brain, studies have shown histological and pathological defects systemically. Autofluorescent material has been shown to accumulate in most tissues outside of the brain, with prevalence in the kidney and spleen (Galvin et al, 2008). AFSM has been seen in the liver, bone, eye, and heart. Cardiac defects have been reported in the PPT1-/- mouse (Galvin et al, 2008). Echocardiography revealed left ventricular hypertrophy and aortic dilatation. It has also been shown that PPT1-/- mice have metabolic dysfunction (Woloszynek et al, 2007). Although PPT1-/- mice have relatively normal plasma chemistry, they have decreased body weights compared to wild-type mice and have significantly decreased adiposity. PPT1-/- mice lose 25% of adiposity and have decreased leptin levels as compared to wild-type mice. However, PPT1-/- mice consume more food than wild-type mice and have a slower metabolic rate. This suggests that PPT1 deficiency leads to altered energy utilization similar to that seen in other LSDs (Woloszynek et al, 2007; Woloszynek et al, 2009). Overall, the PPT1-/- mouse recapitulates most of the features of human INCL and is useful as a model for pre-clinical therapy studies.

INCL Therapy

Small molecule drugs

A number of small molecule drugs have been used to treat human and murine INCL by targeting the primary genetic defect through PPT1 mimetics or by targeting the secondary disease mechanisms. Two PPT1 mimetics have been developed for pre-clinical studies. The development of phosphocysteamine as a small molecule drug for INCL was utilized because it functions similarly to PPT1. Phosphocysteamine was shown *in vitro* to lysosomotrophic and is capable of disrupting thioester linkages. The *in vitro* study of phosphocysteamine showed depletion of lysosomal ceroids (GRODs) and showed a decrease in saposin A and D which have been shown to accumulate in GRODs (Zhang et al, 2001). This *in vitro* study prompted the use of phosphocysteamine in the PPT1-/- mouse model. Unfortunately, delivery of phosphocysteamine showed no improvement of biochemical, histological, or functional parameters of INCL (Roberts et al, 2012). Despite this, a clinical trial was conducted combining cysteamine bitartrate with N-acetylcysteine (Zhang et al, 2001). The children showed minimal improvement in clinical signs of disease as measured by EEG and MRI (Levin et al, 2014).

Another PPT1 mimetic, N-tert-butyl-hydroxlamine (NtBuHA), has recently been developed. NtBuHA has been shown to similarly deplete lysosomal ceroid accumulation *in vitro*. NtBuHA was shown to cross the blood-brain barrier and minimally improve histological and clinical signs of disease in the PPT1-/- mouse (Sarkar et al, 2013). This PPT1 mimetic has not yet been tested in clinical trials.

Other small molecule drugs have been tested in pre-clinical studies on INCL mice or patient fibroblasts. In one study, a stop-codon read-through drug PTC124 was utilized *in vitro*. PPT1 nonsense mutations are one of the most prevalent mutations. PTC124 showed an increase

in PPT1 activity and decreased GRODs (Sarkar et al, 2011). In another study, the secondary

mechanism of disease, neuroinflammation, was targeted using Minozac. Minozac is a small

molecule inhibitor of proinflammatory cytokines in the brain. This small molecule has been

shown to attenuate neuronal loss and prevent behavioral deficits in other models of neurologic

disease (Hu et al, 2007). Given the upregulation of proinflammatory cytokines in INCL, Minozac

was used in a pre-clinical experiment. Treatment with Minozac resulted in decreased seizures,

however, it did not improve other clinical parameters (Macauley et al, 2014). There were slight

improvements in histology with slight decreases in GFAP and CD68 staining, which are markers

of neuroinflammation. Similarly, there were subtle decreases in cytokine upregulation.

Cross-correction

The process of 'cross-correction' is the basis for several therapeutic strategies to treat

soluble lysosomal enzyme deficiencies. It was first proposed by de Duve in 1964 as a treatment

strategy, and has been refined since its actual discovery in the late 1960s (Deduve, 1964). 'Cross-

correction' was a fortuitous discovery by Elizabeth Neufeld and colleagues in 1968 (Fratantoni

et al, 1968). Discoveries about lysosomal enzymes and their trafficking soon followed detailing

the mannose-6-phosphate receptor pathway and the modifications of oligosaccharides on

lysosomal enzymes to mediate lysosomal targeting (Dahms et al, 1989; Kornfeld et al, 1982;

Natowicz et al, 1979; Varki & Kornfeld, 1980). Briefly, mannose-6-phosphate (M6P) groups are

attached post-translationally to proteins destined for the lysosome. Via this modification,

enzymes bind to the M6P/Insulin-growth factor II (M6P/IGFII) receptor in the Golgi and are

transported through the endosomal pathway. Detachment of the modified proteins in the

acidified lysosome allows the M6Pr/IGFIIr to recycle to the Golgi or to the plasma membrane

9

(Dahms et al, 1989). Through an undetermined process, possibly exosomes, a small percentage of lysosomal enzymes are secreted into the extracellular space. These soluble enzymes can be retrieved by neighboring cells through the mannose-6-phosphate or mannose receptor-mediated uptake pathways. The endocytosed enzymes are then trafficked back to the lysosome where they participate in normal cellular functions (Sands & Davidson, 2006). 'Cross-correction' is the process underlying stem-cell transplantation, enzyme replacement therapy, and gene replacement therapy. Stem-cell transplantation and enzyme replacement therapy have become standard of care for a growing number of LSDs.

Cell-mediated Therapy

Cell-mediated therapy has been suggested to treat INCL. It is suggested that a limited number of engrafted cells are necessary to treat the disease by taking advantage of 'cross-correction'. Two methods have been performed pre-clinically, to date. Neural stem cells have been transplanted in INCL mice and this procedure has progressed to a phase one clinical trial. Neural stem cell transplantation provided increased PPT1 activity, decreased AFSM, and delayed motor dysfunction in the mouse (Tamaki et al, 2009). However, the overall effect on lifespan was not examined. A clinical trial was initiated in 2005 (Taupin, 2006); however, the clinical trial was withdrawn prior to enrollment of patients (NCT01238315).

Bone marrow transplantation (BMT) was utilized in a pre-clinical study for INCL. BMT has been shown to play a dual role in lysosomal storage diseases of 'cross-correction' and immunomodulation. In other LSD models, BMT results in varying degrees of efficacy (Birkenmeier et al, 1991; Qin et al, 2012; Reddy et al, 2011; Sands et al, 1993), and has become standard of care in certain patient populations. In INCL, BMT was shown to have a detrimental

effect. INCL mice treated with BMT had a decreased lifespan and impaired motor function (Macauley et al, 2012).

Enzyme replacement therapy

Enzyme replacement therapy (ERT) has been shown to be one of the more promising candidates for INCL therapy. Similar to cell-mediated approaches, ERT takes advantage of 'cross-correction'. Recombinant PPT1 delivered intravenously has been shown to correct the systemic histologic phenotype in INCL mice and improve motor function and longevity (Hu et al, 2012; Lu et al, 2010). Intrathecal injections of rPPT1 were attempted in PPT1-/- mice to target the brain pathology. This study showed that intrathecal injections of rPPT1 were able to partially correct histological hallmarks of INCL in the brain, extend lifespan, and improve motor function (Lu et al, 2015). However, the improvements observed in both studies were minor and rPPT1 had to be administered on a regular basis.

Gene Therapy Studies

Gene therapy was first proposed by Friedmann & Roblin in 1972 as a technique to treat human genetic diseases (Friedmann & Roblin, 1972). Since then, a number of pre-clinical gene transfer studies have been performed with a variety of viral vectors (e.g. lentivirus, adeno-associated virus, adenovirus). In the PPT1-/- mouse, gene therapy experiments have been performed primarily using adeno-associated viral (AAV) vectors targeting the forebrain, hippocampus, and cerebellum. Progressive biochemical, histological, and behavioral improvements have been observed as newer generation vectors have been developed. A first-generation AAV2 vector was utilized to supply a persistent source of PPT1 to the PPT1-/- brain via intracranial injections (Griffey et al, 2004). The vector was able to provide localized enzymatic activity sufficient to correct the biochemistry and histopathology in the area near the

injection site. However, the correction was limited by the diffusion of the AAV2 viral vector and 'cross-corrective' enzyme. An increased dose of the AAV2 vector was able to further improve biochemistry, histopathology, and behavior, but the lifespan of the treated mice was not significantly extended compared to the untreated PPT1-/- mice (Griffey et al, 2006). In subsequent studies, the second-generation AAV2/5 vector was utilized. The intracranial AAV2/5-treated mice had greater biochemical, histopathological, and behavioral improvements compared to AAV2. Importantly, there was also a significant extension in lifespan (Macauley et al, 2012; Macauley et al, 2014; Roberts et al, 2012). This may be explained by the greater transduction efficiency and distribution of the AAV2/5 vector in the brain (Burger et al, 2004). While the improvements have been significant compared to PPT1-/- mice, overall, they have been modest compared to wild-type. Gene therapy has been shown in pre-clinical studies of INCL to be the most effective approach to date. A third-generation vector, AAV2/9, has been shown to have a broader distribution in the CNS of animal models and may increase therapeutic efficacy in INCL (Dayton et al, 2012; Schuster et al, 2014; Swain et al, 2014).

Goals of the Thesis
Spinal Cord pathology

CNS-directed gene therapy was shown to have only modest improvements in lifespan and motor function. This was surprising given the nearly normal levels of PPT1 activity in the brain. Thus, it was hypothesized that there were regions of the central nervous system that were not targeted by brain-directed gene therapy. Therefore, we conducted a more thorough retrospective analysis of the AAV2/9- and AAV2/5-treated central nervous system to determine the extent of CNS correction. In the retrospective analysis from the treated animals, there was an increase in

markers for astrocytosis and neuroinflammation in the spinal cords. A comprehensive temporal and spatial analysis of the PPT1-/- spinal cord was conducted in collaboration with Dr. Jonathan Cooper, King's College.

The retrospective analysis of PPT1-/- animals treated with gene therapy showed that there was the accumulation of AFSM throughout the spinal cord and brain stem similar to the PPT1-/- brain. Furthermore, there was an increase in GFAP and CD68 staining, which are markers for neuroinflammation. The inability of intracranial injections of AAV2/9 to treat the brainstem and spinal cord effectively revealed a potential new target for a combinatorial AAV gene therapy-based approach. Therefore, the first goal of this study was to perform a comprehensive analysis of the central nervous system of treated animals to determine the extent of spinal cord disease not treated via intracranial AAV vector delivery. The second goal of this study was to determine whether targeting both the brain and the spinal cord in PPT1-/- mice would significantly improve efficacy. In this study, we transitioned from the second-generation AAV vector (AAV2/5-hPPT1) to the third-generation AAV vector (AAV2/9-hPPT1) to determine whether a third generation vector would provide significantly increased efficacy. We hypothesized that AAV-based intracranial and intrathecal injection of AAV2/9-hPPT1 would significantly extend the lifespan of PPT1-/- mice and improve both clinical and pathological parameters compared to either treatment alone.

Multiple cell types involved in INCL pathogenesis

Multiple studies of INCL neuropathology have shown that there are many CNS cell types affected by PPT1 deficiency. Murine INCL progresses sequentially from astrocytosis, to neuronal loss, and to microgliosis and immune cell infiltration. This progression has been

documented throughout the central nervous system and has been shown to have a profound impact on the severity of the disease. When reactive astrocytosis is inhibited by preventing the upregulation of intermediate filaments (conducive to astrocyte transition from dormant to reactive), the progression of INCL is accelerated. PPT1-/- mice deficient in intermediate filaments have a shortened lifespan and an increase in neuroinflammatory markers. Macauley et al, (2011) showed that reactive astrocytosis might play a neuroprotective role in INCL pathogenesis (Macauley et al, 2011; Shyng & Sands, 2014). Neuronal loss and cortical thinning have been well documented in INCL, and their loss is both temporal and spatial. Studies have shown that neuronal loss first begins in the thalamus followed by neurodegeneration in the cortex and cerebellum (Kielar et al, 2007; Macauley et al, 2009). It has been shown that a subset of neuronal proteins which are involved in the regulation of axonal and synaptic vulnerability are altered in INCL. Neuronal protein expression changes were present prior to synaptic or axonal morphological alterations and followed a similar spatial progression (Kielar et al, 2009). There are also changes to receptors and channels involved with neuronal function associated with PPT1 deficiency (Aby et al, 2013; Kim et al, 2008; Qiao et al, 2007; Tikka et al, 2016; Virmani et al, 2005; Zhang et al, 2006). Furthermore, PPT1 deficiency has been shown to be involved in blood-brain barrier maintenance, neuroinflammation, and systemic metabolic and cardiac dysfunction (Galvin et al, 2008; Khaibullina et al, 2012; Saha et al, 2008; Saha et al, 2012; Tikka et al, 2016; Wei et al, 2011; Woloszynek et al, 2007). While studies have yet to show that PPT1 deficiency directly influences myelination, preliminary studies have shown changes in the level and organization of myelin (Macauley et al, 2009).

Overall, this suggests that multiples cell types are involved in INCL disease. This may not be surprising since PPT1 is ubiquitously expressed. Unfortunately, our ability to model

cellular and metabolic changes in specific cell types in lysosomal storage diseases has been lacking. This is due primarily to 'cross-correction'. It is beneficial to our understanding of INCL as well as the development of therapeutics to understand the role of PPT1 in specific cell types. This will ultimately guide therapeutic strategies in determining the necessity of correcting all cell types or a specific subset of cell types in order to prevent disease.

Tethered PPT1 to the lysosomal membrane

To understand the cell autonomous roles of specific cell types in INCL, we engineered a chimeric lysosomal membrane tethered form of PPT1 using the transmembrane domain/signaling peptide of lysosomal-associated membrane protein-1 (LAMP1). The transmembrane domain/signaling peptide has been shown to be necessary and sufficient for lysosomal targeting of LAMP1, and may be used as a targeting and retention mechanism for soluble lysosomal hydrolases (Guarnieri et al, 1993; Marathe et al, 2000). Therefore, the second major goal of this thesis was to tether PPT1 to the lysosomal membrane through the transmembrane portion of LAMP1 in order to understand the cell autonomous nature of INCL by taking advantage of the Cre-loxP system. Therefore, we inserted a loxP-STOP-loxP sequence into the chimeric PPT1-LAMP1 transgene to achieve cell specificity. The loxP-STOP-loxP region would prevent both transcription and translation of our chimeric lysosomal enzyme unless in the presence of Cre recombinase. Unfortunately, the transgene appeared to be unstable leading to constitutive and ubiquitous expression of PPT1-LAMP1 and an inability to respond to Cre recombinase. However, we showed that membrane tethered PPT1 retained enzyme activity and was capable of preventing the biochemical, histological, and behavioral phenotype of INCL when expressed ubiquitously. Therefore, this study demonstrates a proof-of-principle that tethering PPT1 to the

lysosomal membrane could be a viable approach to address questions regarding the role of

various cell types in the progression of INCL once cell-specific expression can be achieved.

Chapter 2: A new and effective therapeutic target for Infantile Batten disease

Introduction

The neuronal ceroid lipofuscinoses (Batten disease, NCL) are a group of inherited pediatric neurodegenerative lysosomal storage disorders (Geraets et al, 2016; Mole & Williams, 1993). Infantile Batten disease is the most rapidly progressing form of NCL and is caused by mutations in the *CLN1* gene that codes for palmitoyl-protein thioeseterase-1 (PPT1), a soluble lysosomal hydrolase (Kousi et al, 2012; Vesa et al, 1995). PPT1 cleaves fatty acyl chains from proteins undergoing lysosomal degradation. Deficiency in PPT1 leads to the pathological hallmarks of NCL, which include the accumulation of autofluorescent storage material (AFSM), neurodegeneration, and glial activation (Goebel et al, 1995; Haltia et al, 1973a; Haltia et al, 1973b; Hellsten et al, 1997; Hellsten et al, 1996; Jokiaho et al, 1990; Santavuori et al, 1973; Santavuori et al, 1992; Schriner et al, 1996; Syvanen et al, 1997; Vanhanen et al, 1995a; Vanhanen et al, 1995b; Vanhanen et al, 1997; Vesa et al, 1995). Though patients are typically asymptomatic at birth, by 6 months, INCL patients exhibit progressive degenerative clinical signs in vision, motor function, and cognition, which ultimately lead to a shortened lifespan (Goebel & Wisniewski, 2004; Haltia et al, 1973a; Haltia et al, 1973b; Santavuori et al, 1973; Vanhanen et al, 1995a; Vanhanen et al, 1995b; Vanhanen et al, 1997). Currently, there are no effective treatments or cures available for INCL.

The PPT1-deficient (PPT1-/-) mouse shares most of the biochemical, pathological, and clinical signs of human INCL (Gupta et al, 2001). Histopathological characterization of the disease in the forebrain and the cerebellum demonstrated progressive AFSM accumulation, neurodegeneration, astrocytosis, and neuroinflammation (Bible et al, 2004; Gupta et al, 2001; Kielar et al, 2007; Macauley et al, 2009). There is overall brain atrophy with extensive cortical thinning concurrent with astrocyte and microglial activation. At a terminal time point, the mass of the murine brain is decreased by over 20 percent (Bible et al, 2004). The murine model has

18

functional deficits including, but not limited to retinal dysfunction, loss of motor coordination, seizure activity, cardiac insufficiency, and metabolic imbalances (Galvin et al, 2008; Griffey et al, 2005; Kielar et al, 2007; Macauley et al, 2009; Woloszynek et al, 2007). PPT1-/- mice ultimately have a shortened lifespan with a median lifespan of 8.4 months.

There have been several pre-clinical therapy studies performed in the PPT1-/- mouse. Small molecule drugs that act as PPT1 mimetics such as N-tert-butyl hydroxylamine and Cystagon have resulted in minimal improvements (Levin et al, 2014; Sarkar et al, 2013; Zhang et al, 2001). Enzyme replacement therapy (ERT) through intravenous or intrathecal routes of administration resulted in minor clinical improvements (Levin et al, 2014; Sarkar et al, 2013; Zhang et al, 2001). However, the improvements in PPT1-/- neuropathology is only observed when treatment is provided at an early stage (i.e. before the establishment of the blood-brain barrier) (Hu et al, 2012). To date, the most promising treatment in PPT1-/- mice has been CNS-directed gene therapy either alone or combined with other approaches (Griffey et al, 2004; Griffey et al, 2006; Macauley et al, 2012; Macauley et al, 2014; Roberts et al, 2012).

Pre-clinical gene therapy experiments have been performed using adeno-associated viral (AAV) vectors targeting the forebrain, hippocampus, and cerebellum. Progressive biochemical, histological, and behavioral improvements have been observed as newer generation vectors have been developed. First generation AAV2 vectors resulted in improvement in biochemical and histological pathology in the regions targeted. However, functional improvement was not observed until multiple sites of disease within the INCL brain were targeted by AAV2-hPPT1 (Griffey et al, 2004; Griffey et al, 2006). Overall, AAV2-hPPT1 increased PPT1 activity, reduced AFSM accumulation, and improved histological markers of disease, but did not significantly extend the lifespan. The second-generation AAV2/5 vector was shown to have

improved neural transduction and distribution in the murine brain (Burger et al, 2004). Besides a normalization of PPT1 activity, utilization of AAV2/5-PPT1 showed marked reduction in AFSM and pathology, as well as an extension in median lifespan by approximately two months (Macauley et al, 2012; Macauley et al, 2014; Roberts et al, 2012). The clinical improvements have been modest potentially due to limited distribution of the AAV vector (Aschauer et al, 2013; Gray et al, 2013).

A third generation vector, AAV2/9, has been shown to have a broader distribution in the CNS in several animal models (Dayton et al, 2012; Schuster et al, 2014; Swain et al, 2014). Therefore, in the current study, the AAV2/5-hPPT1 vector used in previous pre-clinical INCL gene therapy studies was transitioned to AAV2/9-hPPT1.

We show that intracranial injection of AAV2/9-hPPT1 provides significantly greater efficacy compared to AAV2/5-hPPT1. However, the lifespan was still significantly less than wildtype animals despite having nearly normal PPT1 levels in the brain. Therefore, we performed a more thorough histological analysis of the central nervous system of treated animals. This analysis revealed significant disease throughout the spinal cord that was not corrected by intracranial AAV vector delivery. These findings suggested that spinal cord pathology could play a significant role in INCL pathogenesis. In collaboration with Hemanth Nelvagal and Jonathan Cooper (King's College, London), we performed a comprehensive temporal and spatial analysis of the spinal cord in INCL mice. A brief summary of the findings from this study will be presented in this Chapter. These data taken together revealed a new region of disease and a possible therapeutic target. Therefore, we targeted the spinal cord with intrathecal gene therapy to determine whether AAV-based gene therapy could ameliorate INCL pathogenesis. Furthermore, we hypothesized that intracranial plus intrathecal injections of

AAV2/9-hPPT1 would significantly extend the lifespan of PPT1-/- mice and improve both clinical and pathological parameters compared to either treatment alone.

Intracranial injection of AAV2/9-hPPT1 resulted in greater therapeutic efficacy than intrathecal injection, although both provide significant biochemical, histological, and behavioral improvements compared to untreated PPT1-/- mice. Simultaneous treatment of both the brain and spinal cord resulted in the greatest efficacy. In fact, targeting these two regions resulted in synergistic improvements in lifespan and motor function. These data suggest that the spinal cord disease plays a major role in the overall pathogenesis of INCL. These data also identify the spinal cord as an important therapeutic target.

Material and Methods
PPT1-/- and WT mice

PPT1-/- mice were created by Gupta et al, (2001). Both congenic PPT1-/- and wild-type (WT) mice were maintained on a C57Bl/6J background at Washington University School of Medicine by MSS. The colonies were maintained separately through homozygous mating. The Thy1-YFP PPT1-/- mouse model was generated by crossing the Thy1-YFP reporter mouse (Feng et al, 2000)(Tg(Thy1-YFP)16Jrs, The Jackson Lab, Bar Harbor, ME) to the PPT1-/- mouse. The reporter mice were maintained as Thy1-YFP+/-, PPT1-/-. All procedures were performed in accordance with a protocol approved by the IACUC at Washington University School of Medicine.

Recombinant AAV production

The rAAV2/9-hPPT1 vector used in this study was packaged at the University of North Carolina Vector Core. Briefly, the vector contained the CAGGS promoter, human PPT1 cDNA,

and a rabbit B-globin polyadenylation signal all flanked by the AAV2 inverted terminal repeats (Griffey et al, 2004). Viral titers were 1×10^{12} vg/ml for all injections.

Intracranial and Intrathecal injections

On postnatal day 1 (PND1) or PND2 PPT1-/- pups received intracranial or intrathecal injections with AAV2/9-hPPT1 or AAV2/5-hPPT1 (1×10^{12} vg/ml) using a Hamilton syringe and a 30-gauge needle. For intracranial injections, two microliters of virus were injected bilaterally into the anterior cortex, hippocampus, and cerebellum as previously described (Griffey et al, 2006). For intrathecal injections, P1 or P2 PPT1-/- pups were injected in the lumbar region as previously described (Elliger et al, 1999; Hawkins-Salsbury et al, 2015). Briefly, 15 microliters of virus was mixed with three microliters of sterile Trypan-blue. Fifteen microliters of the mixture was injected. A successful injection was confirmed by the appearance of Trypan-blue in the tail and the cerebellum. For the combination treatment, both intracranial and intrathecal injections were performed on the same day in the same pup.

Treatment Groups

For the initial AAV2/5 vs AAV2/9 comparison, four groups were generated with 10 mice per group: 1) PPT1-/- mice, 2) AAV2/5-hPPT1 intracranial injected PPT1-/- mice (IC-AAV2/5), 3) AAV2/9-hPPT1-/- intracranial injected PPT1-/- mice (IC-AAV2/9), and 4) wildtype (WT) mice. For the combination study, five treatment groups were generated consisting of 22 mice per group: 1) PPT1-/- mice, 2) IC-AAV2/9, 3) AAV2/9-hPPT1 intrathecal injected PPT1-/- mice (IT-AAV2/9), 4) AAV2/9-hPPT1 intracranial and intrathecal injected PPT1-/- mice (IC/IT-AAV2/9), and 5) WT mice. Randomly selected mice were analyzed at pre-determined time

points (3, 5, 7, and 9 months) for biochemical and histological analyses (n=3 mice/group).

Experimental and control animals were randomly assigned identification numbers such that the

person performing the analyses was blind to the genotype and treatment.

Lifespan

Longevity was assessed in the treatment and control groups (n=10-11 mice/group). The

lifespan was determined by death or euthanasia for humane reasons. A Kaplan-Meier lifespan

curve was used to measure survival and significant differences were determined using a log-rank

analysis ($p<0.05$).

Rotarod Testing

Motor function was assessed in the same treated PPT1-/- and control mice (n=10) used

for longevity using a constant-speed (3 rpm) rotarod beginning at 5 months of age, and every two

months thereafter as previously described (Dearborn et al, 2015; Griffey et al, 2006). Statistical

significance was determined using one-way ANOVA at each time point followed by a

Bonferroni post hoc test.

PPT1 activity and secondary enzyme elevations

Tissue was collected at pre-determined time points. Three mice per treatment group were

euthanized via lethal injection (Fatal Plus, Vortech Pharmaceutical, Dearborn, MI). Blood was

collected from the right ventricle using a 1ml tuberculin syringe and a 26-gauge needle and

allowed to clot for 15 minutes before centrifugation at 1000x*g* for 10 minutes. Serum was

collected and flash frozen. Mice were then transcardially perfused with phosphate-buffered

saline (PBS) until the liver was cleared of blood. Portions of heart, liver, spleen, kidney, and eye

were flash frozen for subsequent biochemical analyses. Additional tissue samples were immersion fixed in 4% paraformaldehyde (PFA) in PBS for 24-hr then cryoprotected in 30% sucrose solution in Tris-buffered saline (TBS). The spine was removed by cutting at the axis/C1 and resecting the spine where the spine enters the tail. The spine was fixed and cryoprotected as described above. The brain was removed, weighed, and bisected sagittally; the left hemisphere was flash frozen while the right hemisphere is fixed and cryoprotected as described above. PPT1 assays were performed on homogenates from the brain, heart, and liver as previously described using the 4-MU-palmitate fluorometric assay and normalized to total protein (van Diggelen et al, 1999). Secondary elevations of another lysosomal enzyme, β-glucuronidase, were determined as previously described using 4-MU-β-D-glucuronide fluorometric assay and normalized to total protein (Sands et al, 1994). Significance was determined using a two-way ANOVA followed by a Bonferroni post-hoc analysis for all enzyme assays.

Thy1-YFP PPT1 spinal cord analysis

Thy1-YFP PPT1-/- and Thy1-YFP PPT1+/- mice spinal cords were isolated, fixed, and cryoprotected as described above. Spinal cords were sectioned longitudinally at 32 micrometers directly onto slides. Confocal images of Thy1-YFP PPT-/- and Thy1-YFP PPT1+/- spinal cords were captured at the lumbar region at 10x magnification. Keeping all the parameters identical from slide to slide, images were analyzed using ImageJ. Relative fluorescence units were calculated by converting the image to a binary black and white image. The number of white pixels were calculated and divided by the total pixel area. Three sections were analyzed per image and averaged. A Student's t-test was performed for significance with $p < 0.05$.

Histochemical Stain

A histochemical stain for PPT1 activity was performed on sagittal brain sections as previously described (Dearborn et al, 2016). Briefly, unfixed tissue was isolated from treated mice and immediately embedded in Optimal Cutting Temperature Compound (OCT; Sakura Finetek USA, Inc., Torrance, CA) on dry ice. Tissues were cryosectioned at 16 micrometers and mounted on Superfrost Plus slides (Thermo Fisher Scientific, Waltham, MA, USA). Tissues were fixed in 4% paraformaldehyde in PBS on the slides for 20 min at 4°C. Slides were then rinsed and equilibrated with 0.2M sodium acetate buffer (pH 4.5). Each slide was covered with the histochemical solution overnight at 37^0C in a humidified chamber. Slides were rinsed with water, counterstained with Nuclear Fast Red (Sigma-Aldrich, St. Louis, MO, USA), and coverslipped.

Brain and Spinal Cord processing and histological analysis

Brain processing and analysis was performed as previously described (Macauley et al, 2012). Briefly, brains from treated and control mice were removed and fixed for 24 hr in 4% PFA in PBS. They were then cryoprotected in 30% sucrose in TBS. Brains were sectioned at 40 micrometers and immunostained for GFAP and CD68, or Nissl. Spinal cords were processed as described in Nelvagal et al, (in preparation). Briefly, spinal cords were removed from treated and control mice, fixed for 24 hr in 4% PFA in PBS, followed by cryoprotection in 30% sucrose. Sections were cut at 40 micrometers and stained with Cresyl Fast Violet (Nissl staining) and immunostained for GFAP and CD68. Regional volumes were calculated as previously described (Kuhl et al, 2013). Briefly, whole volumes and gray matter were measured in 24 sequential

sections. Using the Cavelieri estimation, whole cord volumes and whole gray matter volumes were estimated.

Cytokine Profile Analysis

Cytokine profiling was performed using an Affymetrix multiplex assay through the Center for Human Immunology and Immunotherapy Programs (CHiiPS) Immunomonitoring Lab (IML) at Washington University School of Medicine. Nine analytes (GRO-α, IFN-γ, IL-10, IP-10, MCP-1, MCP-3, MIP-2, RANTES, and TNF- α) were measured in brain homogenates of treated animals. Treated mice were perfused with PBS prior to removal of the brain. Half of the brain was flash frozen and homogenized in 10mM Tris (pH 7.5) 150mM NaCl, 0.2% Triton X-100, and 1mM DTT, as previously described (Macauley et al, 2014). The homogenate was spun at 14,000xg for 1 min, and the supernatant was isolated. Proteinase inhibitor cocktail (P2714, Sigma, St. Louis, MO) and PMSF (17 µg/ml, Sigma, St. Louis, MO) were added to the supernatant. Samples were flash frozen. For the assay, samples were thawed on ice and centrifuged to remove particulates. Samples were then diluted to 10mg of protein/ml. Diluted samples were further diluted 1:2 in PBS with premixed beads. The plate was incubated overnight on a shaker at 4C. The Affymetrix multiplex plate was run and the data was reported as pg/ml.

Statistical analysis

Statistical analyses were performed using two-way or one-way ANOVA utilizing the GraphPad Prism Software. Statistical significance is achieved at $p < 0.05$.

Results

Intracranial AAV2/9-hPPT1 is superior to AAV2/5-hPPT1.

Previous studies have shown that intracranial administration of AAV2/5-hPPT1 significantly improves the lifespan and motor function in the murine model of INCL (Macauley et al, 2012; Macauley et al, 2014; Roberts et al, 2012). Recently, the AAV2/9 vector has been utilized in CNS-related disorders due to its improved distribution and transduction efficiency (Dayton et al, 2012; Foust et al, 2009). Both IC-AAV2/5 and IC-AAV2/9 treated animals had a significant ($p < 0.001$) increase in lifespan compared to untreated PPT1-/- animals. Untreated PPT1-/- mice have a median lifespan of 8.4 months. A direct comparison between IC-AAV2/5 and IC-AAV2/9 administration showed a significant ($p < 0.001$) improvement in median lifespan of IC-AAV2/9 animals (13.5 months) compared to IC-AAV2/5 animals (10.6 months) (Figure 1A). Treatment with IC-AAV2/5 or IC-AAV2/9 significantly increased PPT1 enzyme activity levels in the brain to >50% normal (Figure 1B). There was also a reduction of histological markers of disease in the brains of both groups (data not shown, Figure 1C).
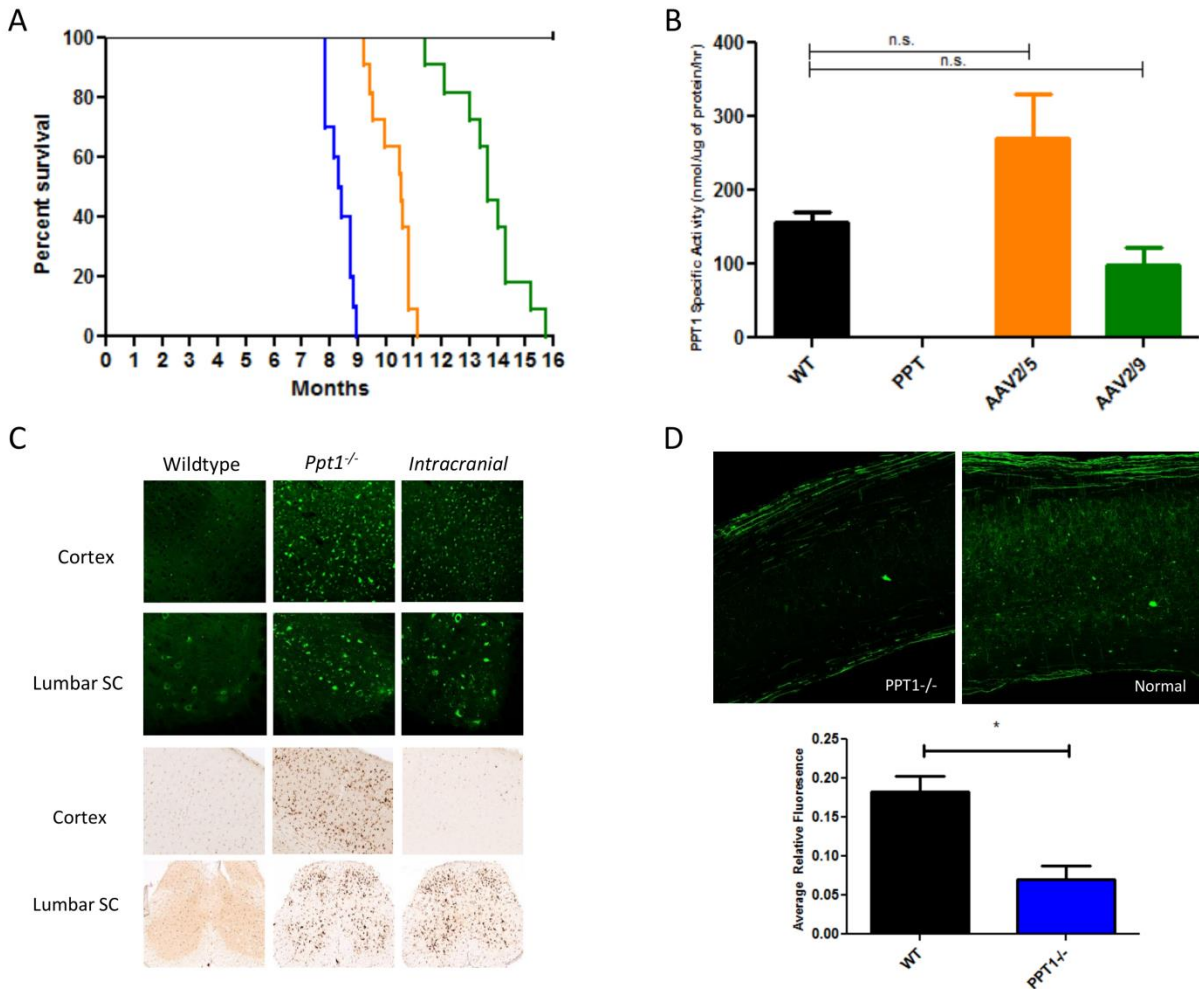
Figure 1. AAV2/9 is superior to AAV2/5 but does not correct the spinal cord. A) Median lifespan of PPT1-/- (8.4 months, blue), IC-AAV2/5 (10.6 months, orange), IC-AAV2/9 (13.7 months, green), and wildtype mice (black). B) PPT1 activity in the terminal brains of IC-AAV2/5 and IC-AAV2/9 mice (n> 3/group. C) Spinal cord and cortical histology from PPT1-/-, WT, and IC-AAV2/9 for AFSM (top) and CD68 (bottom). D) Confocal images of axonal loss in spinal cords of PPT1-/- mice. Comparison of Thy1-YFP-PPT1-/- lumbar spinal cord (left) and Thy1-YFP-PPT1+/- lumbar spinal cord (right). Mean relative fluorescence (*p=0.013).

Spinal Cord disease in IC-treated PPT1-/- animals

Although there was an increase in PPT1 activity to >50% normal levels, the increase in lifespan was modest. Therefore, a more thorough examination of the treated-animal's central nervous system was conducted. Examination of spinal cord from AAV2/9-PPT1 treated animals revealed widespread autofluorescent storage material that was comparable to age-matched PPT1-

/- mice (Figure 1C). There was also increased microgliosis (CD68) in the treated groups. To confirm the presence of spinal cord disease, a Thy1-YFP PPT1-/- reporter mouse model was utilized (Castelvetri et al, 2011; Feng et al, 2000). Axonal blebs and gross axonal degeneration at 7 months are detectable in the INCL spinal cord. There was a significant decrease in axonal fluorescence in the lumbar spinal cord of PPT1 deficient mice compared to wildtype (Figure 1D). These data identified a previously unknown site of disease and uncovered a potential new therapeutic target.

Spinal Cord Pathology in INCL

Spinal cord pathology has not been characterized in models of INCL animals, and only one study has previously reported the possibility of spinal cord disease in INCL patients (Santavuori et al, 1974). A temporal examination of the spinal cord from PPT1-/- and WT mice revealed a progressive increase in AFSM in the cervical, thoracic, and lumbo-sacral regions (Figure 2). A temporal examination of total volume of the spinal cord showed that PPT1-/- mice had significantly decreased spinal cord volumes compared to wildtype beginning at two months. The difference in volume increases until 3 months then the difference in total volume remains essentially constant from three to seven months (Figure 3B, left). Grey matter volume in the PPT1-/- mouse was significantly decreased compared to wildtype grey matter volume beginning at two months and continues until seven months (Figure 3B, center). The white matter volume is significantly decreased in the PPT1-/- spinal cord compared to wildtype from two to seven months (Figure 3B, right).

Histopathological markers of disease were analyzed in the PPT1-/- spinal cords. There was progressive astrocytosis in both the ventral and dorsal horns of the spinal cord in all three

regions (cervical, thoracic, and lumbo-sacral) analyzed. There was a significant increase in

GFAP staining beginning at two months with the percent immunoreactivity increasing until

seven months (Figure 4A, B). Similarly, there was progressive microgliosis in the dorsal and

ventral horns in all regions of the spinal cord analyzed. There was a significant increase in CD68

staining beginning at two months and progressively increasing until seven months (Figure 5A,

B).
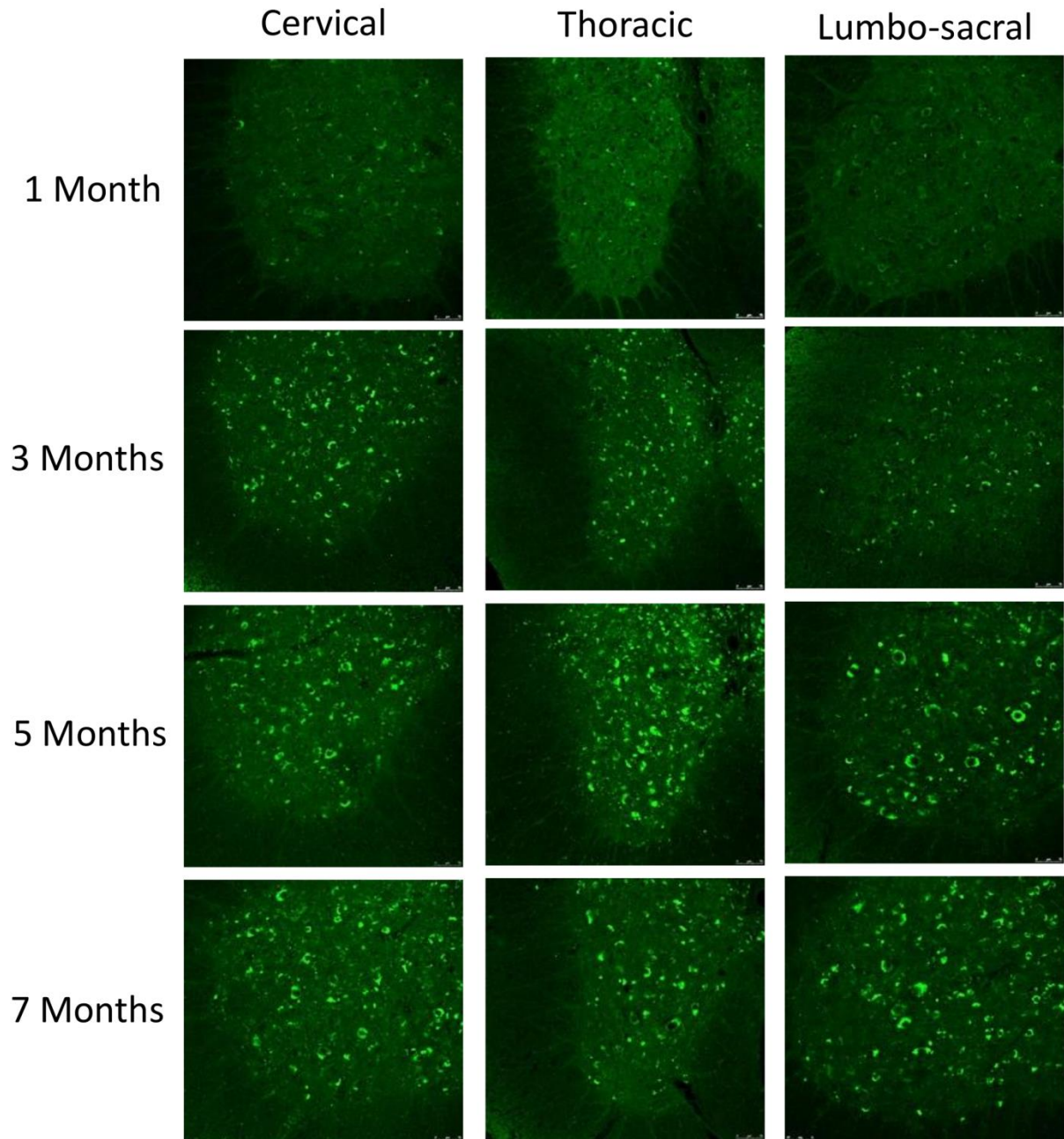
Figure 2. Progressive accumulation of autofluorescent storage material. AFSM in the cervical (left column), thoracic (middle column), and lumbo-sacral (right column) regions at 1, 3, 5, and 7 months.
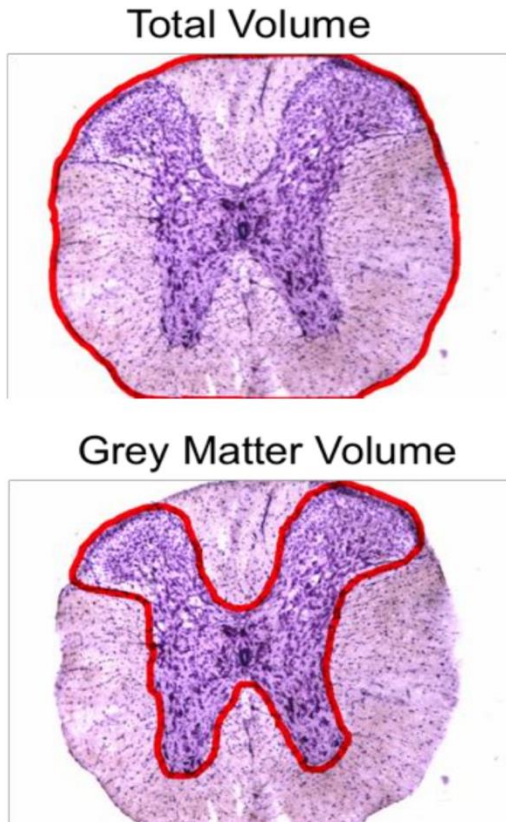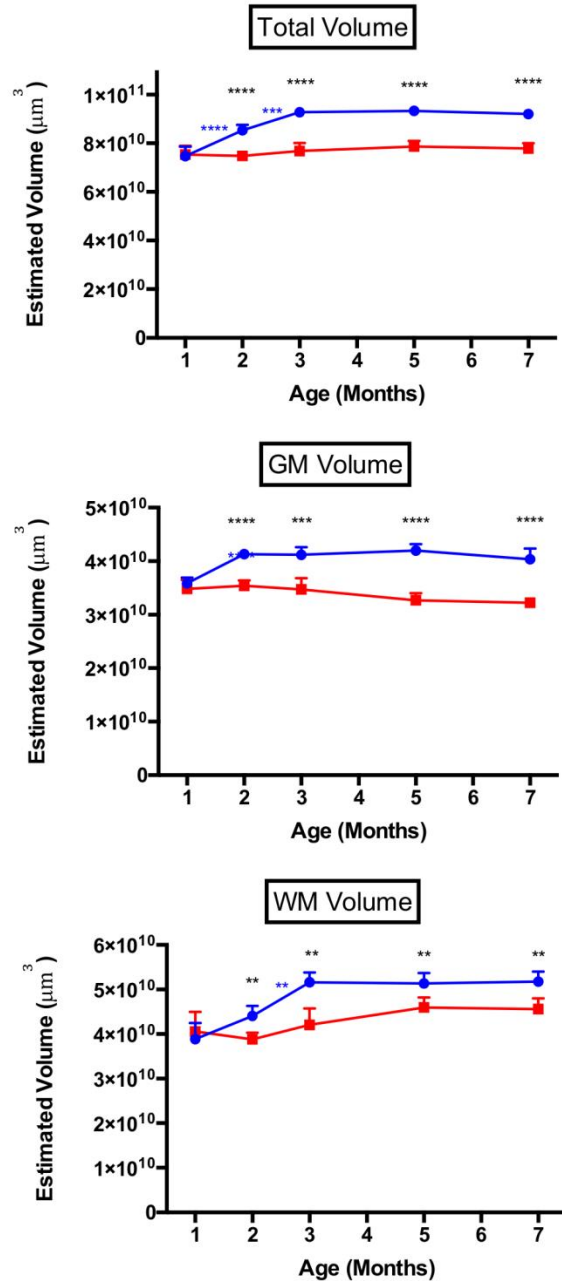
Figure 3. Regional Volume measurements of PPT1-/- spinal cords. A) Diagram for determining total (left) and grey (right) matter volume (outlined in red). White matter volume is determined by subtracting grey matter from total volume. B) Estimated volume for total (left), grey (center), and white (right) matter volumes between PPT1-/- (red) and WT (blue) spinal cords over time (**p,0.01, *** p<0.001, ****p<0.0001).
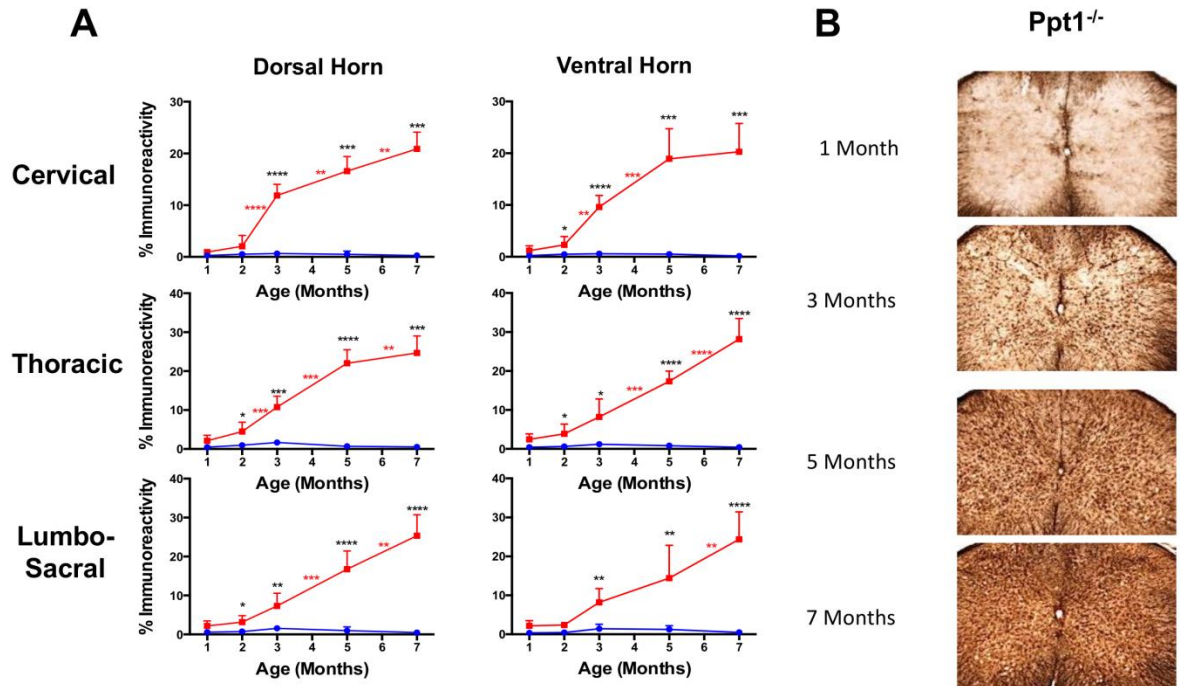
Figure 4. Progressive astrocytosis in the spinal cord. A) Quantitative GFAP staining in the dorsal and ventral horns of PPT1-/- (red) and WT (blue) spinal cords at cervical (top), thoracic (middle), and lumbo-sacral (bottom) regions (**p,0.01, *** p<0.001, ****p<0.0001). B) Image of GFAP staining in the PPT1-/- spinal cord at 1, 3, 5, and 7 months.
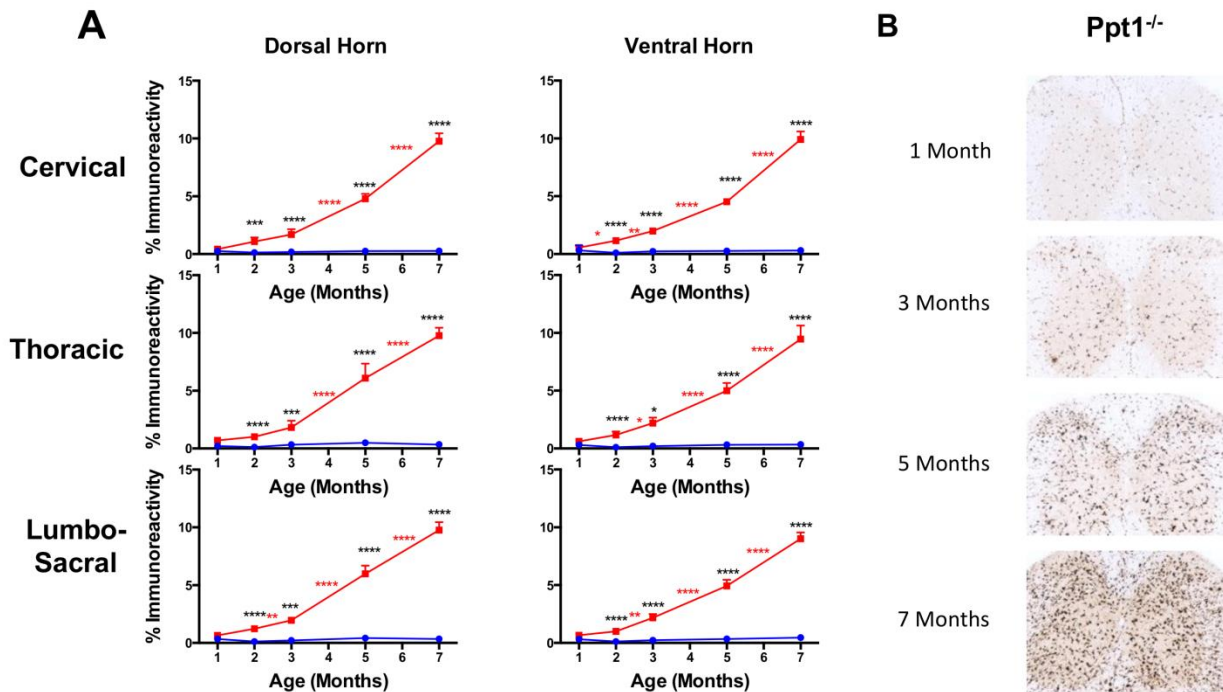
Figure 5. Progressive microgliosis in the spinal cord. A) Quantitative CD68 staining in the dorsal and ventral horns of PPT1-/- (red) and WT (blue) spinal cords at cervical (top), thoracic (middle), and lumbo-sacral (bottom) regions (**p,0.01, *** p<0.001, ****p<0.0001). B) Image of CD68 staining in the PPT1-/- spinal cord at 1, 3, 5, and 7 months.
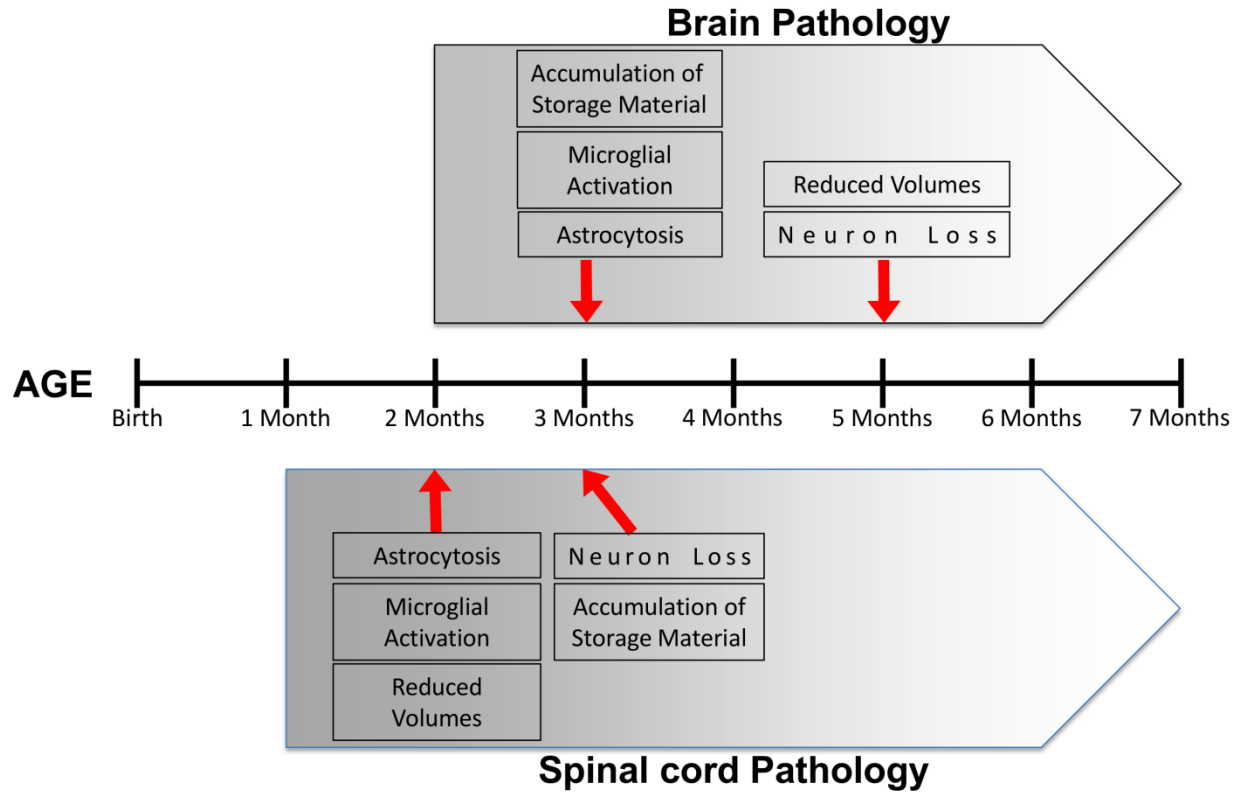
Figure 6. Diagram of temporal pattern of INCL brain and spinal cord pathology

Summary of Brain and Spinal Cord INCL Pathogenesis

As we have shown, there is significant temporal and spatial INCL pathogenesis in the spinal cord. Interestingly, spinal cord pathology precedes the brain pathology and shares many pathological similarities (Figure 6). This is suggestive of regional specificity of INCL progression. For example, significant disease in the thalamus is detectable prior to other regions in the brain (Bible et al, 2004). In the brain, there is an accumulation of AFSM and astrocytosis/microgliosis beginning at 3 months of age (Bible et al, 2004). Following AFSM accumulation and astrocytosis/microgliosis, there is observable neuronal loss and cortical

atrophy. As summarized in Figure 6, in the spinal cord, there is significant astrocytosis/microgliosis and reduced volume beginning at two months. This precedes the neurological disease in the brain by one month. Similarly, neuronal loss precedes INCL disease in the brain. INCL has historically been considered a neurodegenerative disease. However, there is stagnation in spinal cord volume growth suggesting a role for PPT1 in neurodevelopment. Overall, the disease in the spinal cord suggests that this region could be significant in INCL pathogenesis and could be a target for AAV-based gene therapy.

Differential PPT1 activity in the brain and spinal cord following intracranial and intrathecal AAV2/9-hPPT1

In order to determine the significance of the spinal cord disease and whether the spinal cord could be an effective therapeutic target, PPT1-/- mice were treated with intracranial AAV2/9, intrathecal AAV2/9, or a combination of both. Initially, PPT1 activity was measured in the brains and spinal cords of animals treated with IC-AAV2/9 or IT-AAV2/9. When the brain and spinal cord PPT1 enzyme activity levels at one month were examined from IC-AAV2/9 and IT-AAV2/9 mice, PPT1 activity in IC-AAV2/9 brains were significantly higher in the brain than WT (Figure 7A). However, PPT1 activity in the IT-AAV2/9 brains were minimal at approximately 10% of wildtype. This trend was reversed in the spinal cord with supraphysiological levels of PPT1 enzyme activity in IT-AAV2/9 brain but near-PPT1-/- enzyme activity in IC-AAV2/9 mice (Figure 7A).

When determining the temporal patter of expression, PPT1 activity in the wild-type brain was approximately 150 nmol/mg/hr throughout the study. In contrast, PPT1 activity was virtually undetectable in PPT1-/- mice brains throughout the study. IT-AAV2/9 brains had a small

increase in brain PPT1 activity to ~2-5% of wild-type levels. In contrast, IC-AAV2/9 as well as the combination IC/IT-AAV2/9 brains had near wild-type to supraphysiological levels of PPT1 activity (~150-450 nmol/mg/hr)(Figure 7B). Overall, the treatment groups produced a significant ($p < 0.0001$) difference in PPT1 activity between three to seven months (two-way ANOVA). When comparing treatment groups, there was a significant increase in PPT1 activity in the IC-AAV2/9 ($p = 0.0025$), IC/IT-AAV2/9 ($p < 0.0001$), and WT ($p < 0.0001$) brains compared to PPT1-/- brains. IT-AAV2/9 brains had a significant ($p = 0.0001$) albeit small increase in PPT1 activity compared to untreated PPT1-/- brains. There was not a significant difference between the IC-AAV2/9 or IC/IT-AAV2/9 brain PPT1 activities compared to WT ($p = 0.68, 0.12$); however, there was a significant difference between WT and IT-AAV2/9 PPT1 activities ($p < 0.0001$).

A reduction in the secondary elevation of other lysosomal enzymes serves as a biochemical surrogate of therapeutic efficacy (Griffey et al, 2004). Overall, the secondary elevations of β-glucuronidase in the treatment groups and age of the animals were observed to have a significant ($p < 0.0001$) effect in secondary elevations of β-glucuronidase. When comparing treatment groups, there was a significant decrease in β-glucuronidase activity in the IC-AAV2/9 ($p < 0.0001$), IC/IT-AAV2/9 ($p < 0.0001$), and WT ($p < 0.0001$) animals compared to untreated PPT1-/- brains. IT-AAV2/9 brains had a significant ($p = 0.027$) albeit small decrease in β-glucuronidase activity compared to untreated PPT1-/- brains. There was a small but significant increase in β-glucuronidase activity between the IC-AAV2/9 ($p = 0.0002$), IT-AAV2/9 ($p < 0.0001$), IC/IT-AAV2/9 ($p < 0.0001$) brains compared to WT β-glucuronidase activity levels (Figure 7C).

Using a recently developed histochemical stain, the brains of experimental and control animals were analyzed for the distribution of PPT1 activity. The broad, diffuse blue staining

observed in WT brains was not present in the untreated PPT1-/- brain (Figure 8). The IC-

AAV2/9 brains had detectable activity in the cortex and hippocampus with weaker staining in the

thalamus, cerebellum, and other hindbrain regions. In contrast, in the IT-AAV2/9 brains, an

increase in staining in the cerebellum and brainstem was observed with little to no staining in the

forebrain. The IC/IT-AAV2/9 brains had increased staining in both forebrain and hindbrain.

There was still only low levels of PPT1 detected in the thalamus of IC/IT-AAV2/9 treated mice.
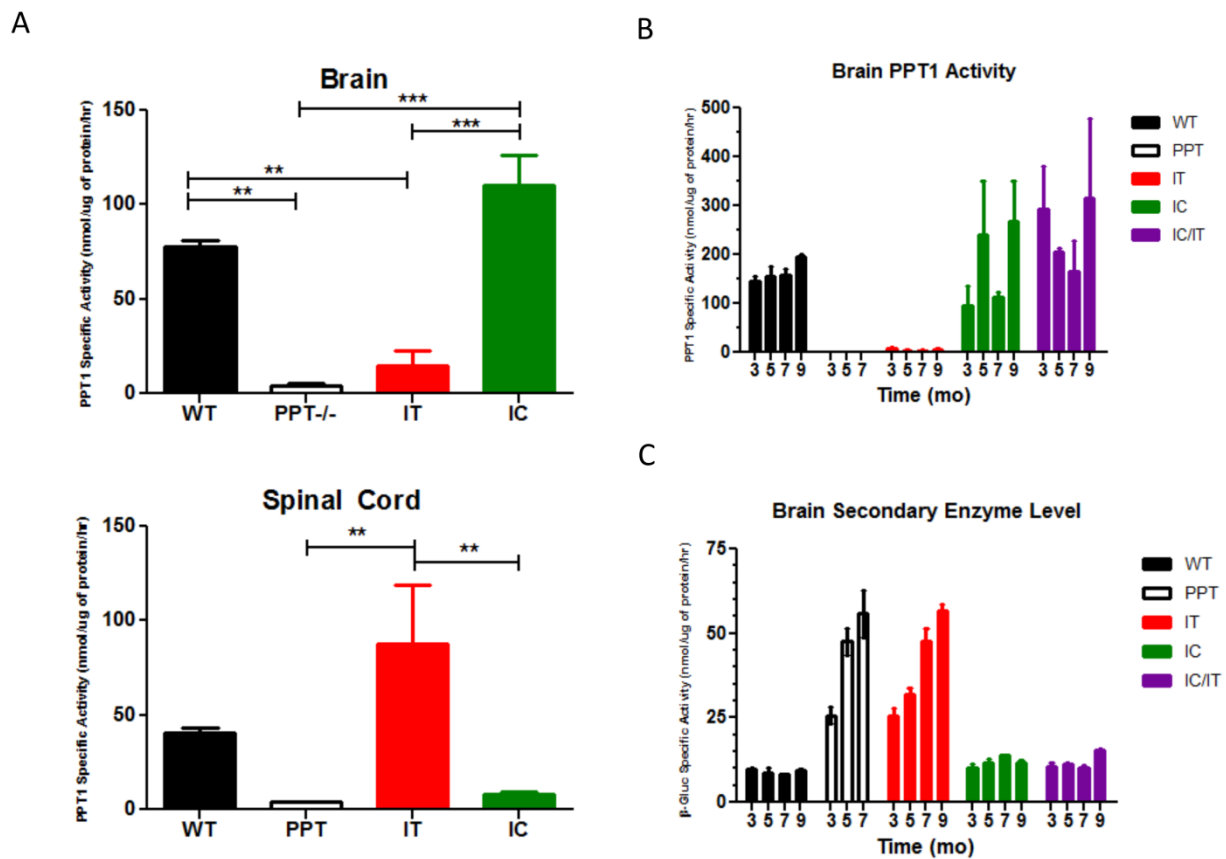
Figure 7. PPT1 and Secondary enzyme activity in treated animals. A) Analysis of PPT1 activity at 1 month in the Brain and Spinal Cord following IT-AAV2/9 and IC-AV2/9 injections. There was reciprocal PPT1 activity between intrathecal and intracranial injections in the brain and spinal cord (**p<0.01, *** p<0.001). B) Temporal analysis of PPT1 activity brain. PPT1 activity was increased in the brain for IC-AAV2/9 and IC/IT-AAV2/9 to near-WT or supraphysiological levels. There was a marginal increase in PPT1 activity in the IT-AAV2/9 brain (approximately 2-5% WT levels). C) Secondary enzyme levels were normalized in the brain. β-glucuronidase levels are increased in the untreated PPT1-/- and IT-AAV2/9 brains. IC-AAV2/9 and IC/IT-AAV2/9 brains have near WT levels of β-glucuronidase.
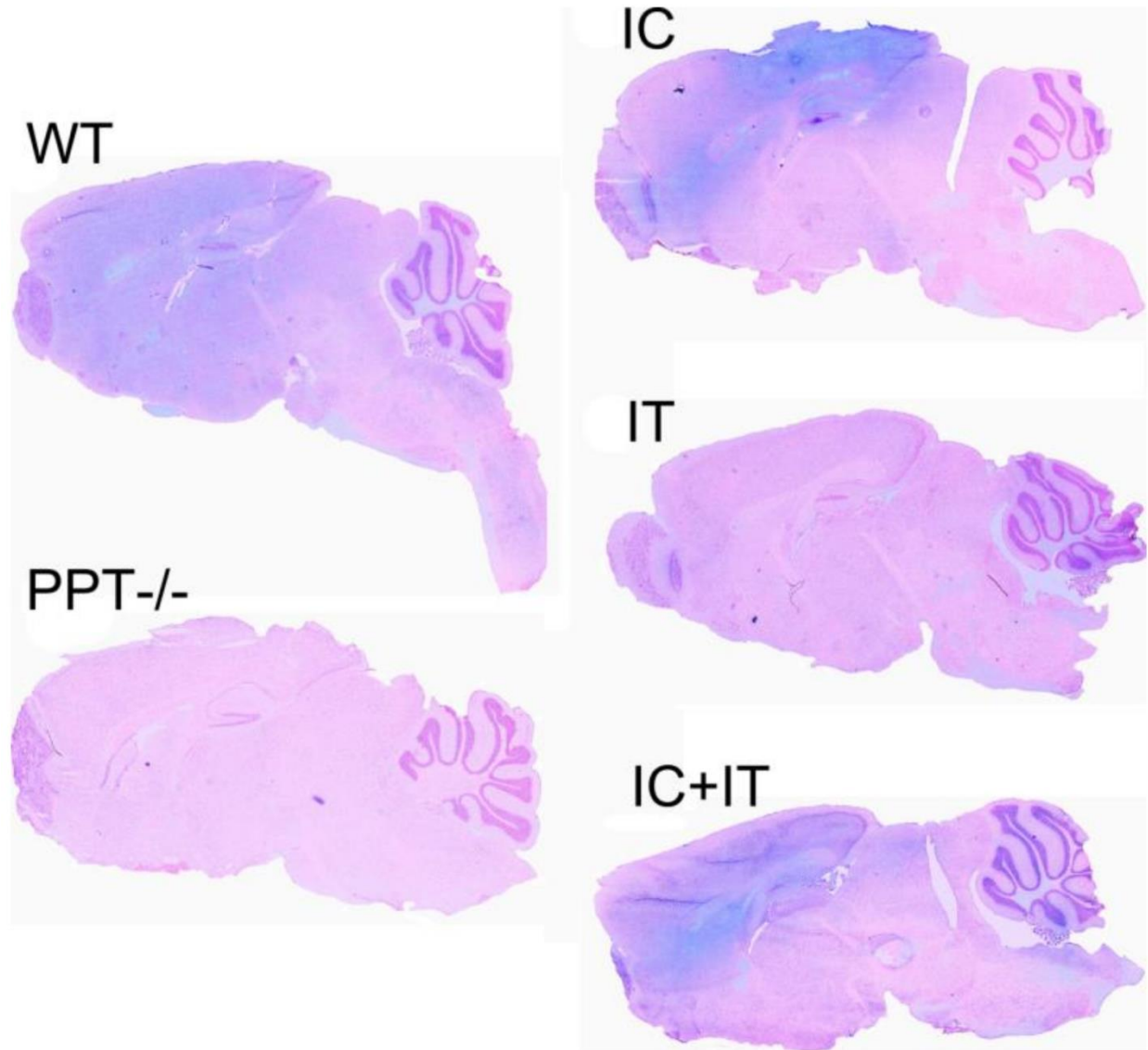
Figure 8. Histochemical Stain for PPT1 activity. PPT1 activity is depicted in blue. Sections were counterstained with nuclear fast red (red).

Intracranial and Intrathecal AAV2/9-hPPT1 reduce histological markers of INCL

The accumulation of autofluorescent storage material, the histological hallmark of NCL, was measured in all the experimental and control animals (Figure 9). A significant increase in AFSM was observed in the PPT1-/- brain and spinal cord compared to wildtype. Following intracranial administration, there was a significant decrease in AFSM in the M1 (motor cortex) and in the VPM/VPL (thalamus), and no decrease in the spinal cord. In contrast, intrathecal

administration led to a reduction of AFSM in the spinal cord but not in the brain. Consistent with

the biochemical and histochemical data, when the brain and spinal cord were simultaneously

targeted, there was a significant reduction in AFSM in the M1, VPM/VPL, and the spinal cord.
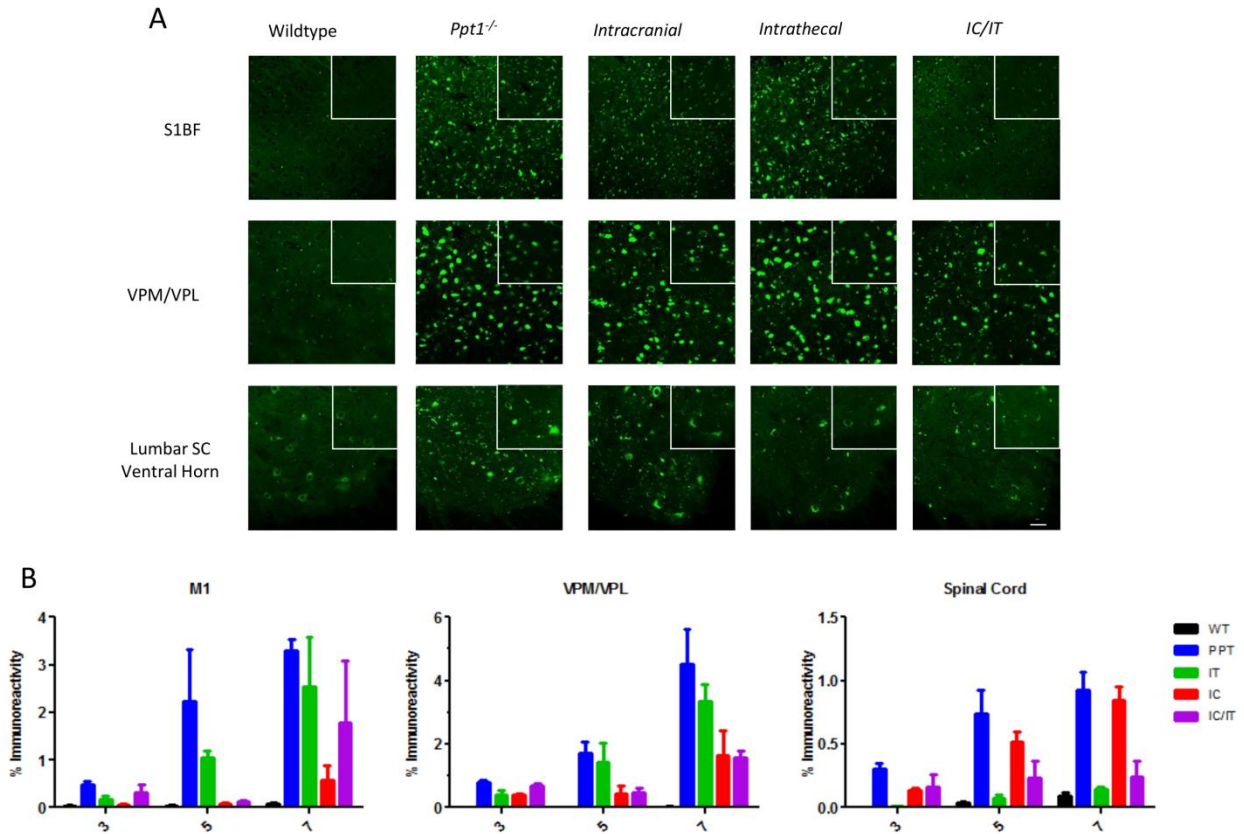
Figure 9. Autofluorescent storage material is reduced in the combination treated animals.
A) Representative images of AFSM in treated animals. Autofluorescent storage material was
examined in the S1 barrel field (S1BF) of the somatosensory cortex (top), the VPM/VPL of the
thalamus (middle), and the ventral horn of the lumbar spinal cord (bottom) of the treated
animals. B) Quantitative graph of AFSM over time examining the M1 of the motor cortex,
VPM/VPL of the thalamus, and the lumbar spinal cord.

IC-AAV2/9 and IC/IT-AAV2/9 decrease cortical atrophy

Profound brain atrophy is another hallmark of INCL. Cortical thickness (Figure 10A) and

brain weight (Figure 10B) were measured as an indicator of brain atrophy. The PPT1-/- brain

significantly decreases in weight from 3 months to 7 months when compared to wildtype. The

decreasing brain weight was reflected in the significant thinning of the PPT1-/- cortices compared to the WT. The IC-AAV2/9 and the IC/IT-AAV2/9 cortices did not show significant cortical thinning or a reduction in brain weight as compared to wildtype. However, IT-AAV2/9 PPT1-/- mice had significant thinning of the cortices, and a progressive decrease in brain weight similar to that of untreated PPT1-/-mice. The brains of the IT-AAV2/9 and untreated PPT1-/- mice are not significantly different at any time point measured. Overall, both the age of the animals and the treatment groups had a significant (p<0.0001) effect on the brain mass. When comparing treatment groups, there was a significant increase in brain weight in the IC-AAV2/9 (p<0.0001), IC/IT-AAV2/9 (p<0.0001), and WT (p<0.0001) animals compared to PPT1-/- brains. IT-AAV2/9 brains had a significant (p=0.032) albeit small increase in brain weight compared to PPT1-/- animals. There was no difference between the IC/IT-AAV2/9 brain weights compared to WT (p=0.862); however, there was a significant albeit small decrease in brain weight between IC-AAV2/9 (p=0.040) and WT brains. There was a significant difference between WT and IT-AAV2/9 PPT1 brain weights (p<0.0001).
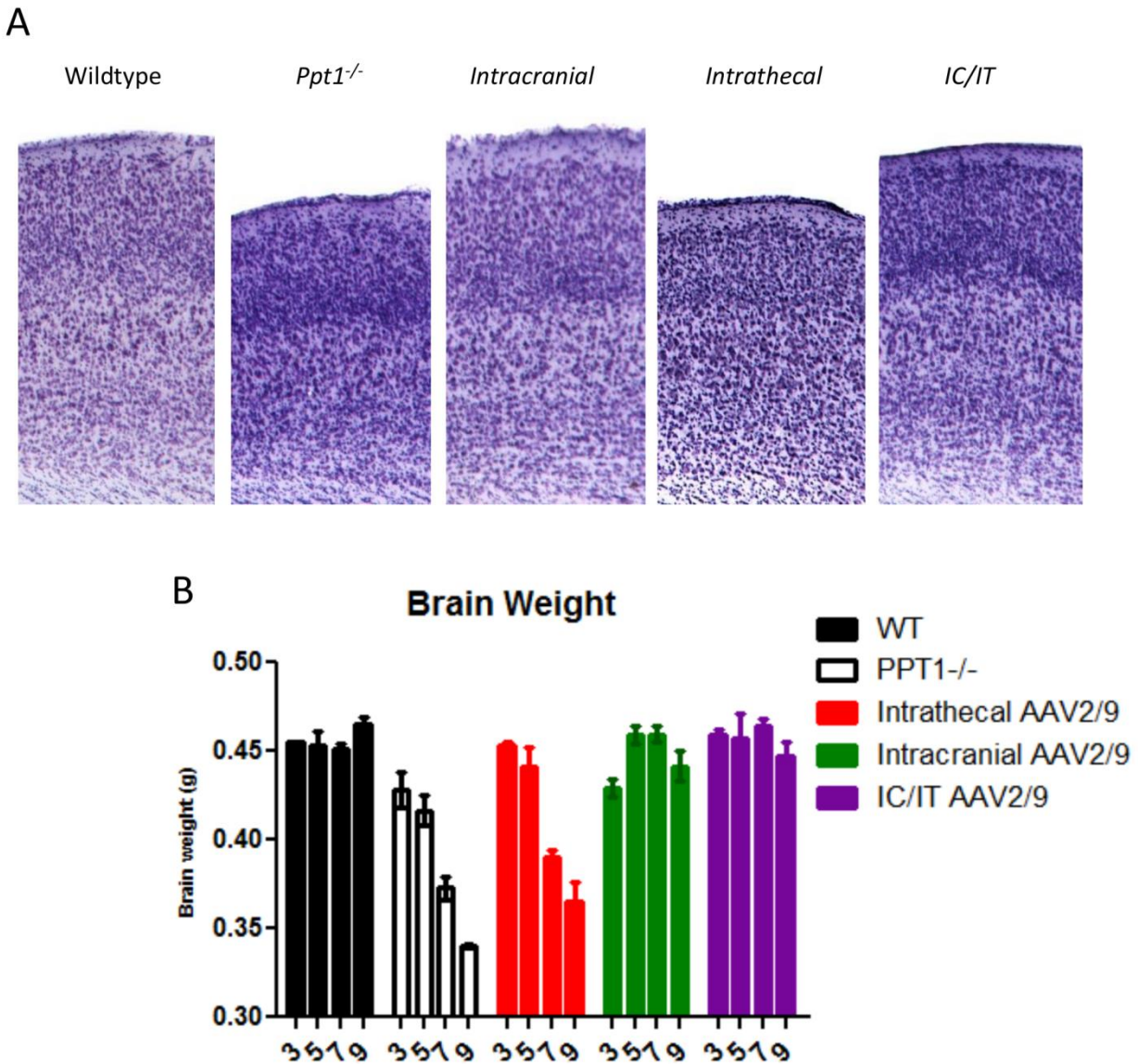
Figure 10. Cortical atrophy and brain mass is normalized in the combination therapy. A) Representative images of cortices from treated animals. Sections were stained with Nissl. B) Brain weight from treated animals over time. Brain weights for IC-AAV2/9 and IC/IT-AAV2/9 brains were essentially normal at all time points examined. IT-AAV2/9 showed a significant reduction in brain weight compared to WT brain weight at 7 and 9 months.

Combination therapy reduces neuroinflammation in brain and spinal cord

Progressive astrocytosis and microgliosis are prominent features of INCL (Kielar et al, 2007). A significant increase in CD68 and GFAP staining in the PPT1-/- brain and spinal cord was observed compared to wildtype (Figure 11A, B & 12A, B). In IC-AAV2/9 brains, there was

a significant decrease in CD68 and GFAP staining in the M1 of the motor cortex and the VPM/VPL of the thalamus. There was no decrease in CD68 or GFAP staining in the IC-AAV2/9 spinal cord. In contrast, in IT-AAV2/9, CD68 and GFAP staining were decreased in the spinal cord but not in the brain. Similar to the accumulation of AFSM, when the brain and spinal cord were simultaneously targeted, there was a reduction in CD68 and GFAP staining in all regions examined: M1 of the motor cortex, VPM/VPL of the thalamus, and the lumbar spinal cord.

Cytokine and chemokine levels in brain homogenates of treated mice and controls were measured as a complementary indicator of neuroinflammation. It had been previously shown in INCL that there is an increase in cytokine and chemokine production as the disease progresses (Macauley et al, 2011; Qiao et al, 2007). There were no significant differences in the levels of tumor-necrosis factor-α (TNF-α) or interferon-γ (IFN-γ) between any of the groups (Figure 13A). In both the CXC motif and CCL motif chemokines, there was a significant increase in PPT1-/- brains compared to wildtype brains. Neither IC-AAV2/9 nor IT-AAV2/9 alone significantly reduced chemokine levels below that of PPT1-/- brains. There was a slight increase above PPT1-/- chemokine levels for IT-AAV2/9 mice in CXCL1, CXCL10, CCL2, and CCL7. In the brains of IC/IT-AAV2/9 PPT1-/- mice, there was a significant decrease in all cytokines and chemokines to near wildtype levels (Figure 13B, C).
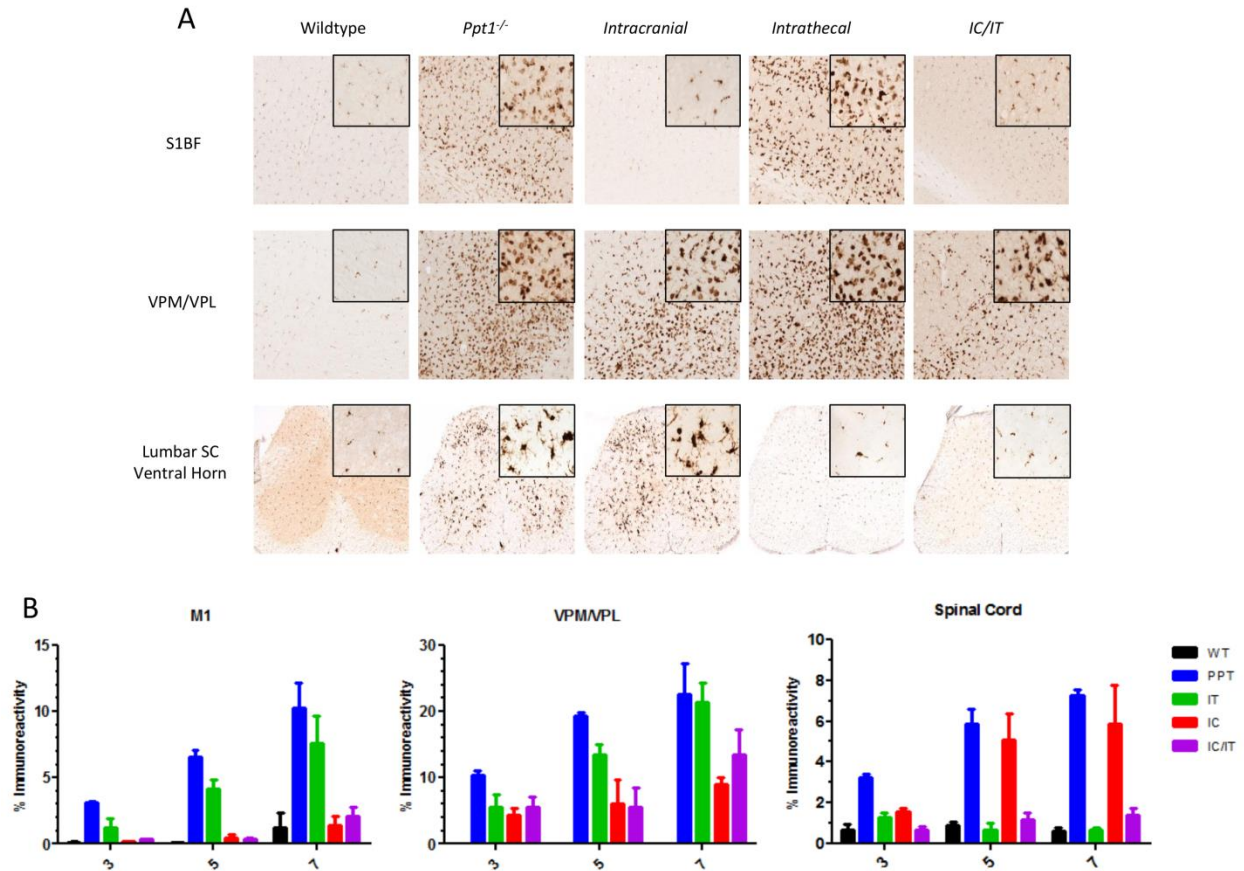
Figure 11. Microgliosis is reduced in the combination treated animals. A) Representative images of CD68 staining in treated animals. CD68 staining was examined in the S1 barrel field (S1BF) of the somatosensory cortex (top), the VPM/VPL of the thalamus (middle), and the ventral horn of the lumbar spinal cord (bottom) of the treated animals. B) Quantitative graph of CD68 over time examining the M1 of the motor cortex, VPM/VPL of the thalamus, and the lumbar spinal cord.
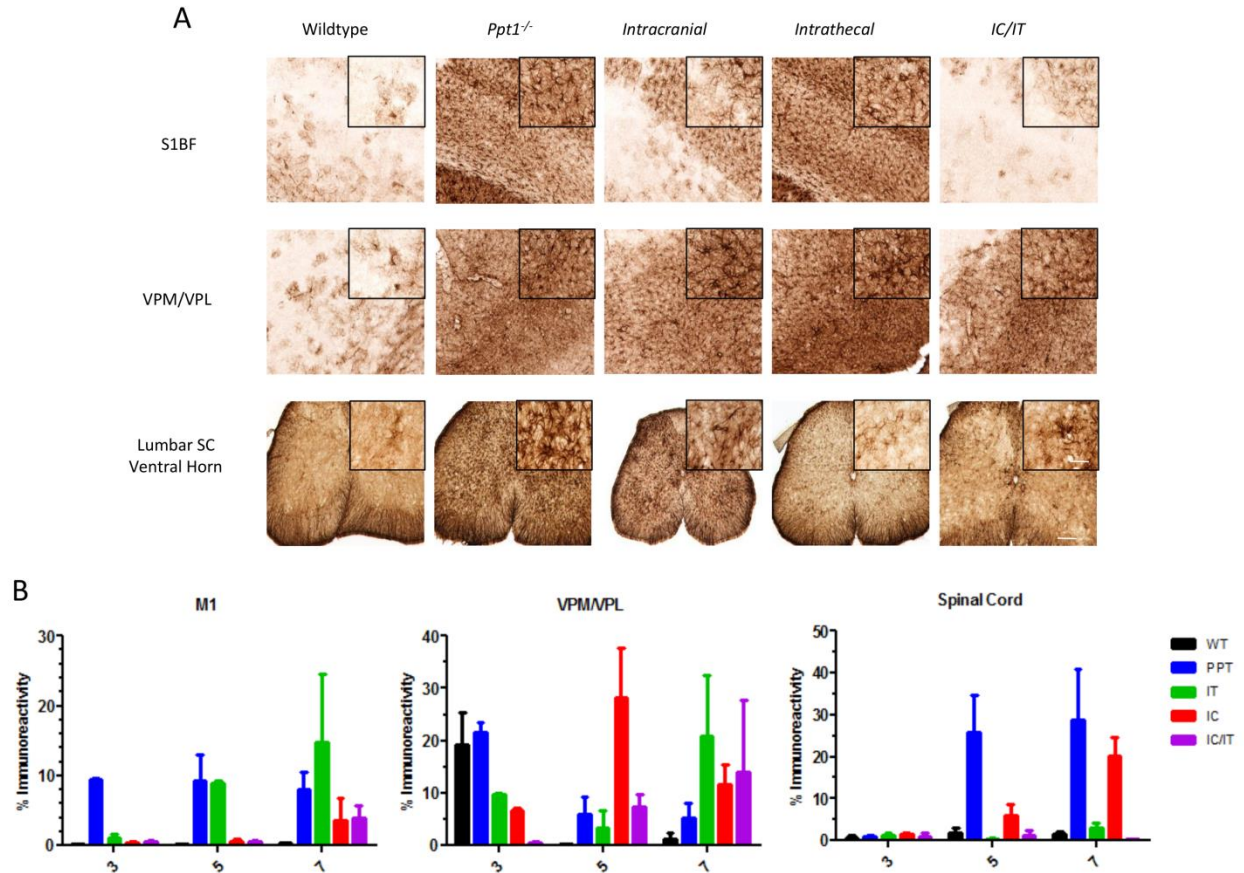
Figure 12. Astrocytosis is reduced in the combination treated animals. A) Representative images of GFAP staining in treated animals. GFAP staining was examined in the S1 barrel field (S1BF) of the somatosensory cortex (top), the VPM/VPL of the thalamus (middle), and the ventral horn of the lumbar spinal cord (bottom) of the treated animals. B) Quantitative graph of GFAP over time examining the M1 of the motor cortex, VPM/VPL of the thalamus, and the lumbar spinal cord.
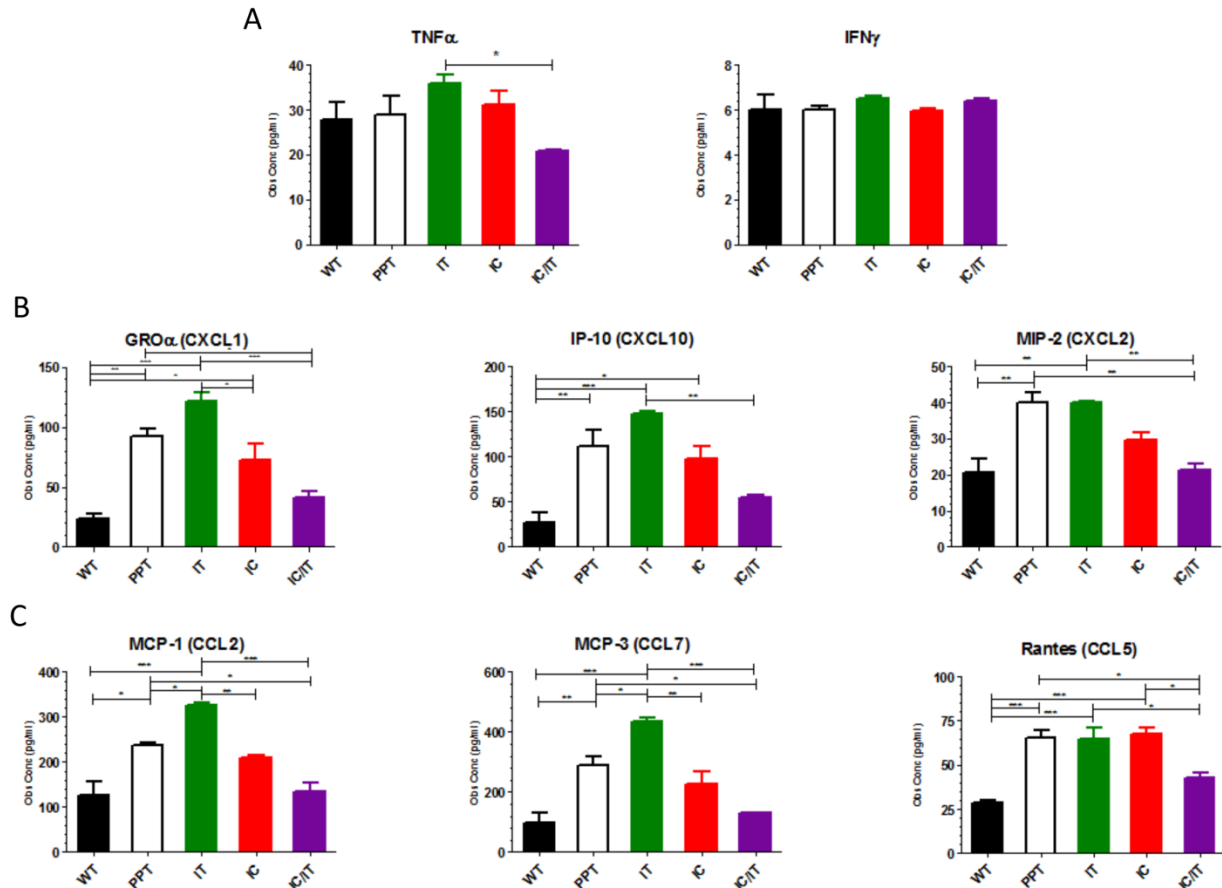
Figure 13. Cytokine analysis of treated animals at 7 months. A) Pro-inflammatory cytokines. B) CXC motif chemokines. C) CC motif chemokines. There were no significant differences in TNFα (with the exception of IT-AAV2/9 vs IC/IT-AAV2/9) or IFNγ between any of the groups. There was a significant ($p<0.05$) increase in CXC and CC motif chemokines in PPT1-/- and IT-AAV2/9. The IC-AAV2/9 chemokine levels had a trend towards normalization to wildtype levels except in RANTES. The IC/IT-AAV2/9 chemokine levels were not significantly different from wildtype.

Improvements in Motor function and Longevity

Gross motor function and longevity are robust endpoints used to score the therapeutic efficacy of treatments in the INCL mouse. Gross motor function was measured by the latency for INCL mice to fall off the rotarod. Wild-type mice remained on the rotarod for 60 seconds for the duration of the study (Figure 14A). Untreated PPT1-/- mice displayed significant motor deficits starting at 5 months and fell off the rotarod at 7 months with an average latency of ~10 seconds.

After 7 months, the untreated PPT1-/- mice were unable to stay on the rotarod. Although IT-AAV2/9 mice had significantly improved motor function, they began to fall off the rotarod at 7 months with an average latency to fall of 48 seconds and continued to decline until 11 months (latency ~18 seconds). IC-AAV2/9 mice had significantly improved motor function compared to IT-AAV2/9 animals. IC-AAV2/9 mice began to fall off the rotarod at 9 months with an average latency to fall of ~58 seconds and continued to decline until 13 months (~14 seconds). The combination IC/IT AAV2/9 mice had significantly improved motor function compared to either IC-AAV2/9 or IT-AAV2/9 mice and displayed significant motor deficits starting at 15 months with an average latency of ~50 seconds. The average latency remained constant at 17 months but declined at 19 months to ~40 seconds. By 21 months, the remaining IC/IT-AAV2/9 mice were unable to stay on the rotarod (Figure 14A).

Untreated PPT1-/- mice had a median lifespan of 8.4 months (Figure 14B). IT-AAV2/9 mice have a significant extension in median lifespan to 11.8 months and the IC-AAV2/9 mice had a median lifespan of ~13.6 months. The IC/IT-AAV2/9 mice had a dramatic and significant extension in median lifespan to 19.3 months, with the longest-lived mouse at 22 months. Only one WT mouse died during the study with the remaining staying alive until the end of the study (~24mo).
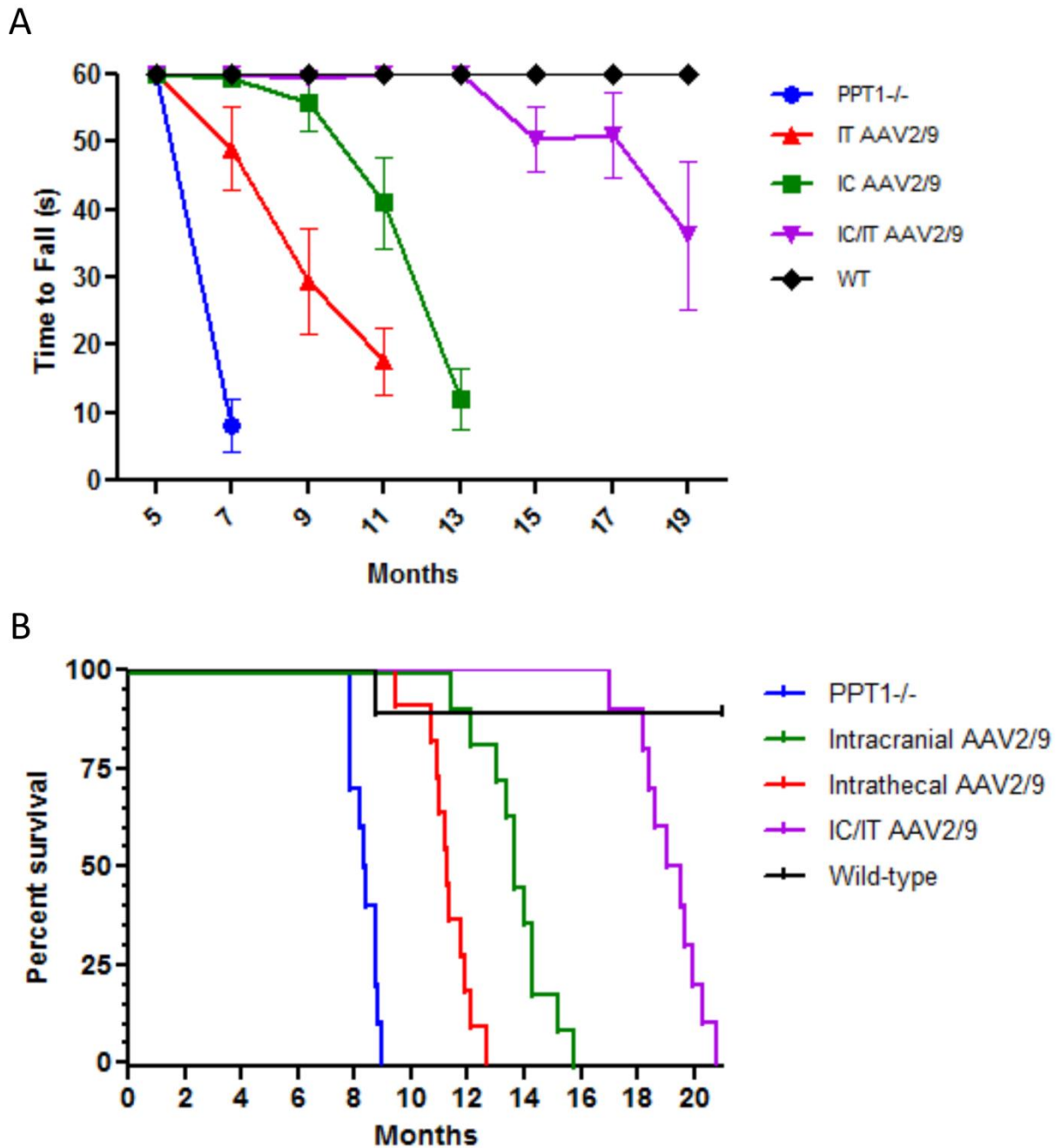
Figure 14. Functional and behavioral phenotype is improved with the combination therapy.
A) Rotarod test for motor function. The PPT1 -/- mice (blue) were unable to stay on the rotarod past 7 mo. IT-AAV2/9 mice (red) showed motor deficits at 7 month and could not stay on past 11 mo. The IC-AAV2/9 mice (green) showed deficits at 9 mo and could not stay on past 13 mo. The combination IC/IT-AAV2/9 mice (purple) showed deficits at 15 mo and could not stay on past 19 mo. B) Lifespan curve. The median lifespan for PPT1-/- mice (blue) was 8.4 mo. IT-AAV2/9 mice (red) had an extension in lifespan of 11.3 mo (+3 mo). IC-AAV2/9 mice (green) had an extension in lifespan of 13.7 mo (+5.3 mo). The combination IC/IT-AAV2/9 mice (purple) had an extension in lifespan of 19.3 mo (+11.5 mo).

Discussion

To date, pre-clinical gene therapy studies for INCL have focused on the delivery of PPT1 to the brain (Griffey et al, 2004; Griffey et al, 2006; Macauley et al, 2012; Macauley et al, 2014; Roberts et al, 2012). Gene therapy studies utilizing a second-generation AAV vector (AAV2/5) have shown that persistent delivery of PPT1 can significantly extend the lifespan, decrease histological markers of disease and improve motor function in INCL mice (Macauley et al, 2012; Macauley et al, 2014; Roberts et al, 2012). In the current study, we show that the third-generation AAV vector, AAV2/9, is superior to AAV2/5. Intracranial injection of AAV2/9-hPPT1 nearly normalized PPT1 activity, and reduced the secondary elevations of another lysosomal enzyme in the brain. However, IC-AAV2/9 mice still had a significantly shortened lifespan compared to their wild-type littermates. We hypothesized that the distribution of PPT1 was not sufficient to treat the entire CNS.

A more thorough analysis of the CNS from a separate cohort of IC-AAV2/9 mice showed no reduction of AFSM accumulation or neuroinflammation in the spinal cord. The persistent spinal cord disease could partially explain the limited efficacy in this and other studies when gene therapy was limited to the brain. This study and previous studies have shown that the brain mass of PPT1-/- mice receiving intracranial injection of an AAV vector does not significantly decrease until near terminal; whereas the brain mass of PPT1-/- animals begin decreasing at 5 months of age (Macauley et al, 2014; Roberts et al, 2012). This suggests that the spinal cord disease may play a significant role in the overall pathogenesis of INCL. The neurological disease observed in the spinal cord of treated PPT1-/- mice is corroborated by the appearance of axonal blebs and axonal degeneration using the Thy1-YFP PPT1-/- reporter mouse. The Thy1-YFP-PPT1-/- reporter model will be a useful tool for the characterization of INCL spinal cord disease and for evaluating efficacy.

A comprehensive temporal and spatial examination of the PPT1-/- murine spinal cord showed progressive AFSM accumulation and neuroinflammation beginning at 2 months of age (Nelvagal et al, in preparation). The disease in the spinal cord affects both the grey matter and white matter tracts. Interestingly, the total volume of the spinal cord in PPT1-/- animals stayed constant from one month to seven months whereas the wildtype volumes increased. This trend was similar for both the grey and white matter volumes. This suggests a potential neurodevelopmental defect in the PPT1-/- animals that has not been previously characterized. In the characterization of the INCL spinal cord pathology, astrocytosis and microgliosis were significantly increased beginning at two months of age. This precedes the onset of disease in the brain which begins at three months of age (Kielar et al, 2007). This finding redefines the age of onset for INCL CNS pathology (Figure 6). Collectively, these data suggest that the spinal cord could be an effective therapeutic target. Interestingly, a previous study showed that intrathecal injections of recombinant PPT1 over three consecutive days was able to extend the lifespan, improve motor function, and modestly decrease histological signs of disease in the spinal cord (Lu et al, 2015). It is possible that some of the efficacy was due to decreasing the spinal cord disease.

Based on these data, we performed a more comprehensive study targeting the spinal cord alone and in combination with brain-directed gene therapy. Similar to previous studies, intracranial AAV mediated gene therapy using an AAV2/9 vector resulted in significantly increased longevity, improved motor function, and decreased pathology in the brain. We discovered that there was no improvement observed in the spinal cord disease following brain-directed gene therapy. While intrathecal AAV2/9 gene therapy alone resulted in decreased pathology in the spinal cord, a significant extension in lifespan, and improved motor function,

the pathology in the brain was not improved. These results are consistent with the reciprocal pattern of enzyme activity in those areas. This small increase in enzymatic activity in the brain following intrathecal injection is not surprising given the limited distribution of AAV2/9 when delivered intrathecally (Schuster et al, 2014).

Surprisingly, no significant differences in cytokine or chemokine levels in the brain between the intracranial treated animals and their PPT1-/- littermates were detected even though there was a decrease in CD68 and GFAP staining. Cytokine and chemokine levels were measured in whole brain homogenates. Both the intracranial and intrathecal injections target specific regions of the CNS. Therefore, INCL disease is still progressing in the CNS regions not targeted by either therapy. It is plausible that cytokines/chemokines from the unresponsive regions distribute throughout the brain. Not surprisingly, there were no decreases in cytokine/chemokine levels in IT-AAV2/9 brains. Cytokine and chemokine levels were only decreased when both the brain and spinal cord were targeted. This is consistent with the biochemical and histological findings.

The different clinical responses of animals treated with either IC- or IT-AAV2/9 provide important insights into the progression of INCL. As mentioned above, the significance of the spinal cord disease to the overall pathogenesis was not known. IT-AAV2/9 corrects much of the pathology in the spinal cord but has little effect on the brain. The fact that motor function was improved and the lifespan was increased when histological correction was limited to the spinal cord suggests that this aspect of INCL is clinically significant. However, it is unclear if IT-AAV2/9 resulted in correction of other, yet unknown, aspects of INCL as well. For example, it is not known if INCL affects the peripheral nervous system (PNS). Intrathecal injection of AAV vectors has been shown to deliver transgene products to the sciatic nerve (Federici et al, 2012;

50

Jacques et al, 2012; Schuster et al, 2014; Vulchanova et al, 2010). It is possible that IT-AAV2/9 is affecting the PNS in INCL. These data also demonstrate that the brain is the most severely and acutely affected region of the CNS, since limiting therapy to the brain is clearly more effective than targeting the spinal cord.

When the intracranial and intrathecal injections are combined, there is a dramatic and significant extension in lifespan and improvement in motor function compared to either therapy alone. This is most likely due to the broader distribution of the AAV-hPPT1 vector in the CNS. Taken together, these data suggest that it will be necessary to treat both the spinal cord and brain disease to achieve maximum efficacy. Interestingly, these data also show that targeting both regions results in synergistic improvements. For example, if the modalities were simply additive, the extension in lifespan would be approximately 16.7 months rather than the 19.3 months observed. Similarly, the improvement in motor function also suggests a synergistic effect. The age at which IC/IT-AAV2/9 mice begin to fall off the rotarod (15 months) is greater than the sum of the increases observed with the IT-AAV2/9 (7 months) or IC-AAV2/9 (9 months) mice.

Although the combination therapy significantly improves lifespan and motor function, the IC/IT-AAV2/9 mice have a reduced lifespan compared to their wildtype littermates. These data suggest that the IC/IT-AAV2/9 mice may either be succumbing to disease outside of the central nervous system or that the minimal correction of the thalamus/mid-brain is not sufficient to prevent neurodegeneration. These data suggest that an intracranial or intrathecal administration route alone is not sufficient to correct the entire CNS (Rosenberg et al, 2014). It has been shown that there is cardiac dysfunction in models of Batten disease and INCL (personal communication with Dr. Jonathan Cooper, (Galvin et al, 2008)) as well as systemic metabolic defects (Woloszynek et al, 2007). Targeting these secondary disease modalities using small

molecule drugs or recombinant PPT1 in combination with gene therapy may further extend the

lifespan and quality of life for treated-INCL mice. Simultaneously targeting multiple pathogenic

mechanisms or different diseased compartments has proven effective in INCL (Macauley et al,

2012; Macauley et al, 2014; Roberts et al, 2012) and other LSDs (Biswas & LeVine, 2002;

Hawkins-Salsbury et al, 2011; Hawkins-Salsbury et al, 2015; Jeyakumar et al, 2001; Lee et al,

2007; O'Connor et al, 1998; Passini et al, 2007; Reddy et al, 2011).

Chapter 3: Cell-limited expression of PPT1

This chapter is adapted from the following manuscript:

Shyng C, Macauley SL, Sands MS. Cell-limited expression of PPT1. In Preparation

Introduction

Soluble lysosomal enzymes are translated and glycosylated in the endoplasmic reticulum then transported to the Golgi apparatus where terminal mannose residues are phosphorylated at the six position (M6P). Binding to the M6P /IGF II receptor in the Golgi targets the phosphorylated enzymes to the lysosome through the endolysosomal pathway. The enzyme-receptor complex uncouples at acidic pH releasing the enzyme for proper lysosomal activity. It has been shown that soluble lysosomal enzymes are secreted from a parent cell and can be captured by neighboring cells via the M6P/IGFII receptor on the plasma membrane (Barton & Neufeld, 1971; Cantor & Kornfeld, 1992; Hickman & Neufeld, 1972; Neufeld & Fratantoni, 1970). Trafficking of the secreted enzymes to the neighboring lysosome allows enzymatic functionality to be restored (Dahms et al, 1989; Neufeld, 1980; Neufeld, 2006; Verkruyse & Hofmann, 1996; Willingham et al, 1981). This inter-cellular trafficking of lysosomal enzymes, termed 'cross-correction', forms the basis of therapeutic approaches using cell-based, virus-based, or enzyme replacement therapies. While 'cross-correction' enhances treatment, it prevents the cell-autonomous study of enzyme deficiencies in lysosomal storage diseases (Sands, 2013; Sands & Davidson, 2006).

For this study, we utilized the soluble lysosomal hydrolase palmitoyl-protein thiosesterase-1 as a model enzyme to study cell autonomy in a lysosomal storage disorder. In humans, deficiency of PPT1 results in infantile neuronal ceroid lipofuscinosis (INCL), a progressive neurodegenerative disease (Hofmann et al, 1999; Vesa et al, 1995). Histopathological characterization of PPT1 deficiency reveals an accumulation of autofluorescent storage material (AFSM), neuronal death, glial activation, and neuroinflammation. This pathology results in progressive clinical deficits in vision, motor function, and cognition. A PPT1-deficient mouse model closely mimics human INCL (Bible et

al, 2004; Gupta et al, 2001). Understanding the role of specific cell types in INCL pathology may lead to an improvement in targeted therapeutics in humans. Using proteomics and metabolomics, studies have shown that PPT1 deficiency leads to alterations in global cellular and metabolic expression profiles. However, modeling cellular and metabolic profile changes in specific cell types has been lacking due to 'cross-correction' (Aby et al, 2013; Scifo et al, 2015; Tikka et al, 2016). By sequestering PPT1 in individual cells, we may begin to understand the role of specific cell types in disease progression, as well as the interactions of PPT1 sufficient and deficient cells in a hypothetical therapeutic environment.

To overcome 'cross-correction', we have engineered a chimeric, lysosomal membrane-tethered form of PPT1 using the transmembrane domain/signaling peptide of lysosomal-associated membrane protein-1 (LAMP1). The transmembrane domain/signaling peptide has been shown to be necessary and sufficient for lysosomal targeting of LAMP1, and may be used as a targeting and retention mechanism for secreted lysosomal hydrolases (Guarnieri et al, 1993; Rohrer et al, 1996). A similar approach has been used to create a milder form of Neiman-Pick A/B disease (acid sphingomyelinase (SMase) deficiency) (Marathe et al, 2000). In our model, we created a chimeric form of PPT1 that is tethered to the lysosomal membrane and would be expressed in a cell-specific manner (PPT1-LAMP1). To accomplish cell-specificity, we employed a genetic approach by inserting a loxP-STOP-loxP sequence into the transgene that would prevent both transcription and translation of PPT1-LAMP1 unless in the presence of Cre recombinase.

We show here that membrane tethered PPT1 retains enzyme activity and is capable of preventing the biochemical, histological, and behavioral phenotype of INCL when expressed ubiquitously *in vivo*. Unfortunately, the transgene rearranged leading to Cre unresponsiveness,

and unregulated and ubiquitous PPT1-LAMP1 expression. Nonetheless, this study demonstrates a proof-of-principle that this general methodology is a viable approach to address questions regarding the role of specific cell types in the progression of INCL.

Materials and Methods
PPT1-LAMP1 transgene

A diagram of the PPT1-LAMP1 transgene is shown in Figure 1. The transgene includes the promoter and first intron of the chicken β-actin gene, a LoxP-STOP-LoxP sequence from pBS302 (Addgene, Cambridge, MA), the human PPT1 cDNA genetically linked to a 120bp sequence encoding the transmembrane domain and lysosomal localization sequence of LAMP1, a six-glycine linker region, followed by a rabbit β-globin polyadenylation signal.

Generation of the PPT1-LAMP1 transgenic mouse

Transgenic mice were generated by microinjection of the transgene into C57Bl/6 embryos. This service was performed by the Transgenic Knockout Microinjection Core at Washington University School of Medicine. Founder lines were identified by PCR using primers flanking the PPT1-LAMP1 junction. Germline founder lines were identified by breeding transgene positive mice to PPT1-/- mice. Germline transgene transmission was identified using the aforementioned PCR primers. When possible, the transgenes were fixed on the PPT1-/- background. Congenic C56Bl/6 wild-type mice were used as controls.

Lentiviral production of PPT1-LAMP1

A 3rd generation SIN lentiviral vector was created for *in vitro* experiments (Dull et al, 1998; Zufferey et al, 1998). Briefly, the transfer plasmid contained the phosphoglycerate kinase

(PGK) promoter, the target gene, a SV40 poly(A) site, and a puromycin resistant cassette. The target gene contained wild-type PPT1 or PPT1-LAMP1. The negative-control, empty lentiviral vector did not contain a target gene. The transfer plasmid was transiently transfected in combination with pMD-Lg/pRRE, pRSV-Rev, and pMD2.G plasmids into HEK293T cells by calcium-phosphate transfection. Media containing lentivirus was collected and concentrated using ultracentrifugation as previously described (Dull et al, 1998; Zufferey et al, 1998). Lentiviral titers were assessed using serial dilutions and puromycin selection.

Transwell experiment

Cross-correction experiments were performed using a transwell system (Corning, Corning, NY). Briefly, PPT1-/- cells were plated on the bottom well, transduced for 24 hours, then exposed to puromycin after 72 hours post-transduction. The bottom well cells were allowed to become confluent. Untransduced PPT1-/- cells were plated on the transwell inserts in a separate dish, and were transferred into the experimental plate. Three days post-incubation, cells and media were collected for PPT1 enzyme activity. Cells were lysed in 10mM Tris pH 7.5, 150mM NaCl, 0.2% Triton X-100 via three freeze-thaw cycles. Cells were centrifuged and supernatant collected for enzyme activity. Cross correction experiments using primary dermal fibroblast cell cultures from one of the transgenic animals were similarly performed with the primary cells being plated on the bottom wells.

RNA isolation, RT-PCR, and Sequencing

RNA was isolated from brain, heart, and liver using TRIzol (Thermo Fischer, Waltham, MA) as described. Briefly, samples were homogenized in TRIzol. RNA was isolated, and cDNA

was generated using a High-Capacity cDNA Reverse Transcription Kit (Thermo Fischer, Waltham, MA). RT-PCR was performed using primers flanking the 6-glycine region. The forward primer was in the PPT1 sequence and the reverse was in the LAMP1 sequence. DNA sequencing was performed using the Protein and Nucleic Acid Chemistry Laboratory using Sanger di-deoxy sequencing. The sequencing primers flanked the loxP-STOP-loxP sequence. qPCR was performed on genomic DNA. Standards for copy number were generated from serial dilutions of the stock PPT1-LAMP1 plasmid. Quantitation for copy number was generated as previously described (Joshi et al, 2008).

SDS-PAGE/Western Blot

To confirm expression of PPT1-LAMP1 protein, lentiviral transduced cells or primary cell lines derived from a transgenic animal and control lines were isolated and homogenized in 50mM Tris-HCl pH 7.5, 1% Triton X-100, 0.5% sodium deoxycholate, 0.1% sodium dodecyl sulfate, 150mM NaCl, and 2mM EDTA (RIPA buffer). Cells were spun at 14000xg for 1 min and the supernatant was collected. The cell supernatant was diluted to 2µg protein/ul and 30ug of protein were loaded onto 12% SDS-PAGE gels (Bio-Rad, Hercules, CA). Protein was transferred onto PVDF (Porex Filtration Group, Fairburn, GA) membrane and probed for human PPT1 (Abcam 89022; 1:1000) or the cytoplasmic domain of LAMP1 (Sigma L1418; 1:1000). Secondary antibodies for mouse-horseradish peroxidase (HRP) or rabbit-HRP were used. Pierce ECL Western Blotting Substrate (ThermoFisher, St. Louis, MO) was used to detect the antibodies.

PPT1 Enzyme Activity and Secondary Enzyme Elevations

Three mice each from transgenic and control groups were euthanized via lethal injection. Mice were transcardially perfused with phosphate-buffered saline (PBS) until the liver was cleared of blood. Portions of visceral organs (heart, liver, spleen, kidney, eye) were flash frozen for subsequent biochemical analyses. Additional tissue samples were fixed in 4% paraformaldehyde in PBS solution for 24-hr fixation then cyroprotected in 30% sucrose solution in Tris-buffered saline (TBS). The brain was removed, weighed, and bisected sagittally; the left hemisphere was flash frozen while the right hemisphere was fixed/cyroprotected. PPT1 assays were performed on the brain, heart, and liver as previously described using the 4-MU-palmitate fluorometric assay and normalized to total protein (Griffey et al, 2004). Secondary elevations of β-glucuronidase was determined using 4-MU-β-D-glucuronide fluorometric assay and normalized to total protein as previously described (Roberts et al, 2012). Significance was determined using a two-way ANOVA followed by a Bonferroni post-hoc analysis for all enzyme assays.

Immunofluorescence

Immunofluorescence was performed as previously described (Hawkins-Salsbury et al, 2013). Briefly, cells were plated on poly-lysine coated coverslips. Cells were fixed then permeabilized with a 0.01% Triton X-100 in TBS solution. After blocking with 5% normal goat serum in TBS, cells were stained for human PPT1 (rabbit anti-rat), the cytoplasmic domain of Lamp1 (rat anti-mouse), and DAPI. Primary antibodies were detected with Alexa Fluor 488 (anti-rat) and 555 (anti-rabbit).

Autofluorescent Storage Material

AFSM was imaged as previously described (Griffey et al, 2004). Briefly, fixed and cryoprotected tissue was frozen in Optimal Cutting Temperature compound (OCT, Tissue-tek, VWR, Radnor, PA). Twelve-micrometer sections were cut and placed onto Superfrost slides. The slides were allowed to dry for 24 hrs at room temperature. The OCT was washed off using diH2O, and allowed to dry. Slides were coverslipped using Vectashield Antifade mounting medium (Vector Labs, Burlingame, CA). Sections were then imaged using confocal microscopy.

Lifespan, Rotarod, and Electroretinography

Longevity was assessed in control groups and transgenic mice (n=10-11 mice/group). The lifespan study was determined by death or euthanasia at one year. A Kaplan-Meier lifespan curve was used to measure survival and significant differences were determined using a log-rank analysis (p<0.05).

Transgenic and control mice (n=10) were tested on a constant-speed rotarod (3 rpm) at 7 months as previously described (Dearborn et al, 2015). Statistical significance was determined using one-way ANOVA at each time point followed by a Bonferroni post hoc test.

Electroretinography (ERG) was performed by the Vision Core at Washington University in St. Louis as previously described (Griffey et al, 2005; Heldermon et al, 2007). Briefly, mice were dark-adapted for mixed rod/cone ERG for a minimum of 2 hours or light adapted for 20 minutes for pure cone ERG measurements. Mice were then anesthetized. A recording electrode was placed on the cornea and a reference electrode was inserted subcutaneously behind the ear. Mice were exposed to flashes of light and the a- and b-waves were recorded using the UTAS-E-3000 LKC testing and analysis system (LKC Technologies, Gaithersburg, MD). b-wave amplitudes were recorded in microvolts and reported.

Results

Lysosomal Membrane-Tethered PPT1

PPT1 is a soluble lysosomal hydrolase that can be secreted then endocytosed by neighboring cells. Studying PPT1 function in a cell autonomous manner is difficult due to 'cross-correction'. Therefore, we generated a tethered form of PPT1 by anchoring the enzyme to the lysosomal membrane (Figure 15A). We genetically engineered the tethered PPT1 such that the enzyme is within the lumen of the lysosome and that the C-terminus of PPT1 is tethered to the transmembrane domain and C-terminus of the lysosomal acidic membrane protein-1 (LAMP-1) via a six glycine linker (PPT1-LAMP1). Conceptually, the six-glycine linker region should not have steric hindrance nor disallow PPT1 to function properly. The transmembrane domain and C-terminus of LAMP-1 is a lysosomal membrane protein and has been shown to be targeted to the lysosome via the YQTI amino-acid motif (Figure 15B).

A
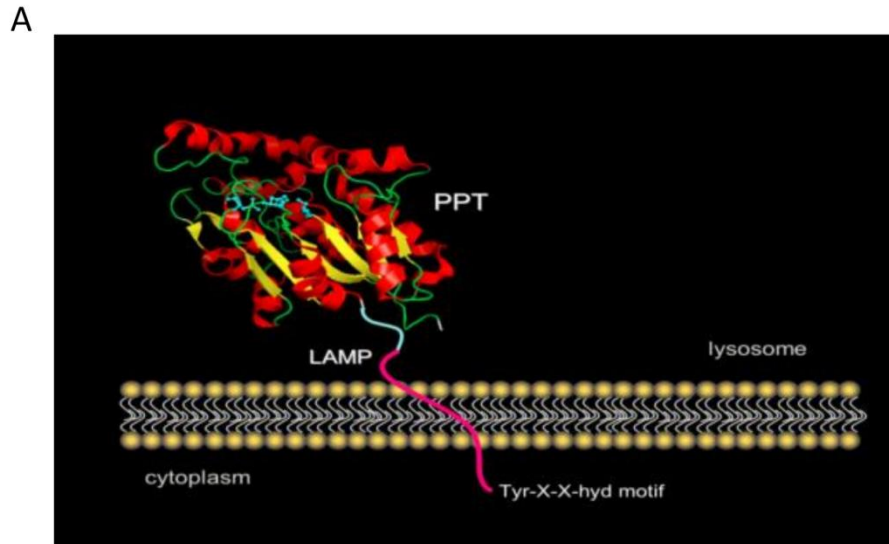
B

MASPGCLWLLAVALLPWTCASRALQHLDPPAPLPLVIWHGMGDSCCNPLSMGAIKK
MVEKKIPGIYVLSLEIGKTLMEDVENSFFLNVNSQVTTVCQALAKDPKLQQGYNAMG
FSQGGQFLRAVAQRCPSPPMINLISVGGQHQGVFGLPRCPGESSHICDFIRKTLNAGA
YSKVVQERLVQAEYWHDPIKEDVYRNHSIFLADINQERGINESYKKNLMALKKFVMV
KFLNDSIVDPVDSEWFGFYRSGQAKETIPLQETSLYTQDRLGLKEMDNAGQLVFLATE
GDHLQLSEEWFYAHIIPFLGGGGGGGGNNMLIPIAVGGALAGLVLIVLIAYLIGRKRSHA
GYQTI-

Figure 15. Mockup and Sequence of PPT1-LAMP1. A) Ribbon diagram of PPT1-LAMP1.
PPT1 is in the lumen of the lysosome (globular structure). It is connected to the C-terminus and
transmembrane domain of LAMP1 (pink) by a six glycine linker (light blue). B) Amino acid
sequence of PPT1-LAMP1. The human PPT1 sequence (green) is genetically tethered to the
transmembrane domain and C-terminus of LAMP-1 (pink) by the six-glycine linker (light blue).
The lysosomal targeting motif is underlined.

PPT1-LAMP1 function in vitro

PPT1-/- fibroblasts were transduced *in vitro* with lentiviral constructs containing hPPT1-

LAMP1, WT-hPPT1, or a negative-control empty vector. Lysosomal localization of PPT1-

LAMP1 was confirmed using immunofluorescence by staining against human PPT1 and LAMP-

1 (Figure 16A). A western blot was performed on protein homogenates from these cells and

showed that there was an increase in molecular weight of the hPPT1-LAMP1 (~40 kDa)

compared to the wildtype human PPT1(~32-36 kDa). This was consistent with the additional

molecular weight of the LAMP1 transmembrane domain and six-glycine linker (~5 kDa).

Blotting against the C-terminus of LAMP-1, both the endogenous LAMP1 (~120 kDa) and a

signal at ~40 kDa were detected. This was the same molecular weight as PPT1-LAMP1 detected

with the anti-PPT1 antibody (Figure 16B).

To confirm that PPT1-LAMP1 retained enzyme activity and was not secreted, a transwell

experiment was performed where the bottom well contained the lentiviral-transduced cells and

the transwell contained untransduced PPT1-/- cells. There was little to no PPT1 activity in cell

transduced with the empty vector (Figure 15C). Following transduction with wildtype PPT1,

significantly higher PPT1 activity (~400 nmol/µg/hr) was detected compared to the empty vector

cells. After transduction with the PPT1-LAMP1 vector, the level of PPT1 activity in the

transduced cells was comparable to the WT-PPT1 transduced cells. Lastly, PPT1-LAMP1 was

not secreted from the transduced cells. In the wild-type hPPT1 transduced wells, there was an

increase in PPT1 activity in the transwell cells (~5% of wild-type levels). However, in the PPT1-

LAMP1 transduced wells, there was little to no detectable activity in the transwell cells from the

PPT1-LAMP1 well. In the negative control, as expected, PPT1 enzymatic activity was

undetectable (Figure 16C).
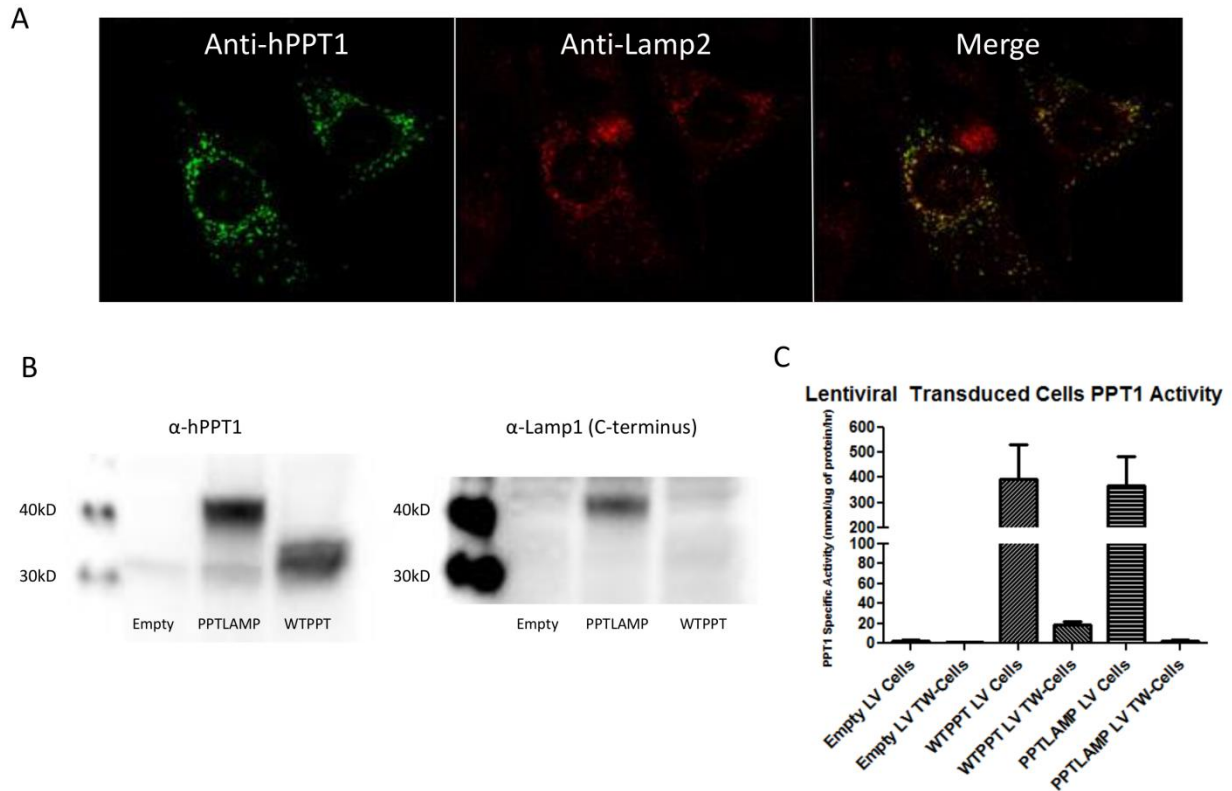
Figure 16. *In vitro* characterization of PPT1-LAMP1. A) Immunofluorescence of PPT1 (green, left) and LAMP-2 (red, center). Co-localization of PPT1 and LAMP2 is in yellow (right). B) Expression of PPT1-LAMP1 *in vitro*. PPT1-/- cells were transduced with lentivirus containing hPPT1-LAMP1 or hPPT1. The left panel is probed for anti-hPPT1. hPPT1 has a predicted molecular weight of ~32 and 36 kDa, and hPPT1-LAMP1 is predicted at ~40 kDa. The right panel was probed for the C-terminus of LAMP-1. LAMP-1 signal was detected in the lane from hPPT1-LAMP1 transduced cells. C) Transwell experiment for 'cross-correction'. Cells were transduced with empty, WT-PPT1, or PPT1-LAMP1 lentiviral vectors. There was a significant increase in enzyme activity in the WT-PPT1 compared to empty. WT-PPT1 cells and PPT1-LAMP1 cells had similar levels of activity. There was a significant increase in PPT1 activity in the transwell inserts in the WTPPT1 transwell compared to Empty and PPT1-LAMP1 transwells (p<0.05).

Generation of a PPT1-LAMP1 transgenic animal

To study the role of specific cell to the pathogenesis of INCL *in vivo*, transgenic animals harboring the PPT1-LAMP1 transgene were generated. For cell-specificity, we included a loxP-STOP-loxP sequence within our transgene (Figure 17A). *In vitro* transfection of PPT1-/- cells with a Cre-recombinase plasmid or the transgene-containing plasmid alone resulted in no

increase in PPT1 activity levels compared to PPT1-/- cells. However, when transfected together, there was a significant increase in PPT1 activity to near WT-PPT1 activity levels (Figure 17B). This confirmed that the transgene-containing plasmid was Cre-responsive.

PPT1-/- animals harboring the transgene were generated after confirmation of *in vitro* feasibility. Transgene-positive founder animals were identified by PCR analysis for the PPT1-LAMP1 junction (Figure 18A, B). Eight transgene-positive animals were identified. Five founder lines demonstrated germ-line transmission. However, three founders were unable to establish productive colonies. Two founders (Founder #38 and #42) were able to generate colonies. Founder #38 did not express PPT1-LAMP1 in the presence or absence of Cre-recombinase. Surprisingly, a PPT1 enzymatic assay of Founder #42 (F42) brain resulted in supraphysiological levels of PPT1 activity in the absence of Cre recombinase (data not shown). While unfortunate, F42 could be utilized as a proof-of-principle transgenic model of sequestered PPT1.

A

Chicken β-actin Promoter & 1st Intron	Lox-STOP-lox	Palmitoyl protein-thioesterase 1	Lamp-1	Rabbit β-globin Poly-(A) terminator
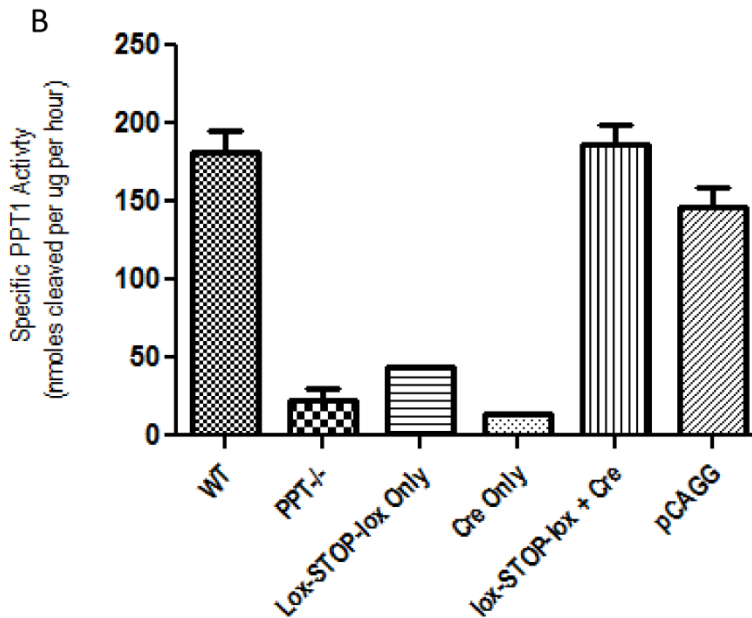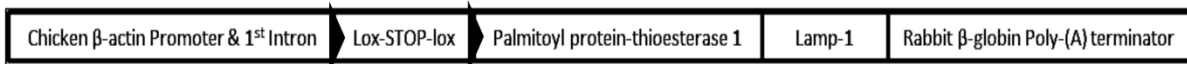
Figure 17. Generation of a cell-specific transgene. A) Structure of the transgene. LoxP sites

are shown in triangles. B) The transgene was first tested *in vitro*. There was not a significant increase in PPT1 activity in the PPT1-/- cells transfected with the transgene alone or the Cre-containing plasmid alone. There was a significant increase in PPT1 activity when the transgene and the Cre-containing plasmid were transfected together. pCAGGs-hPPT1 plasmid was used as a transfection control (p<0.05).

Founder #42 analyses

Molecular and biochemical characterization of F42 revealed a possible spontaneous recombination, and expression of the PPT1-LAMP1 transcript and protein. Further characterization of the transgene was performed using primers flanking the loxP-STOP-loxP sequence (Figure 18A). Surprisingly, a band of approximately 260bp was detected. This fragment was consistent with recombination of the loxP sites (Figure 18C). Further DNA sequencing of the fragment confirmed Cre-independent recombination. Approximate copy numbers were calculated using quantitative PCR. The qPCR confirmed an approximate 11 transgene copies per genome.

Using RT-PCR, PPT1-LAMP1 mRNA was detected in the brain, heart, and liver of F42 mice but was undetectable in wildtype or PPT1-/- mice (Figure 19A). Western blot analysis was performed on primary dermal fibroblasts to confirm the presence of PPT1-LAMP1. In F42 primary fibroblasts, a protein of ~36-40 kDa was detected with an anti-hPPT1 antibody (Figure 19B, left). Similarly, a protein was detected at ~40 kDa with an anti-LAMP1 antibody directed towards the C-terminus domain (Figure 19B, right). This was consistent with the aforementioned *in vitro* studies that reflected the increase in size due to the addition of the LAMP-1 C-terminus and transmembrane domain. Similarly sized proteins were not detected in the primary dermal fibroblasts from murine PPT1-/- and wild-type mice. However, the PPT1 signal was detected in human fibroblast cultures. The two bands likely correspond to unglycosylated (lower band) and glycosylated PPT1 (Das et al, 2001; Lyly et al, 2007). There was a faint band in the F42

66

homogenates that migrated at approximately the same position as the unglycosylated PPT1 in the

human fibroblasts. With further characterization of F42, dermal fibroblasts using a transwell

system showed that PPT1-LAMP1 does not 'cross-correct' (Figure 19C). Approximately 10

nmol/µg/hr PPT1 activity was detected in the transwell cells exposed to media from the wild-

type cells. In contrast, no PPT1 activity was detected in the transwell cells exposed to media

from the F42 cells even though F42 dermal fibroblasts had ~6-fold greater PPT1 activity

compared to wildtype cells.
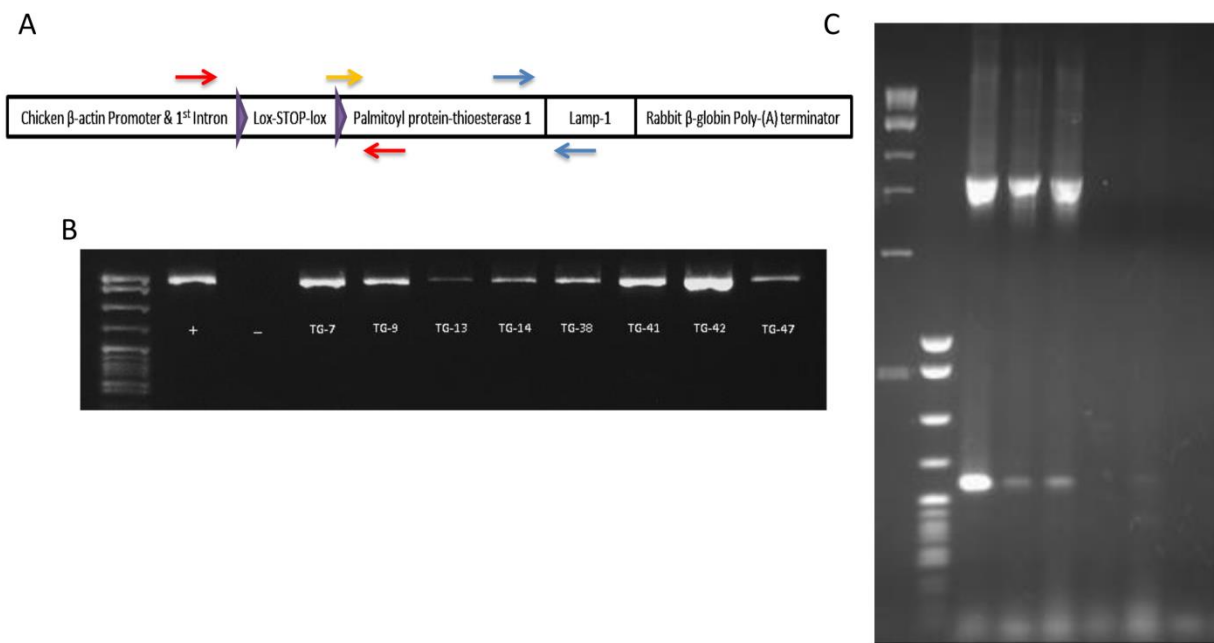
Figure 18. Generation of transgenic animals and identification of loxP site recombination.
A) Structure of the transgene and position of primers. Primers used for the identification of
recombination are shown in red. Primers used for identification of transgenic animals are shown
in forward: yellow and reverse: red. Primers used for RT-PCR are shown in blue. B) PCR gel
image identifying all the transgene positive founders. Lane 1: pBR322-MSPI digest ladder, Lane
2: positive control using the transgene plasmid, Lane 3: pCAGGs-PPT1 plasmid, Lane 4-11:
transgene founder lines. C) PCR gel identifying spontaneous recombination in Founder #42.
Lane 1: 1Kb ladder, Lane 2: pBR322-MSPI digest ladder, Lane 3: *in vitro* Cre recombinase and
transgene plasmid, Lane 4: genomic DNA isolated from F42 brain, Lane 5: genomic DNA
isolated from F42 Liver, Lane 6: genomic DNA isolated from PPT1-/- brain, Lane 7: genomic
DNA isolated from PPT1-/- liver, Lane 8: negative control.
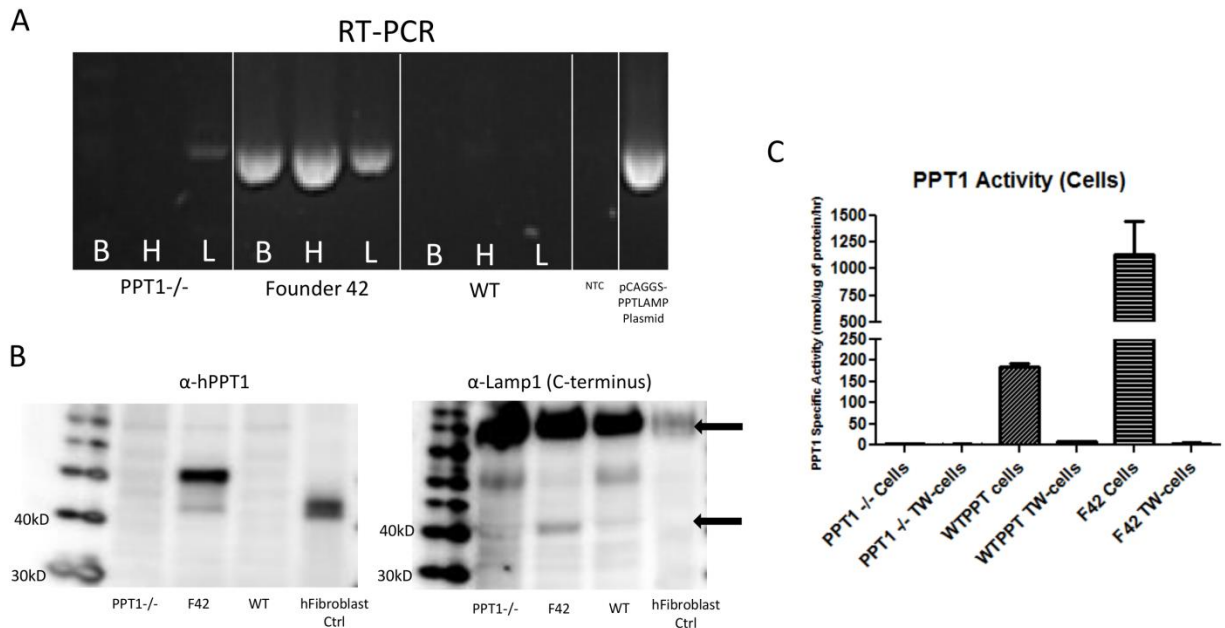
Figure 19. *In vitro* characterization of F42. A) RT-PCR of brain, heart, and liver from PPT1-/-, F42, and WT mice for the PPT1-LAMP1 mRNA transcript. B) Western blot for PPT1-LAMP1 expression. Protein expression of PPT1-LAMP1 was conducted on primary dermal fibroblasts. The left panel was probed for anti-human PPT1. A strong signal was detected at ~40 kDa in the F42 lane, and at the predicted ~32 (unglycosylated) and ~36 kDA (glycosylated) in the human control fibroblasts. The right panel was probed for the C-terminus of LAMP-1. There was a signal at ~120kDa (endogenous LAMP1) in all lanes and ~40kDA (PPT1-LAMP1) signal in the F42 lane. C) Transwell experiment for 'cross-correction'. Primary dermal fibroblast cells were used. There was a significant increase in enzyme activity in the WT-PPT1 compared to PPT1-/- cells. F42 cells have ~6-fold greater levels of PPT1 activity compared to WT cells. There was an increase in PPT1 activity in the transwell inserts in the WTPPT1 transwell compared to PPT1-/- and F42 transwells.

PPT1-LAMP1 expression in vivo is ubiquitous and prevents AFSM

A survey of tissues for PPT1 activity and secondary enzyme elevations was conducted in Founder 42 mice. Supraphysiological levels of PPT1 activity were detected in the brain and heart, and lower enzymatic activity in the kidney and spleen compared to wildtype. Surprisingly we detected very low PPT1 activity in the liver (Figure 20A). As previously shown, there was a secondary elevation in β-glucuronidase activity in the PPT1-/- brain, heart and liver as compared to wildtype (Griffey et al, 2004). This secondary elevation was restored to wildtype β-

glucuronidase activity levels in the brain and heart of F42 animals. However, there was not a significant reduction in the secondary elevation of β-glucuronidase activity in the liver compared to the PPT1-/- liver (Figure 20B). Autofluorescent storage material was examined in the brains and livers of PPT1-/-, WT, and F42 mice. As expected, there was widespread AFSM throughout the brain and liver of PPT1-/- animals and none detected in the wildtype animals. Accumulation of AFSM was not detected in the cortex, hippocampus, thalamus, or cerebellum of F42 brains. However, there was abundant AFSM throughout the liver in hepatocytes and cells of the reticuloendothelial system (Figure 20C & 20D).
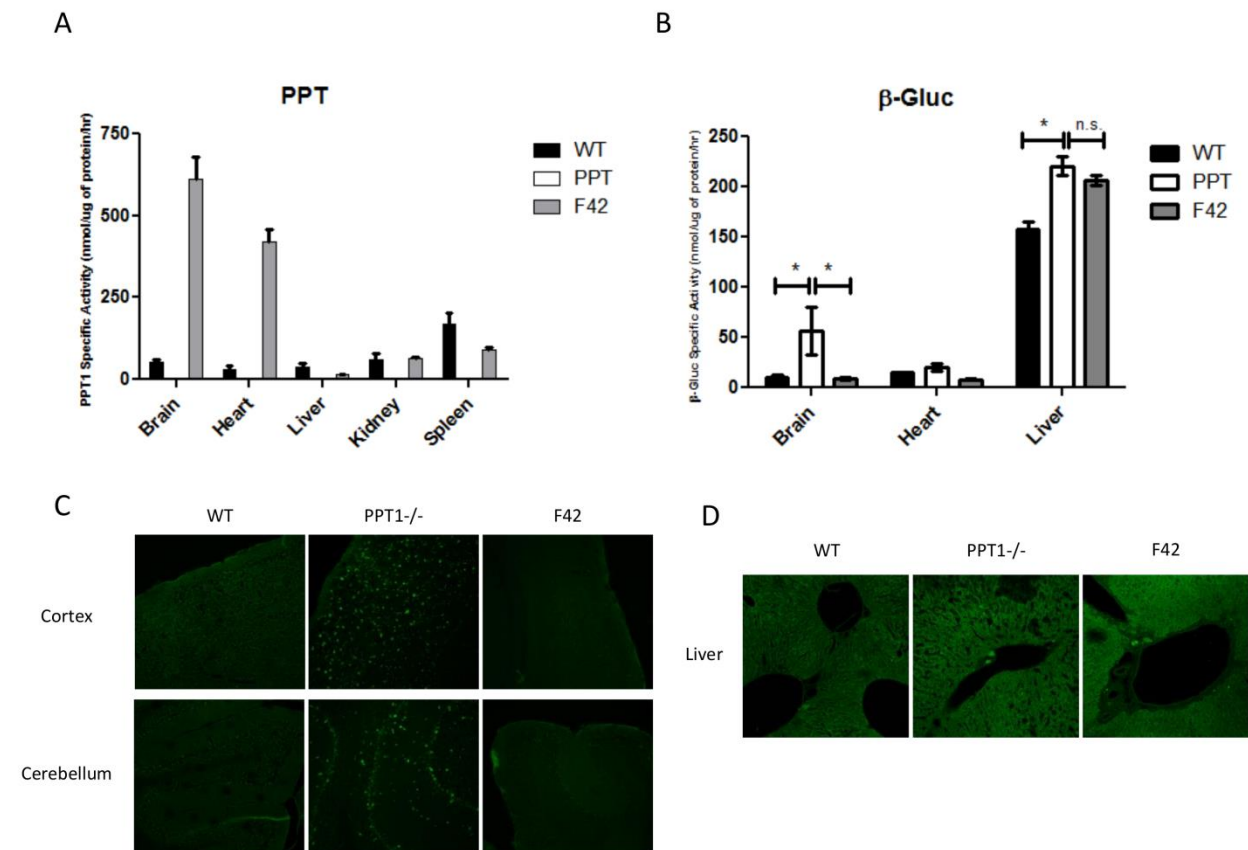
Figure 20. Biochemistry and Histology in F42. A) PPT1 enzyme activity tissue survey. Supraphysiological levels of PPT1 activity were detected in the brain and heart. Near normal levels were detected in the kidney, and ~50% activity in the spleen. The liver had very low activity. B) β-glucuronidase activity in the brain, heart, and liver from F42 and controls. There was a significant increase in β-glucuronidase activity in the brain and liver of PPT1-/- animals compared to WT (p<0.05). β-glucuronidase activity was normalized to WT levels in the F42 brain, however, the β-glucuronidase activity was not reduced in F42 liver. The heart showed a

small increase in β-glucuronidase activity in PPT1-/- animals but this increase was not statistically significant. There appeared to be decreased β-glucuronidase activity in the F42 heart. C) AFSM accumulation in F42 and control brains. Representative images show AFSM accumulation in PPT1-/- brains (cortex and cerebellum). AFSM was not detected in F42 cortex or cerebellum. D) AFSM accumulation in F42 and control liver. Representative images show AFSM accumulation in PPT1-/- and F42 livers.

PPT1-LAMP1 ubiquitous expression in vivo prevents behavioral decline and extends longevity

PPT1-/- mice showed a significant decline in ERG amplitudes and motor function by 7 months of age, and are terminal by ~8.5 months. Physiological characterization of F42 showed that PPT1-LAMP1 expression prevented the decline in both dark-adapted and light-adapted ERG amplitudes (Figure 21A). At 7 months, the motor function of F42 animals, as measured by the latency to fall off the rotarod, was identical to wildtype mice (Figure 21B). Lastly, the F42 mice are able to live to at least one year without any motor deficits or other obvious clinical signs of disease (Figure 21C).
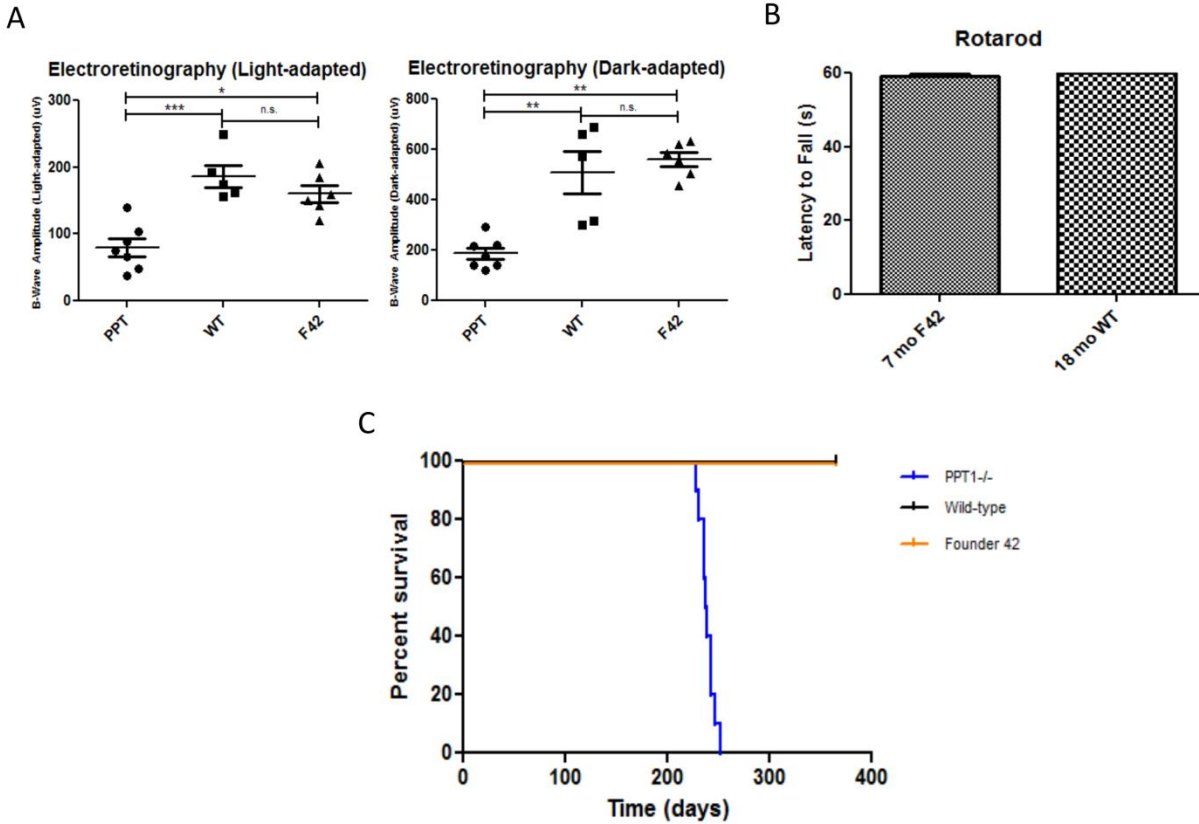
Figure 21. Functional and Clinical parameters of F42. A) Electroretinography of F42 and control eyes. There was a significant increase in b-wave amplitudes in the light-adapted ($p<0.001$) and dark-adapted ($p<0.001$) in WT compared to PPT1-/- mice. Similarly, there was a significant increase in b-wave amplitudes in light-adapted ($p<0.01$) and dark-adapted ($p<0.001$) in F42 compared to PPT1-/-. There was no significant difference between F42 and WT B) Rotarod of F42 mice showed no deficit in motor function at 7 months of age. C) The lifespan of F42 mice (orange) was not reduced compared to WT animals out to one year; PPT1-/- animals had a median lifespan of 238 days (blue)**.**

Discussion

Lysosomal storage diseases are simple monogenic diseases that present with a complex clinical phenotype. This is because lysosomal enzymes are ubiquitously expressed and, when deficient, affect many cell types. A more thorough understanding of the role individual cell types play in the disease process will allow for the rational development of more effective therapies. While 'cross-correction' has been a boon for therapy, it interferes with our ability to address basic biological questions about the role of specific cell types in disease progression. Any

attempt to correct the disease in a cell-specific manner would yield inconclusive, confounding results. Therefore, in this study, a novel method was employed to prevent cross-correction in an attempt to limit PPT1 expression to specific cell types.

A previous study by Marathe et al, (2000) showed that it was possible to prevent the secretion of sphingomyelinase, another soluble lysosomal hydrolase. Sphingomyelinase has been shown to be processed differentially depending on whether it will be targeted to the lysosome or secreted. In an effort to sequester the secreted form, SMase was tethered to the lysosomal membrane using the C-terminus of LAMP-1. The authors created a transgenic/knockout model that had modest lysosomal SMase activity in the brain (approximately 20% WT) and lower activity in visceral tissues (1-14%). This model had no evidence of neurological disease but widespread systemic disease. The original goal of their study was to eliminate the secreted form ubiquitously, which resulted in a hybrid model of Neimann-Pick A/B with visceral disease but no neurological disease.

In the current study, the original goal was to achieve cell-specific expression of PPT1. However, due to spontaneous rearrangement, a model with ubiquitous expression of tethered PPT1 was created. This model (F42) had AFSM in the liver but was otherwise biochemically, histologically, and clinically normal. This demonstrates proof-of-principle that PPT1-LAMP1 can hydrolyze its normal substrates and prevent INCL.

Tethering of PPT1 to the lysosomal membrane using the transmembrane domain and C-terminus of the LAMP-1 protein does not alter the enzymatic activity of PPT1. In addition, PPT1-LAMP1 was faithfully trafficked to the lysosome where it functions similarly to native PPT1. Importantly, PPT1-LAMP1 does not 'cross-correct' neighboring cells. In both *in vitro* experiments using either transduced cells or primary fibroblasts from F42, PPT1 activity was

expressed six-fold greater than normal and no enzymatic activity was detected in the transwell insert.

Ubiquitous expression of PPT1-LAMP1 *in vivo* was capable of preventing the accumulation of AFSM in the brain. This indicated that restoration of PPT1 by tethering it to the lysosomal membrane was sufficient in preventing the accumulation of AFSM. Moreover, the expression of PPT1-LAMP1 ubiquitously was able to prevent the onset of the major clinical/behavioral signs such as shortened lifespan, reduced visual function, and motor dysfunction. Similar to the *in vitro* experiments, there was also no evidence of PPT1-LAMP1 secretion or 'cross-correction' *in vivo*. The brain and heart of F42 have PPT1 activity approximately 10-fold greater than normal, while kidney and spleen have nearly normal and ~50% normal levels of activity, respectively. The liver only expresses ~5% normal levels of PPT1 activity. On histological examination, the liver of F42 has widespread AFSM accumulation. Given the high level of expression in other tissues, if PPT1-LAMP1 were capable of 'cross-correction', we would predict that the liver would have higher levels of activity and no AFSM accumulation.

In order to accomplish our original goal of generating a mouse model that would have cell-specific expression of PPT1LAMP1, a loxP-STOP-loxP system was utilized. However, during the initial characterization of the transgenic lines on a PPT1-/- background, enzymatic activity was detected in the absence of Cre-recombinase indicating a possible spontaneous recombination of the loxP sites. Generation of F42 utilizing the conventional transgenic approach led to multiple copies of the transgene (~11 transgene copies/genome). It has been shown that this method results in the generation of multiple head-to-tail copies (Haruyama et al, 2009). It is possible that the repeat sequences in the concatamers make the transgene prone to

recombination. Consistent with this hypothesis, it has been shown that direct sequence repeats can to lead to deletion of the internal sequence (i.e. loxP-STOP-loxP) (Bill & Nickoloff, 2001; Hendricks et al, 2003; Wurtele et al, 2005). Such an occurrence could lead to excision of the loxP-STOP-loxP region and allow for transcription of the transgene. The varying levels of expression among tissues could be due to the integration site. One potential solution to this problem would be to knock-in the transgene into the ROSA26 locus to control for copy number and random integration.

While the transgenic model may not allow for the study of cell autonomy in an *in vivo* setting, the model provides evidence that this basic approach is sound. In addition, the generation of a constitutively expressing, near-ubiquitous PPT1LAMP1 will allow for the study of cell-cell interactions in an *in vitro* environment. Lastly, this concept of tethering a soluble lysosomal enzyme to the lysosomal membrane may be applied to other LSDs and improve our understanding of cell autonomy in LSDs.

Chapter 4: Summary, Conclusions, and Future Directions

Summary and Conclusions

Infantile neuronal ceroid lipofuscinosis is an inherited metabolic disorder that is caused by a deficiency in the soluble lysosomal hydrolase palmitoyl-protein thioesterease-1 (PPT1) (Haltia et al, 1973b; Santavuori et al, 1973; Vesa et al, 1995). Deficiency in PPT1 leads to lysosomal distention, accumulation of AFSM, and cellular dysfunction. Ultimately, PPT1 deficiency leads to complex clinical signs. The development of the PPT1-/- mouse model has led to a much deeper understanding of disease pathogenesis as well as development of pre-clinical treatments (Gupta et al, 2001). Over the past 15 years, the field has benefited from the characterization of neuropathology in the PPT1-/- mouse. Studies, to date, have shown that INCL disease in the brain is progressive both temporally and spatially (Bible et al, 2004; Kielar et al, 2007; Macauley et al, 2009). There is astrocytosis, neurodegeneration, and neuroinflammation. This histopathology correlates with the clinical signs of disease such as visual deficits, motor dysfunction, and reduced lifespan. Due to the cortical atrophy and dramatic decrease in brain mass, the NCL field has largely focused on disease within the brain while the disease in the spinal cord has been largely overlooked. Similarly, detailed characterization of the peripheral and autonomic nervous systems as well as the systemic disease have not been conducted.

A new target and effective therapy for INCL

This study identified a novel region of disease and sought to treat it using gene transfer. In this study, we transitioned from the second generation AAV2/5 vector to the third generation AAV2/9 vector. The AAV2/9 vector has been shown to have improved distribution and transduction efficiency compared to previously used gene therapy vectors (Dayton et al, 2012; Schuster et al, 2014). Given the AAV2/9 vector's superior characteristics, we predicted that the lifespan of PPT1-/- mice receiving intracranial injections would have been extended longer than

76

the two months observed. This prompted us to perform a more detailed examination of the spinal cord in treated and untreated mice in collaboration with Dr. Jonathan Cooper's lab at King's College, London.

A more comprehensive examination of the PPT1-/- mouse spinal cord revealed gross anatomical changes as well as more subtle histological changes. It was revealed that there was a similar but earlier onset of histopathology in the spinal cord compared to the brain. While the volume of white matter increased temporally in the PPT1-/- spinal cord, the volume did not approach that of wild-type mice. Interestingly, the grey matter in the PPT1-/- spinal cord decreased whereas the wildtype grey matter increased. The hallmark of INCL, autofluorescent storage material, was prevalent in the grey matter and progressively increased starting as early as two months. Astrocytosis and microgliosis were observed as early as two months of age throughout the spinal cord. This was followed by neuronal loss at three months of age. All three parameters continued to degenerate in the PPT1-/- spinal cord compared to the wild-type spinal cord until PPT1-/- mice are terminal. The finding of widespread spinal cord disease was recapitulated in autopsy samples from human INCL patients (Nelvagal et al, In preparation). These data suggest that PPT1-/- leads not only to the progression of INCL, but may also influence neurodevelopment.

In the spinal cords of intracranial-treated mice, the disease was not treated regardless of which AAV vector was used. In this study, we showed that there was accumulation of AFSM, and an increase in histological markers of disease (CD68 and GFAP) when treatment was limited to the brain. This led to the hypothesis that treating the spinal cord directly via gene transfer techniques would prevent disease. This also led to the second hypothesis that treating PPT1-/-

mice by both intracranial and intrathecal routes would significantly improve the histology, improve motor function, and extend the lifespan as compared to either treatment alone.

There appears to be a reciprocal response when comparing intracranial to intrathecal injections in PPT1-/- mice. When PPT1-/- mice are treated with intracranial AAV2/9-hPPT1, the disease in the brain is corrected, however the spinal cord remains diseased. In contrast, when PPT1-/- mice are treated with intrathecal AAV2/9-hPPT1, the disease in the spinal cord is corrected whereas the brain is still affected. A biochemical surrogate for therapeutic efficacy is decreased secondary elevations of other lysosomal enzymes. Secondary elevations of β-glucuronidase in the brain are significantly reduced in intracranial-injected mice alone and only slightly improved in intrathecal-injected mice. The lack of biochemical improvement in the brain following intrathecal injection was somewhat surprising given that two to five percent of wild-type PPT1 activity levels in the brain were detected throughout the study. It has been shown that a very small percentage of wildtype lysosomal enzyme activity levels are required to correct the disease pathology (Sands et al, 1994). In the regions targeted by gene therapy, there was a decrease in histological markers of disease (AFSM, CD68, and GFAP). Particularly in intracranial-injected animals, there were improvements in gross physiology (cortical thickness, brain weight) which was not observed in the intrathecal-injected mice alone. When cytokine levels were examined in the brain, there was a decrease in cytokine/chemokine levels in the brain of intracranial treated mice but not in the intrathecal alone. Interestingly, in the intrathecal-injected mice alone, there was still an upregulation of cytokines/chemokines, which may be due to circulating neuroinflammatory factors in the cerebral spinal fluid. When either disease region was targeted, there was an improvement in motor function and an extension in lifespan. The

histopathology of the treated mice suggest that disease outside of the treated regions could explain the reduced motor function and reduced lifespan as compared to wild-type mice.

When these diseased regions were targeted in combination, there was a significant decrease in histological markers of disease in the brain and spinal cord. Furthermore, there was a return in neuroinflammatory factors in the brain to wild-type levels. There was also a significant improvement in gross brain anatomy. Overall, there was a dramatic and significant improvement in motor function and extension in lifespan. The combination intracranial and intrathecal-injected mice are by far the longest-lived treated PPT1-/- mice (22 months) reported to date.

Conclusion from combination therapy

The identification and characterization of the spinal cord disease and the efficacy of targeting the spinal cord with AAV-based gene therapy are two overarching findings of these studies. First, the disease in the spinal cord begins early in the pathogenesis of INCL. In fact, significant disease in the spinal cord begins about one month earlier than disease in the brain. For therapeutic purposes, this argues for early treatment of the spinal cord. Moreover, our study also shows that persistent expression of PPT1 in the spinal cord is necessary for an extension in the quality of life of PPT1-/- mice. A previous study where enzyme replacement was delivered intrathecally in PPT1-/- mice showed that lifespan was only extended by one month. Taken together, these two aspects suggest that proper identification and treatment for INCL must begin early in life (newborn screening) with methods that supply persistent PPT1 to the entire central nervous system.

Second, while INCL disease has primarily been seen as a brain disease, our work demonstrates that it is necessary to evaluate the disease in the context of the entire central

79

nervous system. As we have shown, targeting the entirety of the central nervous system significantly improves motor function and lifespan of the PPT1-/- mice and slows the progression of INCL-related disease. While intracranial and intrathecal administration of AAV2/9 showed broad distribution in the central nervous system, the histochemical stain determined that the mid-brain was not targeted. Subsequent analysis of this region in treated mice showed significant disease that appeared only minimally decreased upon combination therapy. Recent studies have employed the intrathecal route as a means to target the brain (Gray et al, 2013; Guo et al, 2016; Hordeaux et al, 2015; Schuster et al, 2014). As our study suggests, when using single-stranded AAV2/9 (ssAAV2/9) for intrathecal gene therapy, the correction of the brain is minimal. Therefore, to target the entirety of the central nervous system, it is necessary to utilize multiple routes of injection or to develop vectors that will be better distributed within the brain parenchyma (see Future Directions). Since PPT1 is ubiquitously expressed, it is also necessary to evaluate the disease outside of the central nervous system such as the peripheral and autonomic nervous systems. Given the cardiac dysfunction and metabolic abnormalities associated with INCL, it is also necessary to understand whether neuronal dysfunction plays a vital role in these aspects of disease (see Future Directions).

In a more global context, infantile NCL is one of more than 14 different NCLs. While the age of onset varies depending on the genetic mutation, the accumulation of AFSM, the increase in histopathological markers of disease, the progression of disease within the brain, and the overall clinical signs are relatively similar. The findings from our study along with Nelvagal et al. moves the field forward by broadening the focus of NCL diseases from the brain to the entirety of the central nervous system. It is not difficult to hypothesize that these NCLs would

also have progressive spinal cord disease and that treatment for the NCLs will need to include treatment of the spinal cord.

Future Directions for INCL gene therapy

<u>Developmental defect in the spinal cord and peripheral nervous system disease</u>

Our data, in combination with Nelvagal et al, suggest that there may be a developmental component to INCL particularly in the white matter tracts of the spinal cord. It has been previously shown that there is developmental-dependent PPT1 mRNA expression in the rat brain in early life (Isosomppi et al, 1999; Suopanki et al, 2000; Zhang et al, 1999). This is not surprising given that palmitoylation has been shown to play a key role in neurodevelopment and neural function (Fukata & Fukata, 2010; Young et al, 2012). PPT1 has also been shown to be localized throughout the axon and at synapses (Ahtiainen et al, 2006; Ahtiainen et al, 2003). Furthermore, PPT1 deficiency in mice has shown altered synaptic vesicle recycling (Kim et al, 2008; Virmani et al, 2005). In *Drosophila*, PPT1 has been shown to regulate neural cell fate and specification. In PPT1-/- larvae, there are a variety of defects in axonal guidance and branching (Chu-LaGraff et al, 2010; Glaser et al, 2003). This suggests that PPT1 deficiency may alter neuro-development.

While many studies have been conducted on the progression of INCL in mice after two to three months, it is necessary to study the developmental defects of PPT1 deficiency either at embryonic or early post-natal stages. It has been shown in *Drosophila* that the defects in axonal guidance and targeting affect the entire nervous system. The visualization of axonal guidance and targeting can be addressed with the development of the Thy1-YFP PPT1-/- reporter mouse model. The Thy1-YFP reporter mouse labels some neurons of the motor and sensory cortex, the

corticospinal tract, and the sciatic nerve. Furthermore, this reporter model has been used to examine neuromuscular junctions. With the Thy1-YFP PPT1-/- reporter mouse model we will be able to follow axonal guidance and targeting defects from the brain to the signaling endpoint. By comparing the PPT1-/- mice to the wild-type littermate, we may begin to unravel how PPT1 deficiency contributes to the functional deficits at the cellular level.

Synergy of spinal cord and brain directed therapy

It is necessary to understand the role of the entire central nervous system in disease progression. As shown, while targeting the brain or the spinal cord individually led to modest increases in lifespan and function, targeting both regions simultaneously significantly improved histological and clinical parameters compared to either region alone. In fact, targeting both regions of the CNS leads to an apparent synergistic effect. If the two routes of administration resulted in an additive effect, the median lifespan would have been approximately 17 months. However, the lifespan of mice treated with both intrathecal and intracranial injections was 19.3 months. A similar synergistic effect was observed with motor function. An additive effect would have resulted in motor deficits presenting at 11 months. However, significant motor deficits were not observed until 15 months. A more thorough understanding of this synergy could guide the future development of more effective therapies.

AAV2/9 has been shown to target a variety of cell types, particularly during the early post-natal periods (Foust et al, 2009). To understand the synergy, it may be necessary to limit the expression of PPT1 to select cell types such as neurons or glia using cell-specific promoters in the AAV cassette instead of the ubiquitous CAG promoter. However, utilization of AAV may not correct the entirety of each cell type leading to potential confounding results. To ensure

broad expression of PPT1, it may be more beneficial to develop a mouse model where there could be cell-specific expression of PPT1. We have made significant strides in the development of this model (see Chapter 3: Cell-specific Expression of PPT1).

The synergy that we observed may be due to both a better distribution of PPT1 throughout the central nervous system as well as to the peripheral nervous system. It has been shown that intrathecal injection of an AAV vector can result in significant expression in the peripheral nervous system (Federici et al, 2012; Jacques et al, 2012; Vulchanova et al, 2010). The peripheral and autonomic nervous systems in PPT1 deficient animals have not been characterized. It will be important to examine the impact of CNS-directed gene therapy on the peripheral nervous system. Performing gene therapy experiments in the Thy1-YFP PPT1-/- reporter mouse model might provide insights into the consequences of this approach on the peripheral nervous system. Finally a thorough biochemical, histological, and functional assessment of the systemic disease in AAV-treated mice might be informative..

Improved Combination Therapies

Combination therapy in lysosomal storage diseases has shown tremendous promise (Hawkins-Salsbury et al, 2011). By expanding the region targeted by CNS-directed gene therapy, we were able to more than double the lifespan of PPT1-/- mice. By targeting regions of the central nervous system not previously corrected, we were able to significantly delay disease onset. However, the lifespan of the combination treated animals were still shorter than the wild-type littermates. There is still much more to be accomplished in order to completely correct the disease. In order to treat INCL and other storage disorders effectively, it will be necessary to correct the entirety of the system or organ and not simply a small portion. While 'cross-

correction' is a relatively efficacious method to deliver enzyme, it's radius of correction is limited.

The use of AAV viral vectors to target the CNS in INCL has been beneficial due to the distribution of the AAV vector within the parenchyma. With improving CNS-specific vector serotypes, the distribution of the vectors will only improve. As we showed with the histological stain for PPT1, the PPT1 staining is broad and diffuse throughout the CNS. However, one region that has marginal staining is the thalamus and mid-brain region. The thalamic region has been shown to be the first area affected in INCL with both neuronal loss and glial activation. The thalamic region appeared to have only minimally decreased histological markers of disease in the combination-treated animals and there was no decrease in the animals receiving individual treatments. This suggests yet another therapeutic target using AAV2/9 gene therapy. Another method to target the thalamus would be to employ another AAV vector serotype (e.g. AAV-DJ) or a self-complementary AAV that has a broader distribution and increased transduction efficiency (Fu et al, 2003; Mao et al, 2016).. In either case, this could lead to an increase in the level of enzyme produced and broader correction.

Small molecule drugs have been explored to replace PPT1 activity (PPT1 mimetics) or target secondary effects of PPT1 deficiency (neuroinflammation). Unfortunately, these small molecule therapies have resulted in little to no improvement in functional parameters of INCL such as motor function or longevity. For example, using the anti-inflammatory Minozac, there were minor improvements in histological markers of disease in the brain but functional tests remained unchanged (Macauley et al, 2014). Similarly, using a PPT1 mimetic, phosphocysteamine, there was no biochemical, histological, or functional improvements in INCL mice (Roberts et al, 2012). Although these small molecule drugs provide little or no benefit on

their own, they might interact with another form for therapy (e.g. gene therapy) to greatly increase efficacy.

INCL is considered primarily a neurological disease. However, systemic disease is present in mice and could be relevant for humans (Galvin et al, 2008; Woloszynek et al, 2007). If treatment is limited to the CNS, then the systemic disease could become clinically relevant. To tackle systemic disease, enzyme replacement studies have shown that intravenous delivery of recombinant PPT1 corrects INCL histopathology in the visceral tissues however this does not significantly improve outcome measures such as lifespan or motor function (Hu et al, 2012). Therefore, to treat INCL disease in its entirety, it may be necessary to combine CNS-directed gene therapy with recombinant enzyme replacement therapy.

Another combination therapy that may be useful is gene therapy in combination with substrate reduction. Substrate reduction therapy (SRT) is accomplished by inhibiting the synthesis of the substrates for the enzyme that is deficient. Although in principle SRT is not predicted to stop the disease, it could slow the accumulation of undegraded substrates and potentially slow disease progression. SRT is currently in clinical trials for several LSDs (Cox, 2005; Pastores, 2010; Valayannopoulos, 2013). Therefore, SRT might be an ideal adjunct therapy for INCL. In fact, dramatic results have been achieved in the mouse model of Krabbe disease by combining SRT with CNS-directed gene therapy (Hawkins-Salsbury et al, 2015). SRT could be utilized in INCL by targeting the palmitoylation of proteins. Within the cell, the dynamics of palmitoylation is in equilibrium and has been shown to involve DHHC proteins and acyl-protein thioesterases (Fukata et al, 2015; Fukata et al, 2013; Fukata & Fukata, 2010; Fukata et al, 2016; Martin et al, 2012). Ultimately, palmitoylated proteins are degraded in the lysosome. Therefore, to reduce the influx of palmitoylated proteins into the lysosome, one method could be

a reduction in the cellular pool of free palmitate. Palmitate is produced in the cell by the multimeric enzyme fatty acid synthase (Smith et al, 2003). Inhibition of palmitate synthesis can be accomplished by using small molecule drugs that competitively inhibit fatty acid synthase (Abdel-Magid, 2015). There are a number of FASN inhibitors such as the C75 (a cerulenin derivative), orlistat, and epigallocatechin-3-gallate (EGCG, green tea derived). When combined with CNS-directed gene therapy, it could be possible to attenuate the severity of the disease.

Summary of cell-limited study of PPT1

Given the complex nature of INCL, this study sought to develop a model where INCL could be studied in a cell-specific manner. The cell-specific study of INCL is hindered by 'cross-correction'. For example, correction of neurons with soluble PPT1 would ultimately correct the neighboring glia making the interpretation of the results inconclusive. To prevent cross-correction, we tethered PPT1 to the lumen of the lysosome. This was done by genetically engineering the human PPT1 cDNA to the C-terminus and transmembrane domain of the lysosomal-associated membrane protein-1 (LAMP1).

In this study, PPT1 was tethered to the C-terminus of LAMP-1 using a six-glycine linker. We showed that the PPT1-LAMP1 chimeric protein retained enzymatic function and was incapable of 'cross-correction' *in vitro*. We developed lentiviral constructs that expressed either wild-type human PPT1 or the chimeric PPT1-LAMP1 and transduced PPT1-deficient cells. We showed that PPT1-LAMP1 had similar enzymatic activity as the wild-type PPT1. Using a transwell setting, we further show that PPT1-LAMP1 was incapable of 'cross-correcting' deficient cells in the transwell insert.

Since our overarching goal was to express PPT1 in a cell-specific manner, we sought to limit PPT1-LAMP1 expression to particular cell types. Therefore, we employed current transgenic technology using the Cre-loxP system. We genetically inserted PPT1-LAMP1 into a transgene driven by the ubiquitous CAG promoter. For cell-specificity, we inserted a LoxP-STOP-LoxP sequence within the transgene. This system functions properly *in vitro*. Therefore, we proceeded to create animals harboring this Cre-responsive transgene. A preliminary examination of Founder #42 (F42) revealed PPT1 activity throughout the mouse with supraphysiological levels detected in the brain and heart, and low levels in the liver. This global activity in the absence of Cre recombinase would not allow for cell-specific expression *in vivo.*

Ultimately, we decided to characterize F42 as a proof-of-concept model. We showed that PPT1-LAMP1 is expressed *in vivo* and that it is localized to the lysosome. Using a transwell system, we showed that PPT1-LAMP1 is not secreted from primary dermal fibroblasts derived from F42. This is further confirmed *in vivo* upon examination of the liver. While there were low levels of enzymatic activity in the liver, we observed the hallmark of INCL disease, AFSM, in sporadic cells throughout the liver such as in the hepatocytes and Kupffer cells. This indicated to us that PPT1 is not being secreted and taken up by neighboring cells. Expression of PPT1-LAMP1 corrected all of the INCL clinical signs measured such as visual deficits as measured by ERGs, motor function via rotarod, and lifespan. This shows that expression of PPT1-LAMP1 can complement native soluble PPT1.

Conclusions from cell-specific expression of PPT1

We have generated a model that has cell-limited but ubiquitous expression of PPT1. This was most likely due to a spontaneous recombination of the loxP-STOP-loxP within the transgene

as was detected by PCR analysis of the genome. While this model cannot be used for the intended purpose, the model instead can be used to study *in vitro* effects of sequestered PPT1. Cell-specific studies can still be conducted in a mixed culture setting (discussed further in Future Directions). We have shown that it is possible to sequester a soluble lysosomal hydrolase within the lysosome and that this sequestration does not impede the ability of the enzyme to function. Therefore, with some modifications, it may be possible to express PPT1-LAMP1 in a cell-specific manner and begin to understand the role of different cell types in INCL. On a grander scale, this conceptual approach can be applied to a variety of lysosomal storage disorders that result from deficiencies in a soluble lysosomal hydrolase (e.g. Krabbe disease, MPS disorders). These LSDs suffer from the same confounding nature of 'cross-correction'. By better understanding the pathogenesis of these LSDs and the major cell types that are affected, we may begin to develop more targeted therapies.

Future Directions for Cell-specific Study of INCL

<u>Modification of the Transgene</u>

'Cross-correction' remains a hindrance to the study of specific cell types in lysosomal storage diseases. The generation of the PPT1-LAMP1 chimeric enzyme prevents 'cross-correction' as we have shown. While the F42 model for PPT1-LAMP1 expression may be useful for *in vitro* studies, for cell autonomous studies of INCL *in vivo,* the model is still lacking. The original concept of utilizing the Cre-loxP system for cell-specific expression of PPT1-LAMP1 could still prove to be the most useful. One scenario that may have contributed to spontaneous recombination of the loxP sites in F42 is the methodology in the generation of the transgenic mice. We utilized a conventional transgenic approach where our transgene was micro-injected

into mouse embryos. This method is prone to concatamer formation at a variety of integration sites. The concatamers in turn might be prone to recombination particularly with large regions of repeat sequences. To prevent this, we could take advantage of the ROSA locus. The ROSA26 locus has been shown to be targeted with high efficiency and can be limited to a single copy of the transgene (Beard et al, 2006; Zambrowicz et al, 1997).

It has additionally been shown that a strong promoter can read-through a loxP-STOP-loxP sequence. While infrequent, this could also lead to confounding results. One scenario to overcome this problem would be to utilize the double-floxed inverted orientation (Smedemark-Margulies & Trapani, 2013; Sohal et al, 2009). This system utilizes two sets of incompatible loxP sites that flank the inverted transgene, and, when subjected to Cre-recombinase, result in an inversion of the transgene to its functional form. This method would not require the presence of a STOP sequence in the transgene and any spontaneous recombination would not result in a functional transgene.

Finally, we could re-engineer our transgene to contain loxP sites outside of the expression cassette. In this strategy, we would have ubiquitous expression in the absence of Cre recombinase but could 'turn-off' the expression in a cell-specific manner.

Mixed culture studies

While the current model cannot be used for *in vivo* examination of specific cell types in INCL, *in vitro* studies can be conducted using mixed cultures. We have developed lentiviral vectors that express either hPPT1-LAMP1 or wild-type hPPT1, and an empty vector control. The PGK promoter, a ubiquitous promoter, drives the transgenes in these lentiviral vectors. Moreover, there is a selectable puromycin marker. It will be possible to transduce specific cell

types (e.g. neurons, astrocytes) from PPT1-/- animals and by co-culturing these cells with other cell types, begin to understand how PPT1 deficiency affects intra- and inter-cellular interactions. For example, we may begin to understand the PPT1-/- neuronal phenotype by co-culturing PPT1-/- neurons with lentiviral-transduced PPT1-/- astrocytes *in vitro*. Similar studies can be conducted using isolated primary cell cultures from the F42 transgenic line.

To mimic *in vivo* settings, we could change the promoter of these lentiviral vectors from a ubiquitous promoter to cell-specific promoters. We could inject these lentiviral vectors into newborn mouse brains. While this will not allow for the targeting of every cell for a specific cell type, it will allow for the study of a specific cell type in a defined region. For example, the lentiviral vectors could be injected in the thalamus of PPT1-/- animals, one of the first sites of CNS disease, and these animals could be later observed for changes in biochemistry, histology, and clinical parameters.

References

Abdel-Magid AF (2015) Fatty Acid Synthase (FASN) Inhibitors as Potential Treatment for Cancer, Obesity, and Liver Related Disorders. ACS Med Chem Lett 6**:** 838-839

Aby E, Gumps K, Roth A, Sigmon S, Jenkins SE, Kim JJ, Kramer NJ, Parfitt KD, Korey CA (2013) Mutations in palmitoyl-protein thioesterase 1 alter exocytosis and endocytosis at synapses in Drosophila larvae. Fly 7**:** 267-279

Ahtiainen L, Luiro K, Kauppi M, Tyynela J, Kopra O, Jalanko A (2006) Palmitoyl protein thioesterase 1 (PPT1) deficiency causes endocytic defects connected to abnormal saposin processing. Experimental cell research 312**:** 1540-1553

Ahtiainen L, Van Diggelen OP, Jalanko A, Kopra O (2003) Palmitoyl protein thioesterase 1 is targeted to the axons in neurons. The Journal of comparative neurology 455**:** 368-377

Anderson GW, Goebel HH, Simonati A (2013) Human pathology in NCL. Biochimica et biophysica acta 1832**:** 1807-1826

Aschauer DF, Kreuz S, Rumpel S (2013) Analysis of transduction efficiency, tropism and axonal transport of AAV serotypes 1, 2, 5, 6, 8 and 9 in the mouse brain. PloS one 8**:** e76310

Barton RW, Neufeld EF (1971) The Hurler corrective factor. Purification and some properties. The Journal of biological chemistry 246**:** 7773-7779

Beard C, Hochedlinger K, Plath K, Wutz A, Jaenisch R (2006) Efficient method to generate single-copy transgenic mice by site-specific integration in embryonic stem cells. Genesis 44**:** 23-28

Bennett MJ, Rakheja D (2013) The neuronal ceroid-lipofuscinoses. Dev Disabil Res Rev 17**:** 254-259

Bible E, Gupta P, Hofmann SL, Cooper JD (2004) Regional and cellular neuropathology in the palmitoyl protein thioesterase-1 null mutant mouse model of infantile neuronal ceroid lipofuscinosis. Neurobiology of disease 16**:** 346-359

Bill CA, Nickoloff JA (2001) Spontaneous and ultraviolet light-induced direct repeat recombination in mammalian cells frequently results in repeat deletion. Mutat Res 487**:** 41-50

Birkenmeier EH, Barker JE, Vogler CA, Kyle JW, Sly WS, Gwynn B, Levy B, Pegors C (1991) Increased life span and correction of metabolic defects in murine mucopolysaccharidosis type VII after syngeneic bone marrow transplantation. Blood 78**:** 3081-3092

Biswas S, LeVine SM (2002) Substrate-reduction therapy enhances the benefits of bone marrow transplantation in young mice with globoid cell leukodystrophy. Pediatr Res 51**:** 40-47

Boustany RM (2013) Lysosomal storage diseases--the horizon expands. Nat Rev Neurol 9**:** 583-598

Burger C, Gorbatyuk OS, Velardo MJ, Peden CS, Williams P, Zolotukhin S, Reier PJ, Mandel RJ, Muzyczka N (2004) Recombinant AAV viral vectors pseudotyped with viral capsids from serotypes 1, 2, and 5 display differential efficiency and cell tropism after delivery to different regions of the central nervous system. Molecular therapy : the journal of the American Society of Gene Therapy 10**:** 302-317

Camp LA, Hofmann SL (1993) Purification and properties of a palmitoyl-protein thioesterase that cleaves palmitate from H-Ras. The Journal of biological chemistry 268**:** 22566-22574

Camp LA, Verkruyse LA, Afendis SJ, Slaughter CA, Hofmann SL (1994) Molecular cloning and expression of palmitoyl-protein thioesterase. The Journal of biological chemistry 269**:** 23212-23219

Cantor AB, Kornfeld S (1992) A method for [3H]mannose labeling of Asn-linked oligosaccharides on recombinant glycoproteins synthesized in Xenopus oocytes. Anal Biochem 205**:** 220-226

Castelvetri LC, Givogri MI, Zhu H, Smith B, Lopez-Rosas A, Qiu X, van Breemen R, Bongarzone ER (2011) Axonopathy is a compounding factor in the pathogenesis of Krabbe disease. Acta Neuropathol 122**:** 35-48

Chu-LaGraff Q, Blanchette C, O'Hern P, Denefrio C (2010) The Batten disease Palmitoyl Protein Thioesterase 1 gene regulates neural specification and axon connectivity during Drosophila embryonic development. PloS one 5**:** e14402

Cox TM (2005) Substrate reduction therapy for lysosomal storage diseases. Acta Paediatr Suppl 94**:** 69-75; discussion 57

Cox TM, Cachon-Gonzalez MB (2012) The cellular pathology of lysosomal diseases. The Journal of pathology 226**:** 241-254

Dahms NM, Lobel P, Kornfeld S (1989) Mannose 6-phosphate receptors and lysosomal enzyme targeting. The Journal of biological chemistry 264**:** 12115-12118

Das AK, Lu JY, Hofmann SL (2001) Biochemical analysis of mutations in palmitoyl-protein thioesterase causing infantile and late-onset forms of neuronal ceroid lipofuscinosis. Human molecular genetics 10**:** 1431-1439

Dayton RD, Wang DB, Klein RL (2012) The advent of AAV9 expands applications for brain and spinal cord gene delivery. Expert Opin Biol Ther 12**:** 757-766

Dearborn JT, Harmon SK, Fowler SC, O'Malley KL, Taylor GT, Sands MS, Wozniak DF (2015) Comprehensive functional characterization of murine infantile Batten disease including Parkinson-like behavior and dopaminergic markers. Sci Rep 5**:** 12752

Dearborn JT, Ramachandran S, Shyng C, Lu JY, Thornton J, Hofmann SL, Sands MS (2016) Histochemical localization of palmitoyl protein thioesterase-1 activity. Molecular genetics and metabolism 117**:** 210-216

Deduve C (1964) From Cytases to Lysosomes. Fed Proc 23**:** 1045-1049

Dull T, Zufferey R, Kelly M, Mandel RJ, Nguyen M, Trono D, Naldini L (1998) A third-generation lentivirus vector with a conditional packaging system. Journal of virology 72**:** 8463-8471

Dyken PR (1989) The neuronal ceroid lipofuscinoses. J Child Neurol 4**:** 165-174

Elliger SS, Elliger CA, Aguilar CP, Raju NR, Watson GL (1999) Elimination of lysosomal storage in brains of MPS VII mice treated by intrathecal administration of an adeno-associated virus vector. Gene Ther 6**:** 1175-1178

Federici T, Taub JS, Baum GR, Gray SJ, Grieger JC, Matthews KA, Handy CR, Passini MA, Samulski RJ, Boulis NM (2012) Robust spinal motor neuron transduction following intrathecal delivery of AAV9 in pigs. Gene Ther 19**:** 852-859

Feng G, Mellor RH, Bernstein M, Keller-Peck C, Nguyen QT, Wallace M, Nerbonne JM, Lichtman JW, Sanes JR (2000) Imaging neuronal subsets in transgenic mice expressing multiple spectral variants of GFP. Neuron 28**:** 41-51

Foust KD, Nurre E, Montgomery CL, Hernandez A, Chan CM, Kaspar BK (2009) Intravascular AAV9 preferentially targets neonatal neurons and adult astrocytes. Nat Biotechnol 27**:** 59-65

Fratantoni JC, Hall CW, Neufeld EF (1968) Hurler and Hunter syndromes: mutual correction of the defect in cultured fibroblasts. Science 162**:** 570-572

Friedmann T, Roblin R (1972) Gene therapy for human genetic disease? Science 175**:** 949-955

Fu H, Muenzer J, Samulski RJ, Breese G, Sifford J, Zeng X, McCarty DM (2003) Self-complementary adeno-associated virus serotype 2 vector: global distribution and broad dispersion of AAV-mediated transgene expression in mouse brain. Molecular therapy : the journal of the American Society of Gene Therapy 8**:** 911-917

Fukata M, Sekiya A, Murakami T, Yokoi N, Fukata Y (2015) Postsynaptic nanodomains generated by local palmitoylation cycles. Biochemical Society transactions 43**:** 199-204

Fukata Y, Dimitrov A, Boncompain G, Vielemeyer O, Perez F, Fukata M (2013) Local palmitoylation cycles define activity-regulated postsynaptic subdomains. The Journal of cell biology 202**:** 145-161

Fukata Y, Fukata M (2010) Protein palmitoylation in neuronal development and synaptic plasticity. Nat Rev Neurosci 11**:** 161-175

Fukata Y, Murakami T, Yokoi N, Fukata M (2016) Local Palmitoylation Cycles and Specialized Membrane Domain Organization. Curr Top Membr 77**:** 97-141

Fuller M, Meikle PJ, Hopwood JJ (2006) Epidemiology of lysosomal storage diseases: an overview. In Fabry Disease: Perspectives from 5 Years of FOS, Mehta A, Beck M, Sunder-Plassmann G (eds). Oxford

Galvin N, Vogler C, Levy B, Kovacs A, Griffey M, Sands MS (2008) A murine model of infantile neuronal ceroid lipofuscinosis-ultrastructural evaluation of storage in the central nervous system and viscera. Pediatric and developmental pathology : the official journal of the Society for Pediatric Pathology and the Paediatric Pathology Society 11**:** 185-192

Geraets RD, Koh S, Hastings ML, Kielian T, Pearce DA, Weimer JM (2016) Moving towards effective therapeutic strategies for Neuronal Ceroid Lipofuscinosis. Orphanet J Rare Dis 11**:** 40

Glaser RL, Hickey AJ, Chotkowski HL, Chu-LaGraff Q (2003) Characterization of Drosophila palmitoyl-protein thioesterase 1. Gene 312**:** 271-279

Goebel HH, Vesa J, Reitter B, Goecke TO, Schneider-Ratzke B, Merz E (1995) Prenatal diagnosis of infantile neuronal ceroid-lipofuscinosis: a combined electron microscopic and molecular genetic approach. Brain & development 17**:** 83-88

Goebel HH, Wisniewski KE (2004) Current state of clinical and morphological features in human NCL. Brain pathology 14**:** 61-69

Gray SJ, Nagabhushan Kalburgi S, McCown TJ, Jude Samulski R (2013) Global CNS gene delivery and evasion of anti-AAV-neutralizing antibodies by intrathecal AAV administration in non-human primates. Gene Ther 20**:** 450-459

Griffey M, Bible E, Vogler C, Levy B, Gupta P, Cooper J, Sands MS (2004) Adeno-associated virus 2-mediated gene therapy decreases autofluorescent storage material and increases brain mass in a murine model of infantile neuronal ceroid lipofuscinosis. Neurobiology of disease 16**:** 360-369

Griffey M, Macauley SL, Ogilvie JM, Sands MS (2005) AAV2-mediated ocular gene therapy for infantile neuronal ceroid lipofuscinosis. Molecular therapy : the journal of the American Society of Gene Therapy 12**:** 413-421

Griffey MA, Wozniak D, Wong M, Bible E, Johnson K, Rothman SM, Wentz AE, Cooper JD, Sands MS (2006) CNS-directed AAV2-mediated gene therapy ameliorates functional deficits in a murine model of infantile neuronal ceroid lipofuscinosis. Molecular therapy : the journal of the American Society of Gene Therapy 13**:** 538-547

Guarnieri FG, Arterburn LM, Penno MB, Cha Y, August JT (1993) The motif Tyr-X-X-hydrophobic residue mediates lysosomal membrane targeting of lysosome-associated membrane protein 1. The Journal of biological chemistry 268**:** 1941-1946

Guo Y, Wang D, Qiao T, Yang C, Su Q, Gao G, Xu Z (2016) A Single Injection of Recombinant Adeno-Associated Virus into the Lumbar Cistern Delivers Transgene Expression Throughout the Whole Spinal Cord. Mol Neurobiol 53**:** 3235-3248

Gupta P, Soyombo AA, Atashband A, Wisniewski KE, Shelton JM, Richardson JA, Hammer RE, Hofmann SL (2001) Disruption of PPT1 or PPT2 causes neuronal ceroid lipofuscinosis in knockout mice. Proceedings of the National Academy of Sciences of the United States of America 98**:** 13566-13571

Haltia M, Rapola J, Santavuori P (1973a) Infantile type of so-called neuronal ceroid-lipofuscinosis. Histological and electron microscopic studies. Acta Neuropathol 26**:** 157-170

Haltia M, Rapola J, Santavuori P, Keranen A (1973b) Infantile type of so-called neuronal ceroid-lipofuscinosis. 2. Morphological and biochemical studies. Journal of the neurological sciences 18**:** 269-285

Haruyama N, Cho A, Kulkarni AB (2009) Overview: engineering transgenic constructs and mice. Curr Protoc Cell Biol Chapter 19**:** Unit 19 10

Hawkins-Salsbury JA, Parameswar AR, Jiang X, Schlesinger PH, Bongarzone E, Ory DS, Demchenko AV, Sands MS (2013) Psychosine, the cytotoxic sphingolipid that accumulates in globoid cell leukodystrophy, alters membrane architecture. Journal of lipid research 54**:** 3303-3311

Hawkins-Salsbury JA, Reddy AS, Sands MS (2011) Combination therapies for lysosomal storage disease: is the whole greater than the sum of its parts? Human molecular genetics 20**:** R54-60

Hawkins-Salsbury JA, Shea L, Jiang X, Hunter DA, Guzman AM, Reddy AS, Qin EY, Li Y, Gray SJ, Ory DS et al (2015) Mechanism-based combination treatment dramatically increases therapeutic efficacy in murine globoid cell leukodystrophy. The Journal of neuroscience : the official journal of the Society for Neuroscience 35**:** 6495-6505

Heldermon CD, Hennig AK, Ohlemiller KK, Ogilvie JM, Herzog ED, Breidenbach A, Vogler C, Wozniak DF, Sands MS (2007) Development of sensory, motor and behavioral deficits in the murine model of Sanfilippo syndrome type B. PloS one 2**:** e772

Hellsten E, Vesa J, Jalanko A, Peltonen L (1997) From locus to cellular disturbances: positional cloning of the infantile neuronal ceroid lipofuscinosis gene. Neuropediatrics 28**:** 9-11

Hellsten E, Vesa J, Olkkonen VM, Jalanko A, Peltonen L (1996) Human palmitoyl protein thioesterase: evidence for lysosomal targeting of the enzyme and disturbed cellular routing in infantile neuronal ceroid lipofuscinosis. The EMBO journal 15**:** 5240-5245

Hendricks CA, Almeida KH, Stitt MS, Jonnalagadda VS, Rugo RE, Kerrison GF, Engelward BP (2003) Spontaneous mitotic homologous recombination at an enhanced yellow fluorescent protein (EYFP) cDNA direct repeat in transgenic mice. Proceedings of the National Academy of Sciences of the United States of America 100**:** 6325-6330

Hers HG (1965) Inborn Lysosomal Diseases. Gastroenterology 48**:** 625-633

Hickman S, Neufeld EF (1972) A hypothesis for I-cell disease: defective hydrolases that do not enter lysosomes. Biochemical and biophysical research communications 49: 992-999

Hofmann SL, Das AK, Lu JY, Soyombo AA (2001a) Positional candidate gene cloning of CLN1. Advances in genetics 45: 69-92

Hofmann SL, Das AK, Lu JY, Wisniewski KE, Gupta P (2001b) Infantile neuronal ceroid lipofuscinosis: no longer just a 'Finnish' disease. European journal of paediatric neurology : EJPN : official journal of the European Paediatric Neurology Society 5 Suppl A: 47-51

Hofmann SL, Das AK, Yi W, Lu JY, Wisniewski KE (1999) Genotype-phenotype correlations in neuronal ceroid lipofuscinosis due to palmitoyl-protein thioesterase deficiency. Molecular genetics and metabolism 66: 234-239

Hordeaux J, Dubreil L, Deniaud J, Iacobelli F, Moreau S, Ledevin M, Le Guiner C, Blouin V, Le Duff J, Mendes-Madeira A et al (2015) Efficient central nervous system AAVrh10-mediated intrathecal gene transfer in adult and neonate rats. Gene Ther 22: 316-324

Hu J, Lu JY, Wong AM, Hynan LS, Birnbaum SG, Yilmaz DS, Streit BM, Lenartowicz EM, Thompson TC, Cooper JD et al (2012) Intravenous high-dose enzyme replacement therapy with recombinant palmitoyl-protein thioesterase reduces visceral lysosomal storage and modestly prolongs survival in a preclinical mouse model of infantile neuronal ceroid lipofuscinosis. Molecular genetics and metabolism

Hu W, Ralay Ranaivo H, Roy SM, Behanna HA, Wing LK, Munoz L, Guo L, Van Eldik LJ, Watterson DM (2007) Development of a novel therapeutic suppressor of brain proinflammatory cytokine up-regulation that attenuates synaptic dysfunction and behavioral deficits. Bioorg Med Chem Lett 17: 414-418

Isosomppi J, Heinonen O, Hiltunen JO, Greene ND, Vesa J, Uusitalo A, Mitchison HM, Saarma M, Jalanko A, Peltonen L (1999) Developmental expression of palmitoyl protein thioesterase in normal mice. Brain research Developmental brain research 118: 1-11

Jacques SJ, Ahmed Z, Forbes A, Douglas MR, Vigenswara V, Berry M, Logan A (2012) AAV8(gfp) preferentially targets large diameter dorsal root ganglion neurones after both intra-dorsal root ganglion and intrathecal injection. Molecular and cellular neurosciences 49: 464-474

Jadav RH, Sinha S, Yasha TC, Aravinda H, Gayathri N, Rao S, Bindu PS, Satishchandra P (2014) Clinical, electrophysiological, imaging, and ultrastructural description in 68 patients with neuronal ceroid lipofuscinoses and its subtypes. Pediatric neurology 50: 85-95

Jadav RH, Sinha S, Yasha TC, Aravinda H, Rao S, Bindu PS, Satishchandra P (2012) Magnetic resonance imaging in neuronal ceroid lipofuscinosis and its subtypes. Neuroradiol J 25**:** 755-761

Jardim LB, Villanueva MM, de Souza CF, Netto CB (2010) Clinical aspects of neuropathic lysosomal storage disorders. Journal of inherited metabolic disease 33**:** 315-329

Jeyakumar M, Norflus F, Tifft CJ, Cortina-Borja M, Butters TD, Proia RL, Perry VH, Dwek RA, Platt FM (2001) Enhanced survival in Sandhoff disease mice receiving a combination of substrate deprivation therapy and bone marrow transplantation. Blood 97**:** 327-329

Jokiaho I, Puhakka L, Santavuori P, Manninen T, Nyman K, Peltonen L (1990) Infantile neuronal ceroid-lipofuscinosis is not an allelic form of Batten disease: exclusion of chromosome 16 region with linkage analyses. Genomics 8**:** 391-393

Joshi M, Keith Pittman H, Haisch C, Verbanac K (2008) Real-time PCR to determine transgene copy number and to quantitate the biolocalization of adoptively transferred cells from EGFP-transgenic mice. Biotechniques 45**:** 247-258

Khaibullina A, Kenyon N, Guptill V, Quezado MM, Wang L, Koziol D, Wesley R, Moya PR, Zhang Z, Saha A et al (2012) In a model of Batten disease, palmitoyl protein thioesterase-1 deficiency is associated with brown adipose tissue and thermoregulation abnormalities. PloS one 7**:** e48733

Kielar C, Maddox L, Bible E, Pontikis CC, Macauley SL, Griffey MA, Wong M, Sands MS, Cooper JD (2007) Successive neuron loss in the thalamus and cortex in a mouse model of infantile neuronal ceroid lipofuscinosis. Neurobiology of disease 25**:** 150-162

Kielar C, Wishart TM, Palmer A, Dihanich S, Wong AM, Macauley SL, Chan CH, Sands MS, Pearce DA, Cooper JD et al (2009) Molecular correlates of axonal and synaptic pathology in mouse models of Batten disease. Human molecular genetics 18**:** 4066-4080

Kim SJ, Zhang Z, Sarkar C, Tsai PC, Lee YC, Dye L, Mukherjee AB (2008) Palmitoyl protein thioesterase-1 deficiency impairs synaptic vesicle recycling at nerve terminals, contributing to neuropathology in humans and mice. The Journal of clinical investigation 118**:** 3075-3086

Kornfeld S, Reitman ML, Varki A, Goldberg D, Gabel CA (1982) Steps in the phosphorylation of the high mannose oligosaccharides of lysosomal enzymes. Ciba Found Symp**:** 138-156

Kousi M, Lehesjoki AE, Mole SE (2012) Update of the mutation spectrum and clinical correlations of over 360 mutations in eight genes that underlie the neuronal ceroid lipofuscinoses. Human mutation 33**:** 42-63

Kuhl TG, Dihanich S, Wong AM, Cooper JD (2013) Regional brain atrophy in mouse models of neuronal ceroid lipofuscinosis: a new rostrocaudal perspective. J Child Neurol 28**:** 1117-1122

Lee JP, Jeyakumar M, Gonzalez R, Takahashi H, Lee PJ, Baek RC, Clark D, Rose H, Fu G, Clarke J et al (2007) Stem cells act through multiple mechanisms to benefit mice with neurodegenerative metabolic disease. Nature medicine 13**:** 439-447

Lehtovirta M, Kyttala A, Eskelinen EL, Hess M, Heinonen O, Jalanko A (2001) Palmitoyl protein thioesterase (PPT) localizes into synaptosomes and synaptic vesicles in neurons: implications for infantile neuronal ceroid lipofuscinosis (INCL). Human molecular genetics 10**:** 69-75

Levin SW, Baker EH, Zein WM, Zhang Z, Quezado ZM, Miao N, Gropman A, Griffin KJ, Bianconi S, Chandra G et al (2014) Oral cysteamine bitartrate and N-acetylcysteine for patients with infantile neuronal ceroid lipofuscinosis: a pilot study. Lancet Neurol 13**:** 777-787

Lu JY, Hu J, Hofmann SL (2010) Human recombinant palmitoyl-protein thioesterase-1 (PPT1) for preclinical evaluation of enzyme replacement therapy for infantile neuronal ceroid lipofuscinosis. Molecular genetics and metabolism 99**:** 374-378

Lu JY, Nelvagal HR, Wang L, Birnbaum SG, Cooper JD, Hofmann SL (2015) Intrathecal enzyme replacement therapy improves motor function and survival in a preclinical mouse model of infantile neuronal ceroid lipofuscinosis. Molecular genetics and metabolism 116**:** 98-105

Lyly A, von Schantz C, Salonen T, Kopra O, Saarela J, Jauhiainen M, Kyttala A, Jalanko A (2007) Glycosylation, transport, and complex formation of palmitoyl protein thioesterase 1 (PPT1)--distinct characteristics in neurons. BMC cell biology 8**:** 22

Macauley SL, Pekny M, Sands MS (2011) The role of attenuated astrocyte activation in infantile neuronal ceroid lipofuscinosis. The Journal of neuroscience : the official journal of the Society for Neuroscience 31**:** 15575-15585

Macauley SL, Roberts MS, Wong AM, McSloy F, Reddy AS, Cooper JD, Sands MS (2012) Synergistic effects of central nervous system-directed gene therapy and bone marrow transplantation in the murine model of infantile neuronal ceroid lipofuscinosis. Annals of neurology

Macauley SL, Wong AM, Shyng C, Augner DP, Dearborn JT, Pearse Y, Roberts MS, Fowler SC, Cooper JD, Watterson DM et al (2014) An anti-neuroinflammatory that targets dysregulated glia enhances the efficacy of CNS-directed gene therapy in murine infantile neuronal ceroid

lipofuscinosis. The Journal of neuroscience : the official journal of the Society for Neuroscience 34**:** 13077-13082

Macauley SL, Wozniak DF, Kielar C, Tan Y, Cooper JD, Sands MS (2009) Cerebellar pathology and motor deficits in the palmitoyl protein thioesterase 1-deficient mouse. Experimental neurology 217**:** 124-135

Madhavarao CN, Arun P, Anikster Y, Mog SR, Staretz-Chacham O, Moffett JR, Grunberg NE, Gahl WA, Namboodiri AM (2009) Glyceryl triacetate for Canavan disease: a low-dose trial in infants and evaluation of a higher dose for toxicity in the tremor rat model. Journal of inherited metabolic disease 32**:** 640-650

Maire I (2001) Is genotype determination useful in predicting the clinical phenotype in lysosomal storage diseases? Journal of inherited metabolic disease 24 Suppl 2**:** 57-61; discussion 45-56

Mao Y, Wang X, Yan R, Hu W, Li A, Wang S, Li H (2016) Single point mutation in adeno-associated viral vectors -DJ capsid leads to improvement for gene delivery in vivo. BMC Biotechnol 16**:** 1

Marathe S, Miranda SR, Devlin C, Johns A, Kuriakose G, Williams KJ, Schuchman EH, Tabas I (2000) Creation of a mouse model for non-neurological (type B) Niemann-Pick disease by stable, low level expression of lysosomal sphingomyelinase in the absence of secretory sphingomyelinase: relationship between brain intra-lysosomal enzyme activity and central nervous system function. Human molecular genetics 9**:** 1967-1976

Martin BR, Wang C, Adibekian A, Tully SE, Cravatt BF (2012) Global profiling of dynamic protein palmitoylation. Nature methods 9**:** 84-89

Mole SE, Williams RE (1993) Neuronal Ceroid-Lipofuscinoses. In GeneReviews, Pagon RA, Bird TD, Dolan CR, Stephens K, Adam MP (eds). Seattle (WA)

Natowicz MR, Chi MM, Lowry OH, Sly WS (1979) Enzymatic identification of mannose 6-phosphate on the recognition marker for receptor-mediated pinocytosis of beta-glucuronidase by human fibroblasts. Proceedings of the National Academy of Sciences of the United States of America 76**:** 4322-4326

Neufeld EF (1980) The uptake of enzymes into lysosomes: an overview. Birth Defects Orig Artic Ser 16**:** 77-84

Neufeld EF (1991) Lysosomal storage diseases. Annu Rev Biochem 60**:** 257-280

Neufeld EF (2006) Enzyme replacement therapy - a brief history. In Fabry Disease: Perspectives from 5 Years of FOS, Mehta A, Beck M, Sunder-Plassmann G (eds). Oxford

Neufeld EF, Fratantoni JC (1970) Inborn errors of mucopolysaccharide metabolism. Science 169**:** 141-146

O'Connor LH, Erway LC, Vogler CA, Sly WS, Nicholes A, Grubb J, Holmberg SW, Levy B, Sands MS (1998) Enzyme replacement therapy for murine mucopolysaccharidosis type VII leads to improvements in behavior and auditory function. The Journal of clinical investigation 101**:** 1394-1400

Ostergaard JR, Rasmussen TB, Molgaard H (2011) Cardiac involvement in juvenile neuronal ceroid lipofuscinosis (Batten disease). Neurology 76**:** 1245-1251

Palmer DN, Barry LA, Tyynela J, Cooper JD (2013) NCL disease mechanisms. Biochimica et biophysica acta 1832**:** 1882-1893

Parenti G, Andria G, Ballabio A (2015) Lysosomal storage diseases: from pathophysiology to therapy. Annu Rev Med 66**:** 471-486

Passini MA, Bu J, Fidler JA, Ziegler RJ, Foley JW, Dodge JC, Yang WW, Clarke J, Taksir TV, Griffiths DA et al (2007) Combination brain and systemic injections of AAV provide maximal functional and survival benefits in the Niemann-Pick mouse. Proceedings of the National Academy of Sciences of the United States of America 104**:** 9505-9510

Pastores GM (2010) Therapeutic approaches for lysosomal storage diseases. Ther Adv Endocrinol Metab 1**:** 177-188

Platt FM, Lachmann RH (2009) Treating lysosomal storage disorders: current practice and future prospects. Biochimica et biophysica acta 1793**:** 737-745

Qiao X, Lu JY, Hofmann SL (2007) Gene expression profiling in a mouse model of infantile neuronal ceroid lipofuscinosis reveals upregulation of immediate early genes and mediators of the inflammatory response. BMC neuroscience 8**:** 95

Qin EY, Hawkins-Salsbury JA, Jiang X, Reddy AS, Farber NB, Ory DS, Sands MS (2012) Bone marrow transplantation increases efficacy of central nervous system-directed enzyme replacement therapy in the murine model of globoid cell leukodystrophy. Molecular genetics and metabolism 107**:** 186-196

Reddy AS, Kim JH, Hawkins-Salsbury JA, Macauley SL, Tracy ET, Vogler CA, Han X, Song SK, Wozniak DF, Fowler SC et al (2011) Bone marrow transplantation augments the effect of brain- and spinal cord-directed adeno-associated virus 2/5 gene therapy by altering inflammation in the murine model of globoid-cell leukodystrophy. The Journal of neuroscience : the official journal of the Society for Neuroscience 31**:** 9945-9957

Roberts MS, Macauley SL, Wong AM, Yilmas D, Hohm S, Cooper JD, Sands MS (2012) Combination small molecule PPT1 mimetic and CNS-directed gene therapy as a treatment for infantile neuronal ceroid lipofuscinosis. Journal of inherited metabolic disease

Rohrer J, Schweizer A, Russell D, Kornfeld S (1996) The targeting of Lamp1 to lysosomes is dependent on the spacing of its cytoplasmic tail tyrosine sorting motif relative to the membrane. The Journal of cell biology 132**:** 565-576

Rosenberg JB, Sondhi D, Rubin DG, Monette S, Chen A, Cram S, De BP, Kaminsky SM, Sevin C, Aubourg P et al (2014) Comparative efficacy and safety of multiple routes of direct CNS administration of adeno-associated virus gene transfer vector serotype rh.10 expressing the human arylsulfatase A cDNA to nonhuman primates. Hum Gene Ther Clin Dev 25**:** 164-177

Saha A, Kim SJ, Zhang Z, Lee YC, Sarkar C, Tsai PC, Mukherjee AB (2008) RAGE signaling contributes to neuroinflammation in infantile neuronal ceroid lipofuscinosis. FEBS letters 582**:** 3823-3831

Saha A, Sarkar C, Singh SP, Zhang Z, Munasinghe J, Peng S, Chandra G, Kong E, Mukherjee AB (2012) The blood-brain barrier is disrupted in a mouse model of infantile neuronal ceroid lipofuscinosis: amelioration by resveratrol. Human molecular genetics 21**:** 2233-2244

Sands MS (2013) Considerations for the treatment of infantile neuronal ceroid lipofuscinosis (infantile Batten disease). J Child Neurol 28**:** 1151-1158

Sands MS, Barker JE, Vogler C, Levy B, Gwynn B, Galvin N, Sly WS, Birkenmeier E (1993) Treatment of murine mucopolysaccharidosis type VII by syngeneic bone marrow transplantation in neonates. Lab Invest 68**:** 676-686

Sands MS, Davidson BL (2006) Gene therapy for lysosomal storage diseases. Molecular therapy : the journal of the American Society of Gene Therapy 13**:** 839-849

Sands MS, Vogler C, Kyle JW, Grubb JH, Levy B, Galvin N, Sly WS, Birkenmeier EH (1994) Enzyme replacement therapy for murine mucopolysaccharidosis type VII. The Journal of clinical investigation 93**:** 2324-2331

Santavuori P, Haltia M, Rapola J (1974) Infantile type of so-called neuronal ceroid-lipofuscinosis. Developmental medicine and child neurology 16**:** 644-653

Santavuori P, Haltia M, Rapola J, Raitta C (1973) Infantile type of so-called neuronal ceroid-lipofuscinosis. 1. A clinical study of 15 patients. Journal of the neurological sciences 18**:** 257-267

Santavuori P, Raininko R, Vanhanen SL, Launes J, Sainio K (1992) MRI of the brain, EEG sleep spindles and SPECT in the early diagnosis of infantile neuronal ceroid lipofuscinosis. Developmental medicine and child neurology 34**:** 61-65

Sarkar C, Chandra G, Peng S, Zhang Z, Liu A, Mukherjee AB (2013) Neuroprotection and lifespan extension in Ppt1(-/-) mice by NtBuHA: therapeutic implications for INCL. Nat Neurosci 16**:** 1608-1617

Sarkar C, Zhang Z, Mukherjee AB (2011) Stop codon read-through with PTC124 induces palmitoyl-protein thioesterase-1 activity, reduces thioester load and suppresses apoptosis in cultured cells from INCL patients. Molecular genetics and metabolism 104**:** 338-345

Schonherr E, Jarvelainen HT, Sandell LJ, Wight TN (1991) Effects of platelet-derived growth factor and transforming growth factor-beta 1 on the synthesis of a large versican-like chondroitin sulfate proteoglycan by arterial smooth muscle cells. The Journal of biological chemistry 266**:** 17640-17647

Schriner JE, Yi W, Hofmann SL (1996) cDNA and genomic cloning of human palmitoyl-protein thioesterase (PPT), the enzyme defective in infantile neuronal ceroid lipofuscinosis. Genomics 34**:** 317-322

Schultz ML, Tecedor L, Chang M, Davidson BL (2011) Clarifying lysosomal storage diseases. Trends in neurosciences 34**:** 401-410

Schuster DJ, Dykstra JA, Riedl MS, Kitto KF, Belur LR, McIvor RS, Elde RP, Fairbanks CA, Vulchanova L (2014) Biodistribution of adeno-associated virus serotype 9 (AAV9) vector after intrathecal and intravenous delivery in mouse. Front Neuroanat 8**:** 42

Scifo E, Szwajda A, Soliymani R, Pezzini F, Bianchi M, Dapkunas A, Debski J, Uusi-Rauva K, Dadlez M, Gingras AC et al (2015) Proteomic analysis of the palmitoyl protein thioesterase 1 interactome in SH-SY5Y human neuroblastoma cells. Journal of proteomics 123**:** 42-53

Shyng C, Sands MS (2014) Astrocytosis in infantile neuronal ceroid lipofuscinosis: friend or foe? Biochemical Society transactions 42**:** 1282-1285

Siegismund G, Goebel HH, Loblich HJ (1982) Ultrastructure and visceral distribution of lipopigments in infantile neuronal ceroid-lipofuscinosis. Pathol Res Pract 175**:** 335-347

Simonati A, Tessa A, Bernardina BD, Biancheri R, Veneselli E, Tozzi G, Bonsignore M, Grosso S, Piemonte F, Santorelli FM (2009) Variant late infantile neuronal ceroid lipofuscinosis because of CLN1 mutations. Pediatric neurology 40**:** 271-276

Smedemark-Margulies N, Trapani JG (2013) Tools, methods, and applications for optophysiology in neuroscience. Front Mol Neurosci 6**:** 18

Smith S, Witkowski A, Joshi AK (2003) Structural and functional organization of the animal fatty acid synthase. Prog Lipid Res 42**:** 289-317

Sohal VS, Zhang F, Yizhar O, Deisseroth K (2009) Parvalbumin neurons and gamma rhythms enhance cortical circuit performance. Nature 459**:** 698-702

Suopanki J, Partanen S, Ezaki J, Baumann M, Kominami E, Tyynela J (2000) Developmental changes in the expression of neuronal ceroid lipofuscinoses-linked proteins. Molecular genetics and metabolism 71**:** 190-194

Swain GP, Prociuk M, Bagel JH, O'Donnell P, Berger K, Drobatz K, Gurda BL, Haskins ME, Sands MS, Vite CH (2014) Adeno-associated virus serotypes 9 and rh10 mediate strong neuronal transduction of the dog brain. Gene Ther 21**:** 28-36

Syvanen AC, Jarvela I, Paunio T, Vesa J (1997) DNA diagnosis and identification of carriers of infantile and juvenile neuronal ceroid lipofuscinoses. Neuropediatrics 28**:** 63-66

Tamaki SJ, Jacobs Y, Dohse M, Capela A, Cooper JD, Reitsma M, He D, Tushinski R, Belichenko PV, Salehi A et al (2009) Neuroprotection of host cells by human central nervous system stem cells in a mouse model of infantile neuronal ceroid lipofuscinosis. Cell stem cell 5**:** 310-319

Taupin P (2006) HuCNS-SC (StemCells). Curr Opin Mol Ther 8**:** 156-163

Tikka S, Monogioudi E, Gotsopoulos A, Soliymani R, Pezzini F, Scifo E, Uusi-Rauva K, Tyynela J, Baumann M, Jalanko A et al (2016) Proteomic Profiling in the Brain of CLN1 Disease Model Reveals Affected Functional Modules. Neuromolecular medicine 18**:** 109-133

Tyynela J, Palmer DN, Baumann M, Haltia M (1993) Storage of saposins A and D in infantile neuronal ceroid-lipofuscinosis. FEBS letters 330**:** 8-12

Valayannopoulos V (2013) Enzyme replacement therapy and substrate reduction therapy in lysosomal storage disorders with neurological expression. Handb Clin Neurol 113**:** 1851-1857

van Diggelen OP, Keulemans JL, Winchester B, Hofman IL, Vanhanen SL, Santavuori P, Voznyi YV (1999) A rapid fluorogenic palmitoyl-protein thioesterase assay: pre- and postnatal diagnosis of INCL. Molecular genetics and metabolism 66**:** 240-244

Vanhanen SL, Raininko R, Autti T, Santavuori P (1995a) MRI evaluation of the brain in infantile neuronal ceroid-lipofuscinosis. Part 2: MRI findings in 21 patients. J Child Neurol 10**:** 444-450

Vanhanen SL, Raininko R, Santavuori P, Autti T, Haltia M (1995b) MRI evaluation of the brain in infantile neuronal ceroid-lipofuscinosis. Part 1: Postmortem MRI with histopathologic correlation. J Child Neurol 10**:** 438-443

Vanhanen SL, Sainio K, Lappi M, Santavuori P (1997) EEG and evoked potentials in infantile neuronal ceroid-lipofuscinosis. Developmental medicine and child neurology 39**:** 456-463

Varki A, Kornfeld S (1980) Structural studies of phosphorylated high mannose-type oligosaccharides. The Journal of biological chemistry 255**:** 10847-10858

Verkruyse LA, Hofmann SL (1996) Lysosomal targeting of palmitoyl-protein thioesterase. The Journal of biological chemistry 271**:** 15831-15836

Verkruyse LA, Natowicz MR, Hofmann SL (1997) Palmitoyl-protein thioesterase deficiency in fibroblasts of individuals with infantile neuronal ceroid lipofuscinosis and I-cell disease. Biochimica et biophysica acta 1361**:** 1-5

Vesa J, Hellsten E, Verkruyse LA, Camp LA, Rapola J, Santavuori P, Hofmann SL, Peltonen L (1995) Mutations in the palmitoyl protein thioesterase gene causing infantile neuronal ceroid lipofuscinosis. Nature 376**:** 584-587

Virmani T, Gupta P, Liu X, Kavalali ET, Hofmann SL (2005) Progressively reduced synaptic vesicle pool size in cultured neurons derived from neuronal ceroid lipofuscinosis-1 knockout mice. Neurobiology of disease 20**:** 314-323

Vitner EB, Platt FM, Futerman AH (2010) Common and uncommon pathogenic cascades in lysosomal storage diseases. The Journal of biological chemistry 285**:** 20423-20427

Vulchanova L, Schuster DJ, Belur LR, Riedl MS, Podetz-Pedersen KM, Kitto KF, Wilcox GL, McIvor RS, Fairbanks CA (2010) Differential adeno-associated virus mediated gene transfer to sensory neurons following intrathecal delivery by direct lumbar puncture. Mol Pain 6**:** 31

Wei H, Zhang Z, Saha A, Peng S, Chandra G, Quezado Z, Mukherjee AB (2011) Disruption of adaptive energy metabolism and elevated ribosomal p-S6K1 levels contribute to INCL pathogenesis: partial rescue by resveratrol. Human molecular genetics 20**:** 1111-1121

Weleber RG, Gupta N, Trzupek KM, Wepner MS, Kurz DE, Milam AH (2004) Electroretinographic and clinicopathologic correlations of retinal dysfunction in infantile neuronal ceroid lipofuscinosis (infantile Batten disease). Molecular genetics and metabolism 83**:** 128-137

Willingham MC, Pastan IH, Sahagian GG, Jourdian GW, Neufeld EF (1981) Morphologic study of the internalization of a lysosomal enzyme by the mannose 6-phosphate receptor in cultured Chinese hamster ovary cells. Proceedings of the National Academy of Sciences of the United States of America 78**:** 6967-6971

Wisniewski KE, Zhong N, Philippart M (2001) Pheno/genotypic correlations of neuronal ceroid lipofuscinoses. Neurology 57**:** 576-581

Woloszynek JC, Coleman T, Semenkovich CF, Sands MS (2007) Lysosomal dysfunction results in altered energy balance. The Journal of biological chemistry 282**:** 35765-35771

Woloszynek JC, Kovacs A, Ohlemiller KK, Roberts M, Sands MS (2009) Metabolic adaptations to interrupted glycosaminoglycan recycling. The Journal of biological chemistry 284**:** 29684-29691

Wurtele H, Gusew N, Lussier R, Chartrand P (2005) Characterization of in vivo recombination activities in the mouse embryo. Mol Genet Genomics 273**:** 252-263

Young FB, Butland SL, Sanders SS, Sutton LM, Hayden MR (2012) Putting proteins in their place: Palmitoylation in Huntington disease and other neuropsychiatric diseases. Progress in neurobiology 97**:** 220-238

Zambrowicz BP, Imamoto A, Fiering S, Herzenberg LA, Kerr WG, Soriano P (1997) Disruption of overlapping transcripts in the ROSA beta geo 26 gene trap strain leads to widespread

expression of beta-galactosidase in mouse embryos and hematopoietic cells. Proceedings of the National Academy of Sciences of the United States of America 94**:** 3789-3794

Zhang Z, Butler JD, Levin SW, Wisniewski KE, Brooks SS, Mukherjee AB (2001) Lysosomal ceroid depletion by drugs: therapeutic implications for a hereditary neurodegenerative disease of childhood. Nature medicine 7**:** 478-484

Zhang Z, Lee YC, Kim SJ, Choi MS, Tsai PC, Xu Y, Xiao YJ, Zhang P, Heffer A, Mukherjee AB (2006) Palmitoyl-protein thioesterase-1 deficiency mediates the activation of the unfolded protein response and neuronal apoptosis in INCL. Human molecular genetics 15**:** 337-346

Zhang Z, Mandal AK, Wang N, Keck CL, Zimonjic DB, Popescu NC, Mukherjee AB (1999) Palmitoyl-protein thioesterase gene expression in the developing mouse brain and retina: implications for early loss of vision in infantile neuronal ceroid lipofuscinosis. Gene 231**:** 203-211

Zufferey R, Dull T, Mandel RJ, Bukovsky A, Quiroz D, Naldini L, Trono D (1998) Self-inactivating lentivirus vector for safe and efficient in vivo gene delivery. Journal of virology 72**:** 9873-9880

Curriculum Vitae

Charles Shyng

Division of Biology and Biomedical Sciences
Washington University in St. Louis Medical School
St. Louis, MO 63108
Tel: (404)-729-3933
Email: shyng@wustl.edu

Education:

Ph. D – Molecular Cell Biology
Washington University School of Medicine – Division of Biology and Biomedical Sciences,
   August 2016
   Thesis Mentor: Mark Sands, PhD
   Dissertation Title: Infantile Batten Disease: Effective Therapy and Novel Model

B.A. – Biology, Neuroscience Track
Washington University in St. Louis, December 2009

Citizenship:

United States citizen

Research Experience:

Washington University in St. Louis School of Medicine
   DBBS Graduate Student (2010-present)
      Principal Investigator: Mark Sands, Professor
         Understanding the role of neurons and astrocytes in Infantile Neuronal Ceroid
         Lipofuscinoses (INCL, Batten disease). Developing a mouse model that limits the
         capability of palmitoyl-protein thioesterase-1, the enzyme deficient in INCL, from
         cross-correcting neighboring cells. Studying the spinal cord pathology in the mouse
         model of INCL. Developing novel combinatorial therapies to combat disease
         pathogenesis in Infantile Batten disease using small molecule drugs. Utilizing AAV-
         based gene transfer vectors and methodologies to target both the CNS and spinal cord.

Washington University in St. Louis School of Medicine
   Research Technician (2010)
   Undergraduate Research Assistant (2008-2009)
      Principal Investigator: James Huettner, Professor

The temporal expression of sodium channel subunits during *in vitro* induction of human embryonic stem cells

Atlanta Department of Veteran Affairs Lipid Research Laboratory (Summer 2008)
Undergraduate Research Assistant, Lipid Research Laboratory
Principal Investigator: Ngoc-Anh Le, Associate Professor
The effects of a modernized first world diet on lipid oxidation in second world nations

University of Georgia Young Scholars Program (Summer 2005, 2004)
High School Internship
Principal Investigator: Amy Batal, Associate Professor, Department of Poultry Science
Supplemental amino acids to standard feed impact the development of broiler chicken immunity

Principal Investigator: Steven Stice, Professor, Department of Animal and Dairy Science
The efficacy of growing human stem cells on mouse embryonic fibroblasts using qPCR

Teaching Experience:

Biology 404 – Laboratory of Neurophysiology
Teaching Assistant, Fall 2011

Peer Reviewed Publications

Shyng C, Nelvagal HR, Cooper JD, Sands MS. Cell-limited expression of palmitoyl-protein thioesterase-1: a novel model to study Infantile Batten disease. In Preparation.

Shyng C, Nelvagal HR, Dearborn JT, Cooper JD, Sands MS. Therapeutic efficacy of multi-locale CNS-directed gene therapy in Infantile Neuronal Ceroid Lipofuscinoses. In Preparation.

Pearce Y, **Shyng C**, Sands MS, Cooper JD, et al. Cardiac pathology in murine models of NCL. In Preparation

Nelvagal HR, **Shyng C**, Sands MS, Cooper JD, et al. Onset and progression of spinal cord pathology in a murine model of INCL. In Preparation

Dearborn JT, Ramachandran S, **Shyng C**, Lu JY, Thornton J, Hofmann SL, Sands MS. Histochemical Localization of Palmitoyl Protein Thioesterase-1 Activity. *Mol Gen Met*. 2015. PMID: 26597320

Shyng C and Sands MS. Astrocytosis in Infantile Neuronal Ceroid Lipofuscinosis: Friend or Foe?. *Biochem Soc Trans*., 42(5): 1282–1285, 2014. PMID: 25233404

Macauley SL, Wong AM, **Shyng C**, Augner DP, Dearborn JT, Pearse Y, Roberts MS, Fowler SC, Cooper JD, Watterson DM, Sands MS. An anti-neuroinflammatory that targets

dysregulated glia enhances the efficacy of CNS-directed gene therapy in murine infantile neuronal ceroid lipofuscinosis. *J Neurosci*, 34(39):13077–13082, 2014. PMID: 25253854

Abstracts

Shyng C, Nelvagal H, Dearborn JT, Cooper JD, Sands MS. A new and effective target for Infantile Batten Disease. Batten Disease Support and Research Association Conference, St. Louis, Missouri, USA. July 2016. Poster Presentation.

Shyng C, Nelvagal HR, Dearborn JT, Cooper JD, Sands MS. Therapeutic Efficacy of Intracranial and Intrathecal AAV2/9-PPT1 in Infantile Batten Disease. 19th American Society of Gene and Cell Therapy Annual Meeting, Washington D.C., USA, 2016. Oral Presentation.

Shyng C, Macauley SL, Sands MS. Cell-specific expression of Palmitoyl-protein thioesterase-1: utilizing a novel method to study Infantile Batten disease. 14th International Conference on Neuronal Ceroid Lipofuscinosis, Cordoba, Argentina, 2014. Podium Presentation.

Shyng C, Macauley SL, Cooper JD, Pekny M, Sands MS. Neuroinflammation in Infantile Neuronal Ceroid Lipofuscinosis. Astrocytes in Health and Neurodegerative Disease: Joint Biochemical Society/British Neuroscience Association Focused Meeting. Institute of Child Health, London, UK. April 2014. Abstract.

Macauley SL, Roberts MS, Augner DP, Pearse Y, Wong AM, **Shyng C**, Cooper JD, Sands MS. A small molecule anti-inflammatory enhances the therapeutic effects of AAV-mediated CNS-directed gene therapy for infantile neuronal ceroid lipofuscinoses. 13th International Conference on Neuronal Ceroid Lipofuscinoses, London, England, 2012. Podium Presentation.

Shyng C, Macauley SL, Roberts MS, Cooper JD, Watterson DM, Wozniak DF, Sands MS. Combination Therapies dramatically improve the biochemical, histological, and clinical features of Infantile Batten Disease. Batten Disease Support and Research Association Conference, Charlotte, North Carolina, USA. July 2012. Poster Presentation.

Academic and Professional Honors

2016	Meritorious Abstract Travel Award to the 19th American Society of Gene and Cell Therapy Annual Meeting, Washington D.C., USA, 2016
2014	Award for Best Talk at 2014 Washington University School of Medicine Division of Biology and Biomedical Sciences Molecular and Cellular Biology Program Retreat
2014	Travel Award to the 14th International Conference on Neuronal Ceroid Lipofuscinosis, Cordoba, Argentina, 2014.

Professional Organizations

American Society of Cell and Gene Therapy

Associate Member (2016-present)

<u>Volunteer/Leadership Activities:</u>

St. Louis Pick-Up Soccer (over 2,000 members)
 Community and Game Organizer, 2011-present
St. Louis Undergraduate Research Symposium
 Judge, 2012
Division of Biology and Biological Sciences
 Student Advisory Committee (2010-2012)
 Graduate Student Senate DBBS Senator (2011-2012)
 Future Educators Co-chair (2011-2012)
Missouri Junior Science and Humanities Symposium
 Judge, 2011
College of Arts and Sciences Student Council
 Treasurer, Fall 2009, resigned (early graduation)
 Executive Editor of APEX, Arts & Sciences Undergraduate Journal, 2008-09
 Secretary, 2008-09